EXAMINATION OF THE EXPLOSION CHARACTERISTICS OF METHANE/COAL DUST/DOLOMITE/AIR MIXTURES

FINAL REPORT

BY

Cape Breton Development Corporation
P.O. Box 2500
Sydney, Nova Scotia
Canada B1P 6K9

Work on this project was conducted under the auspices of the Department of Energy, Mines and Resources.

116 pp

DSS FILE NUMBER: 009SQ.23440-8-9077

DSS CONTRACT NUMBER: 23440-8-9077/01-SQ

EMR SCIENTIFIC AUTHORITY: Dr. K.J. Mintz

MICROMEDIA

90-03965/

EXAMINATION OF THE EXPLOSION CHARACTERISTICS OF METHANE/COAL DUST/DOLOMITE/AIR MIXTURES

BY

P.R. Amyotte, M.J. Pegg, and Y.-H. Sun

Department of Chemical Engineering
Technical University of Nova Scotia
P.O. Box 1000
Halifax, Nova Scotia
Canada B3J 2X4

FOR

Cape Breton Development Corporation
P.O. Box 2500
Sydney, Nova Scotia
Canada B1P 6K9

January, 1990

DSS CONTRACT: 23440-8-9077/01-SQ

CBDC PURCHASE ORDER: 15022 (CER-88/9-23)

EXECUTIVE SUMMARY

An experimental investigation of coal dust explosions has been conducted in a 26-L, spherical chamber. The coal was run-of-mine and came from the Prince, Lingan and Phalen mines of the Cape Breton Development Corporation. The overall objectives of the work were to investigate the explosion behaviour and dolomite inerting requirements of each of the three coals, alone and also with admixed methane.

Two size fractions were produced for each of the Prince, Lingan and Phalen coals. For each coal type, particle size and methane concentration (0%, 1%, 2%), tests were conducted at coal dust concentrations ranging from the lean flammability limit to 1.0 kg/m^3. The explosion parameters measured for each test were the maximum explosion pressure, P_{max}, and the maximum rate of pressure rise, $(dP/dt)_{max}$. In the portion of the study dealing with inerting requirements, the same matrix of coal type, particle size and methane concentration was used, along with a single coal dust concentration of 0.5 kg/m^3. Dolomite concentrations ranged from 20% of the total solids mixture to the percentage required to suppress an explosion.

The influence of methane addition to the coal dust/air mixtures was determined to be an increase in both P_{max} and $(dP/dt)_{max}$, with the effect being most significant at low dust concentrations. A reduction in mass mean diameter of the parent coal or an increase in coal volatile content was found to have a similar effect on P_{max} and $(dP/dt)_{max}$. All of these observations are consistent with a description of coal dust flame propagation by combustion of devolatilization products.

The explosion inerting data showed that methane admixture brings about an increase in the dolomite percentage and the total incombustible content required for suppression. The additional dolomite required in the presence of methane was predicted reasonably well by an empirical relationship developed by the U.S. Bureau

of Mines. Coal particle size and volatility were also found to strongly affect the inerting level, with more dolomite being required for finer or higher volatility coals. The results from this work show that there is no rationale for relaxing the current rock dusting regulations in Canada.

SOMMAIRE EXECUTIF

Une investigation expérimentale sur les coups de poussière du charbon a été effectuée dans une chambre sphérique d'une capacité de 26 litres. Le charbon a été du genre tout venant en provenance des trois mines, Prince, Lingan et Phalen, gérées par la Société du développement du Cap Bréton. L'objectif général de ce travail a été d'étudier le comportement explosif de ces trois variétés du charbon et de la quantité nécessaire de la dolomite pour les rendre inerte sans ou avec un mélange du méthane.

Des particules de deux grandeurs ont été utilisées pour chaque échantillon du charbon originant des mines Prince, Lingan et Phalen. Les épreuves ont été effectuées sur les concentrations de poussière du charbon qui s'étendaient de la limite maigre de l'inflammabilité jusqu'à 1.0 kg/m^3 pour chaque variété, grandeur de particule et concentration du méthane. Les paramètres d'explosion mésurés pour chaque essai ont été à la pression maximum d'explosion, P_{max}, et à la vitesse maximum de l'augmentation de pression, $(dP/dt)_{max}$. Dans la parties de l'étude qu s'occupe des conditions réquises pour rendre inerte, on a utilisé la même matrice pour chaque variété du charbon, la même grandeur de particule et la même concentration du méthane à une seule concentration de poussière du charbon à 0.5 kg/m^3. Les concentrations de dolomite s'étendaient du 20% de la totalité du mélange des solides jusqu'au pourcentage nécessaire pour supprimer l'explosion.

Il a été déterminé que l'influence du méthane ajouté aux mélanges de poussière du charbon et d'air a causé un accroissement dans la pression maximum d'explosion, P_{max}, ainsi que dans la vitesse maximum de l'augmentation de pression, $(dP/dt)_{max}$: l'effet le plus important produit aux basses concentrations de poussière du charbon. Une réduction dans le diamètre de la masse moyenne du charbon ou une augmentation dans la teneur en matière volatile du charbon a produit un résultat

semblable sur le P_{max} et le $(dP/dt)_{max}$. Toutes ces observations conforment à la description de la propagation de la flamme de poussière du charbon par la combustion des produits dévolatilisés.

L'information sur la suppression de l'explosion a démontré qu'un mélange du méthane opère une augmentation dans le pourcentage de dolomite et dans le total contenu noncombustible nécessaire. Le Bureau des mines de Etats-Unis a bien prédit par un rapport empirique le montant de dolomite supplémentaire qui est nécessaire dans la présence du méthane. On a découve que la grandeur de particule et la volatilité du charbon ont fortement influencé le niveau d'inertement; plus de dolomite a été nécessaire pour le fin charbon ou le charbon à haute volatilité. Les résultats de cette étude épreuvent qu'il n'y a aucune base de diminuer les régulations en vigeur sur le saupoudrage du rocher au Canada.

TABLE OF CONTENTS

		Page
EXECUTIVE SUMMARY		i
SOMMAIRE EXECUTIF		iii
LIST OF TABLES		vii
LIST OF FIGURES		viii
ACKNOWLEDGEMENTS		xiii
CHAPTER 1	INTRODUCTION	1
	1.1 Scope and Objectives of Present Work	2
	1.2 Hybrid Mixtures	2
	1.3 Explosion Inerting	4
CHAPTER 2	EXPERIMENTAL	5
	2.1 Coal Dust and Dolomite	5
	2.2 Experimental Program	9
	2.3 Apparatus and Procedure	12
	2.3.1 Methane tests	12
	2.3.2 Dolomite tests	14
	2.3.3 Chemical ignitors	14
	2.3.4 Data acquisition and analysis	14
CHAPTER 3	RESULTS	19
CHAPTER 4	DISCUSSION	56
	4.1 Phase I Results	56
	4.1.1 Methane admixture	59
	4.1.2 Coal particle size	61
	4.1.3 Coal volatile content	70
	4.1.4 Lean flammability limit	70
	4.2 Phase II Results	78
	4.2.1 Methane admixture	81
	4.2.2 Coal particle size	84
	4.2.3 Coal volatile content	90
	4.3 Applicability to Coal Mining Industry	91
	4.3.1 Turbulence level	91
	4.3.2 Ignition source	92
	4.3.3 Coal particle size	92
	4.3.4 Coal ash content	95

		Page
CHAPTER 5	CONCLUSIONS AND RECOMMENDATIONS	97
	5.1 Summary of Conclusions	97
	5.2 Recommendations for Further Work	98
REFERENCES		100

LIST OF TABLES

		Page
Table 2.1	Particle size analyses of coals and dolomite.	7
Table 2.2	Proximate analyses of coals.	8
Table 2.3	Phase I tests (coal dust/air and methane/coal dust/air).	10
Table 2.4	Phase II tests (coal dust/dolomite/air and methane/coal dust/dolomite/air).	11
Table 4.1	Lean flammability limits for coal dust/air and methane/coal dust/air mixtures.	73
Table 4.2	Dolomite inerting requirements for coal dust/air and methane/coal dust/air mixtures.	83
Table 4.3	Experimental and predicted values of additional dolomite due to methane addition.	88
Table 4.4	Particle size analyses of CBDC colliery dust samples.	93

LIST OF FIGURES

		Page
Fig. 2.1	Sample particle size distribution (Prince 1) determined by Malvern Instruments (2600 Series) analyzer.	6
Fig. 2.2	Schematic diagram of 26-L explosion vessel and auxiliary equipment.	13
Fig. 2.3	Relationship between mass of dolomite and dolomite percentage.	15
Fig. 2.4	Sample pressure-time trace.	17
Fig. 3.1	P_{max} and $(dP/dt)_{max}$ at various coal dust concentrations (Prince 1, 0% methane).	20
Fig. 3.2	P_{max} and $(dP/dt)_{max}$ at various coal dust concentrations (Prince 1, 1% methane).	21
Fig. 3.3	P_{max} and $(dP/dt)_{max}$ at various coal dust concentrations (Prince 1, 2% methane).	22
Fig. 3.4	P_{max} and $(dP/dt)_{max}$ at various coal dust concentrations (Prince 2, 0% methane).	23
Fig. 3.5	P_{max} and $(dP/dt)_{max}$ at various coal dust concentrations (Prince 2, 1% methane).	24
Fig. 3.6	P_{max} and $(dP/dt)_{max}$ at various coal dust concentrations (Prince 2, 2% methane).	25
Fig. 3.7	P_{max} and $(dP/dt)_{max}$ at various coal dust concentrations (Lingan 1, 0% methane).	26
Fig. 3.8	P_{max} and $(dP/dt)_{max}$ at various coal dust concentrations (Lingan 1, 1% methane).	27
Fig. 3.9	P_{max} and $(dP/dt)_{max}$ at various coal dust concentrations (Lingan 1, 2% methane).	28
Fig. 3.10	P_{max} and $(dP/dt)_{max}$ at various coal dust concentrations (Lingan 2, 0% methane).	29

		Page
Fig. 3.11	P_{max} and $(dP/dt)_{max}$ at various coal dust concentrations (Lingan 2, 1% methane).	30
Fig. 3.12	P_{max} and $(dP/dt)_{max}$ at various coal dust concentrations (Lingan 2, 2% methane).	31
Fig. 3.13	P_{max} and $(dP/dt)_{max}$ at various coal dust concentrations (Phalen 1, 0% methane).	32
Fig. 3.14	P_{max} and $(dP/dt)_{max}$ at various coal dust concentrations (Phalen 1, 1% methane).	33
Fig. 3.15	P_{max} and $(dP/dt)_{max}$ at various coal dust concentrations (Phalen 1, 2% methane).	34
Fig. 3.16	P_{max} and $(dP/dt)_{max}$ at various coal dust concentrations (Phalen 2, 0% methane).	35
Fig. 3.17	P_{max} and $(dP/dt)_{max}$ at various coal dust concentrations (Phalen 2, 1% methane).	36
Fig. 3.18	P_{max} and $(dP/dt)_{max}$ at various coal dust concentrations (Phalen 2, 2% methane).	37
Fig. 3.19	P_{max} and $(dP/dt)_{max}$ at various dolomite concentrations (Prince 1, 0.5 kg/m^3 coal dust, 0% methane).	38
Fig. 3.20	P_{max} and $(dP/dt)_{max}$ at various dolomite concentrations (Prince 1, 0.5 kg/m^3 coal dust, 1% methane).	39
Fig. 3.21	P_{max} and $(dP/dt)_{max}$ at various dolomite concentrations (Prince 1, 0.5 kg/m^3 coal dust, 2% methane).	40
Fig. 3.22	P_{max} and $(dP/dt)_{max}$ at various dolomite concentrations (Prince 2, 0.5 kg/m^3 coal dust, 0% methane).	41
Fig. 3.23	P_{max} and $(dP/dt)_{max}$ at various dolomite concentrations (Prince 2, 0.5 kg/m^3 coal dust, 1% methane).	42
Fig. 3.24	P_{max} and $(dP/dt)_{max}$ at various dolomite concentrations (Prince 2, 0.5 kg/m^3 coal dust, 2% methane).	43

		Page
Fig. 3.25	P_{max} and $(dP/dt)_{max}$ at various dolomite concentrations (Lingan 1, 0.5 kg/m^3 coal dust, 0% methane).	44
Fig. 3.26	P_{max} and $(dP/dt)_{max}$ at various dolomite concentrations (Lingan 1, 0.5 kg/m^3 coal dust, 1% methane).	45
Fig. 3.27	P_{max} and $(dP/dt)_{max}$ at various dolomite concentrations (Lingan 1, 0.5 kg/m^3 coal dust, 2% methane).	46
Fig. 3.28	P_{max} and $(dP/dt)_{max}$ at various dolomite concentrations (Lingan 2, 0.5 kg/m^3 coal dust, 0% methane).	47
Fig. 3.29	P_{max} and $(dP/dt)_{max}$ at various dolomite concentrations (Lingan 2, 0.5 kg/m^3 coal dust, 1% methane).	48
Fig. 3.30	P_{max} and $(dP/dt)_{max}$ at various dolomite concentrations (Lingan 2, 0.5 kg/m^3 coal dust, 2% methane).	49
Fig. 3.31	P_{max} and $(dP/dt)_{max}$ at various dolomite concentrations (Phalen 1, 0.5 kg/m^3 coal dust, 0% methane).	50
Fig. 3.32	P_{max} and $(dP/dt)_{max}$ at various dolomite concentrations (Phalen 1, 0.5 kg/m^3 coal dust, 1% methane).	51
Fig. 3.33	P_{max} and $(dP/dt)_{max}$ at various dolomite concentrations (Phalen 1, 0.5 kg/m^3 coal dust, 2% methane).	52
Fig. 3.34	P_{max} and $(dP/dt)_{max}$ at various dolomite concentrations (Phalen 2, 0.5 kg/m^3 coal dust, 0% methane).	53
Fig. 3.35	P_{max} and $(dP/dt)_{max}$ at various dolomite concentrations (Phalen 2, 0.5 kg/m^3 coal dust, 1% methane).	54

		Page
Fig. 3.36	P_{max} and $(dP/dt)_{max}$ at various dolomite concentrations (Phalen 2, 0.5 kg/m^3 coal dust, 2% methane).	55
Fig. 4.1	Actual values (upper plot) and mean values (lower plot) of P_{max} as a function of coal dust concentration (Prince 2, 0% methane).	57
Fig. 4.2	Actual values (upper plot) and mean values (lower plot) of $(dP/dt)_{max}$ as a function of coal dust concentration (Prince 2, 0% methane).	58
Fig. 4.3	Effect of methane admixture on P_{max} and $(dP/dt)_{max}$ of Phalen 2 coal.	60
Fig. 4.4	Effect of methane admixture on $(dP/dt)_{max}$ of Prince 1 coal (upper plot) and Prince 2 coal (lower plot).	62
Fig. 4.5	Effect of coal particle size on P_{max} and $(dP/dt)_{max}$ of Lingan coals (1% methane).	63
Fig. 4.6	Comparison of effect of methane admixture on $(dP/dt)_{max}$ of Lingan 1 coal with effect of coal particle size on $(dP/dt)_{max}$ of Lingan coals (0% methane).	66
Fig. 4.7	Scanning electron micrographs of unburned Prince 1 coal dust.	67
Fig. 4.8	Scanning electron micrographs of Prince 1 char residue at 0% methane, 0.1 kg/m^3 coal dust (upper plot) and 0% methane, 0.4 kg/m^3 coal dust (lower plot).	68
Fig. 4.9	Scanning electron micrographs of Prince 1 char residue at 1% methane, 1.0 kg/m^3 coal dust (upper plot) and 2% methane, 0.1 kg/m^3 coal dust (lower plot)	69
Fig. 4.10	Effect of coal volatile content on P_{max} and $(dP/dt)_{max}$ (0% methane).	71
Fig. 4.11	Lean flammability limits of Prince 1 coal (upper plot) and Prince 2 coal (lower plot).	75
Fig. 4.12	Lean flammability limits of Lingan 1 coal (upper plot) and Lingan 2 coal (lower plot).	76

		Page
Fig. 4.13	Lean flammability limits of Phalen 1 coal (upper plot) and Phalen 2 coal (lower plot).	77
Fig. 4.14	P_{max} and $(dP/dt)_{max}$ at various dolomite concentrations (Lingan 1, 0.5 kg/m^3 coal dust, 0% methane).	79
Fig. 4.15	P_{max} and $(dP/dt)_{max}$ at various dolomite concentrations (Phalen 2, 0.5 kg/m^3 coal dust, 0% methane).	80
Fig. 4.16	Effect of methane admixture on dolomite inerting requirements of Prince 2 coal.	82
Fig. 4.17	Effect of methane addition on inerting ratio for Prince coals.	85
Fig. 4.18	Effect of methane addition on inerting ratio for Lingan coals.	86
Fig. 4.19	Effect of methane addition on inerting ratio for Phalen coals.	87
Fig. 4.20	Relationship between experimental and predicted values of additional dolomite due to methane addition.	89
Fig. 4.21	P_{max} and $(dP/dt)_{max}$ at various coal dust concentrations (Phalen "pure", 0% methane).	96

ACKNOWLEDGEMENTS

It is a pleasure to acknowledge the contributions of the following organizations and people: Energy, Mines and Resources Canada and the Cape Breton Development Corporation, for funding the work; Dr. K.J. Mintz and Mr. J.C. Campbell, for their scientific and technical insight; Dr. K.I. Wilkie, for developing the computerized system for dust dispersion and ignition and data acquisition; Mr. S. Carr and Mr. T Mosher, for their help in preparing the experimental apparatus; Mr. G. Ward and Mr. A. Snow, for their help in performing the experiments; Ms. D. Laffin, for typing the manuscript.

CHAPTER 1

INTRODUCTION

Combustible dusts such as flour, sugar, metals, plastics and coal are produced as end- or by-products in many industries. The risk of fire or explosion in the handling of such dusts has prompted considerable research effort in the areas of explosion prevention and mitigation. Recognition of the need for good housekeeping practices, removal of ignition sources, sensible location of physical plant, admixture of inerts to hazardous materials and venting of enclosures has resulted in safer plant operation. However, the dust explosion hazard has not been eliminated.

There have been more than 500 major dust or gas (or both) explosions in coal mines in the United States during the past 100 years (Cashdollar et al., 1987); a recent mine explosion in Nova Scotia claimed 11 lives (Watson, 1981). Between 1977 and 1985 there were 26 coal dust fire or explosion accidents in cement plants throughout the United States (Alameddin and Luzik, 1987). In 1982, serious explosions occurred in sugar refineries in the north of France and in Belgium (Geysen et al., 1987). Abrahamsen (1987) reports that between 1962 and 1980 there were 485 explosions and 715 fires in the United Kingdom which involved flammable dusts. Although more recent statistics are not readily available, the most serious dust explosion incidents in the last few years in the United Kingdom involved aluminum powder at Holyhead (1983), rapeseed dust at Hull (1984) and flour at Ashford (1984). Kauffman (1987) has presented a compilation of dust explosion statistics for the United States, and has shown that from 1979 to 1986 there have been 160 dust explosion incidents in grain handling facilities.

1.1 Scope and Objectives of Present Work

The scope of the present work is an investigation of small-scale, confined, deflagrative dust explosions. It is primarily an experimental study, with the major piece of apparatus being a 26-L, spherical explosion chamber. The material examined was coal dust which was produced from run-of-mine coal from three Cape Breton Development Corporation (CBDC) mines (Prince, Lingan and Phalen). Two size fractions were generated for each of the three coals.

The objectives of the present work are summarized as follows:

(1) to investigate the explosion behaviour of the Prince, Lingan and Phalen coals in terms of the maximum explosion pressure, P_{max}, the maximum rate of pressure rise, $(dP/dt)_{max}$, and the lean flammability limit;

(2) to examine the dolomite inerting requirements of each of the coals; and

(3) to investigate the effects of methane admixture on the explosion behaviour and dolomite inerting requirements of each of the coals.

1.2 Hybrid Mixtures

One of the broadest ways of explosion classification is by fuel type: flammable gas, combustible dust, or hybrid mixture (mixture of flammable gas and combustible dust). Strictly speaking, therefore, the present work involved not only dust explosions but also hybrid mixture explosions. This is because a major part of the investigation dealt with methane admixture to the combustion atmosphere, as indicated by objective (3) in the previous section.

Of the three fuel types, hybrid mixtures have received the least attention by researchers. The hazard associated with such mixtures is significant, however, and exists in several industries. Examples of typical hybrid mixtures given by Lee et al. (1984) include hexane with soya bean meal, pentane with styrene and polystyrene, and cyclopentane with wood.

Perhaps the most common hybrid mixture is the one reported on here, namely methane and coal dust, which is a combination most prevalent in the coal mining industry. An appreciation of the hazard associated with methane and coal dust can be gained by examining the steps leading to a fully developed mine explosion. These steps have been outlined by Hertzberg et al. (1982a) as follows:

(1) Growth of a large, flammable methane/air zone near the face that is being mined. The flammable zone growth results from increasing methane emissions as the mining process advances into the fresh seam. If the ventilation is inadequate to dilute and carry away the increased emissions, then significant flammable volumes are generated.

(2) Ignition of that flammable volume by the frictional heating of cutting bits, by an electric or electrostatic spark, or by an explosive shot.

(3) Development of a localized methane/air explosion and flame acceleration outward from the face.

(4) Lifting of coal dust accumulations by the flow generated ahead of the accelerating methane/air flame, and mixing of that dust with air to create a flammable coal dust/air mixture.

(5) Ignition of the dust/air mixture by the methane/air flame.

(6) Further turbulent acceleration of the dust flame front which lifts more coal dust, mixing it with air throughout an increasingly lengthening zone ahead of the flame.

(7) Propagation of a dust explosion throughout the mine.

The above scenario considers the methane explosion and the coal dust explosion to be separate events, and thus does not really provide a description of a hybrid mixture explosion. However, the presence of methane further away from the working face means that step (4) would involve mixing of coal dust with not just air, but

air and methane. This could result in a flammable methane/coal dust/air hybrid mixture which ignites and propagates through the mine workings according to steps (5) to (7).

1.3 Explosion Inerting

Inerting is the term applied to the practice of adding inhibitors to combustible dusts, the purpose being to arrest explosion propagation. Inerting agents can be separated into two categories, those that act thermally and those that act chemically. Examples of thermal inhibitors include fly ash, limestone, dolomite, nitrogen, carbon dioxide and helium. Typical chemical inhibitors are salt and ammonium phosphate.

Government regulations in Canada, the United States and many other countries require the use of rock dust (generally limestone or dolomite) as the inerting agent in coal mines. Dolomite was used, therefore, in the portion of the current work which involved explosion inerting. A good description of inerting requirements in coal mines, written from a practical point of view, has been given by Nagy (1981).

CHAPTER 2

EXPERIMENTAL

In this chapter, the materials and methods used to conduct the explosion tests are described.

2.1 Coal Dust and Dolomite

Coal samples from the Prince, Lingan and Phalen mines, and dolomite from the Kelly Cove (Cape Breton) deposit, were obtained from CBDC. The coal was run-of-mine and had not been processed prior to delivery to TUNS. At TUNS, each coal was ground and sieved to produce two size fractions. There were thus six coal dust samples prepared for testing. They are referred to throughout this report as Prince 1 and Prince 2, Lingan 1 and Lingan 2, and Phalen 1 and Phalen 2. The dolomite was not processed in any manner after receipt at TUNS.

After grinding and sieving, each coal dust sample was thoroughly mixed and samples were withdrawn for particle size analysis (performed by the Mining and Metallurgical Engineering Department, TUNS) and ultimate and proximate analyses (performed by the Nova Scotia Research Foundation Corporation). Particle size measurements were made using a Malvern Instruments (2600 Series) analyzer based on the principle of laser diffraction or ensemble light scattering. A sample distribution is shown in Fig. 2.1.

The particle size analyses of all the coals are shown in Table 2.1, along with that of the dolomite which was used in the inerting studies. The arithmetic volume or mass mean diameter, D_w, is the last entry in each row of Table 2.1. A calcium/magnesium analysis of the dolomite (performed by the Mining and Metallurgical Engineering Department, TUNS) indicated 31 weight% CaO and 17 weight % MgO. Proximate analyses of the coals are given in Table 2.2; the bold-faced

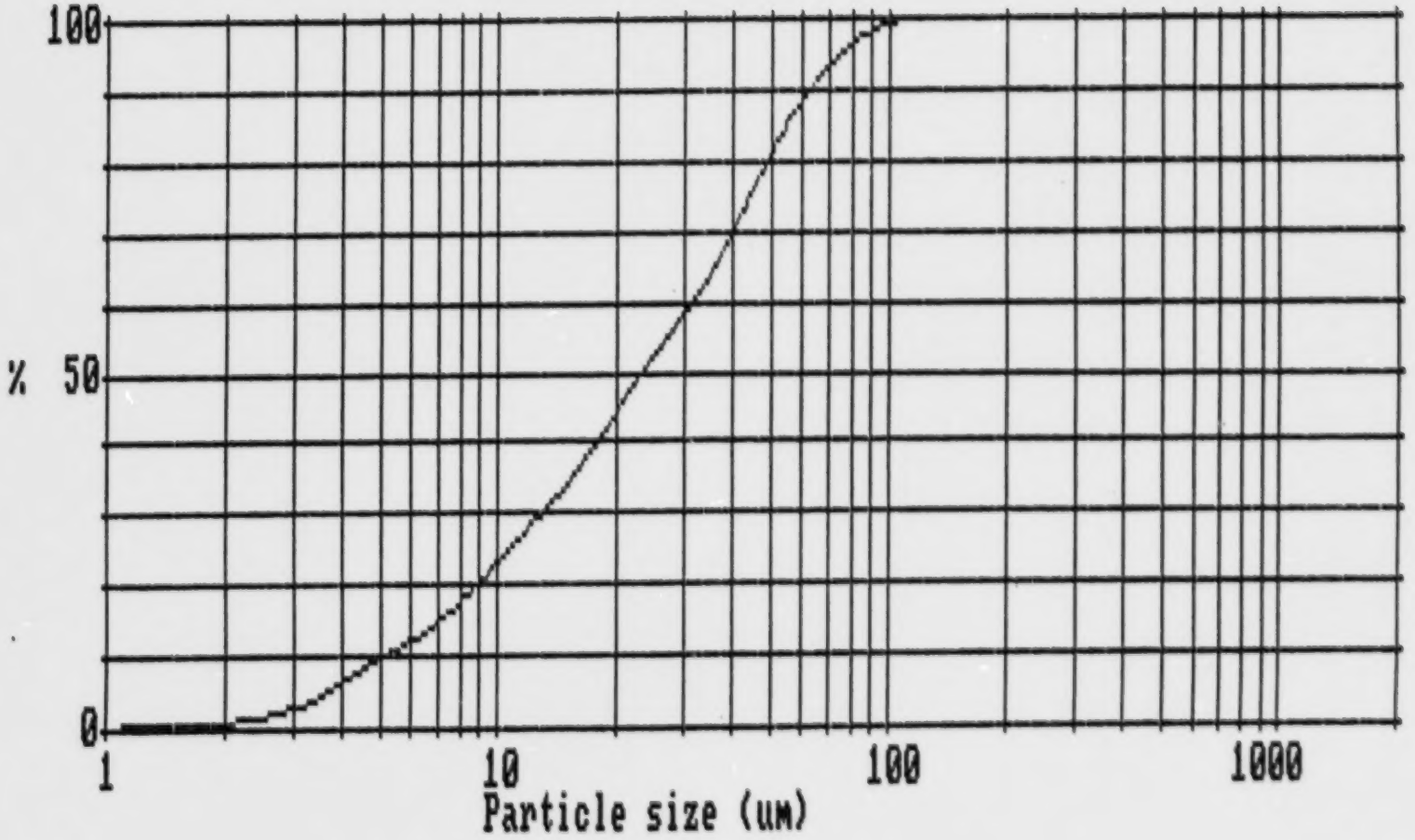

Fig. 2.1 Sample particle size distribution (Prince 1) determined by Malvern Instruments (2600 Series) analyzer.

Table 2.1 Particle size analyses of coals and dolomite.

Coal Dust	< 125 μm [weight %]	<75 μm [weight %]	<45 μm [weight%]	<20 μm [weight%]	D_w [μm]
Prince 1	100	95	76	44	23
Prince 2	100	100	88	53	19
Lingan 1	100	87	65	41	27
Lingan 2	100	98	83	53	18
Phalen 1	100	89	68	45	24
Phalen 2	100	100	89	60	15
Dolomite	94	76	56	32	37

Table 2.2 Proximate analyses of coals.

Coal Dust	Moisture [%]	Ash [%]	Volatiles [%]	Fixed Carbon [%]
Prince 1	0.7	15.1	35.8	48.4
	0.6	15.3	36.0	48.1
	0.7	15.0	36.2	48.1
	0.7	**15.1**	**36.0**	**48.2**
Prince 2	0.9	14.7	34.4	50.0
	1.0	14.6	33.9	50.5
	1.0	14.7	34.7	49.6
	1.0	**14.7**	**34.3**	**50.0**
Lingan 1	0.2	18.5	31.6	49.7
	0.2	18.5	32.4	48.9
	0.2	18.3	31.8	49.7
	0.2	**18.4**	**31.9**	**49.5**
Lingan 2	0.3	15.1	31.2	53.4
	0.3	15.0	31.1	53.6
	0.2	15.1	32.7	52.0
	0.3	**15.1**	**31.7**	**52.9**
Phalen 1	0.3	35.4	25.8	38.5
	0.3	35.1	26.1	38.5
	0.3	35.1	27.0	37.6
	0.3	**35.2**	**26.3**	**38.2**
Phalen 2	0.5	33.0	26.5	40.0
	0.5	32.9	26.3	40.3
	0.5	33.0	26.0	40.5
	0.5	**33.0**	**26.3**	**40.2**

entries are the averages of the three analyses done for each of the six dust samples. The Prince and Lingan analyses (particularly the Prince) are typical of coals from CBDC mines prior to cleaning. The Phalen analyses are not typical, however, and indicate an abnormal level of ash in the run-of-mine coal. This is discussed further in section 4.3.4 of the report.

To prevent excessive loss of volatiles and surface oxidation, the coal dust was kept in an inert atmosphere over the duration of testing. This involved first placing the dust in glass mason jars, the tops of which had been fitted with inlet and outlet valves. Each jar was filled with dust to about three-quarters full, and the remaining space was evacuated with a small vacuum pump. The jar was then flushed through with nitrogen to provide the inert atmosphere. The evacuation and purging procedure was repeated for each jar at regular intervals throughout the testing.

2.2 Experimental Program

The experimental program was divided into two phases. Phase I addressed objectives (1) and (3) in section 1.1. and dealt with coal dust/air and methane/coal dust/air tests according to the scheme outlined in Table 2.3. For each coal type, particle size and methane concentration, tests were conducted at coal dust concentrations ranging from the lean flammability limit (LFL) to 1.0 kg/m^3.

In phase II, which addressed objectives (2) and (3) in section 1.1, experiments were carried out on coal dust/dolomite/air mixtures and methane/coal dust/dolomite/air mixtures as shown in Table 2.4. For each coal type, particle size and methane concentration, tests were conducted at one coal dust concentration (0.5 kg/m^3) and dolomite concentrations ranging from 20% of the total solids mixture to the percentage required to suppress an explosion.

Table 2.3 Phase I tests (coal dust/air and methane/coal dust/air).

Coal Type and Size	Methane Concentration [%]	Coal Dust Concentration [kg/m^3]
Prince 1	0, 1, 2	LFL to 1.0
Prince 2	0, 1, 2	LFL to 1.0
Lingan 1	0, 1, 2	LFL to 1.0
Lingan 2	0, 1, 2	LFL to 1.0
Phalen 1	0, 1, 2	LFL to 1.0
Phalen 2	0, 1, 2	LFL to 1.0

Table 2.4 Phase II tests (coal dust/dolomite/air and methane/coal dust/dolomite/air).

Coal Type and Size	Methane Concentration [%]	Coal Dust Concentration [kg/m^3]	Dolomite Concentration [%]
Prince 1	0, 1, 2	0.5	20 to suppression
Prince 2	0, 1, 2	0.5	20 to suppression
Lingan 1	0, 1, 2	0.5	20 to suppression
Lingan 2	0, 1, 2	0.5	20 to suppression
Phalen 1	0, 1, 2	0.5	20 to suppression
Phalen 2	0, 1, 2	0.5	20 to suppression

2.3 Apparatus and Procedure

The explosion tests were conducted in a stainless steel, spherical vessel having a volume of 26 L (Fig. 2.2). Prior to each run, the required mass of coal dust was placed in a curved tube located beneath a nozzle housed in the chamber bottom. Dust dispersion through the nozzle was achieved by an air blast from a 1–L reservoir pressurized to 13.8 bar (g). Also before each run, the explosion vessel was evacuated to 0.53 bar so that the dispersion pulse raised the vessel pressure to 1 bar at the time of ignition. Ignition was by a chemical ignitor having a stored energy of 5 kJ, centrally mounted in the chamber. A fixed time delay of 400 ms between commencement and ending of dust dispersion, followed by a 10–ms delay before ignition (i.e. a total ignition delay time of 410 ms), was used in all tests.

Pressure development during an explosion was measured by a piezoelectric transducer mounted flush with the interior of the vessel. An IBM PC was used to record the pressure-time data from which values of P_{max} and $(dP/dt)_{max}$ were obtained. The PC was also used to control the dust dispersion and ignition sequence by opening and closing the solenoid valve shown in Fig. 2.2 and firing the chemical ignitor at the appropriate times.

2.3.1 Methane tests

For tests involving methane, the procedure described above was modified slightly. Methane/air mixtures with the same concentration of methane were made up by the partial pressure method in both the dispersion reservoir and the explosion vessel prior to dust dispersion. The vessel pressure at the time of ignition was still 1 bar, but now the combustion atmosphere contained either 1% or 2% methane depending on the test.

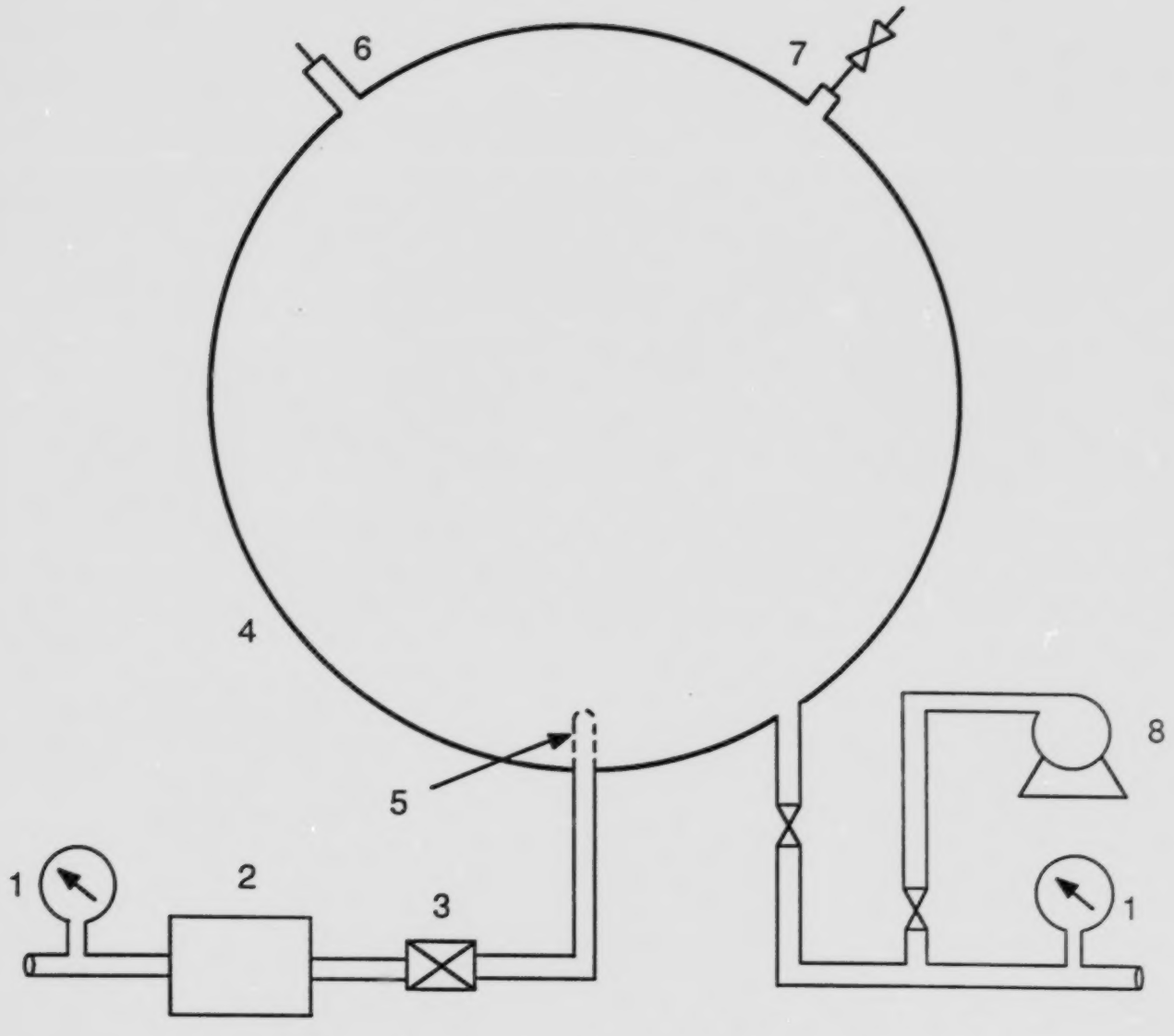

1	Pressure gauge	5	Dispersion nozzle
2	Dispersion reservoir	6	Pressure transducer
3	Solenoid valve	7	Exhaust
4	Explosion chamber	8	Vacuum pump

Fig. 2.2 Schematic diagram of 26-L explosion vessel and auxiliary equipment.

2.3.2 Dolomite tests

For tests involving dolomite, the experimental procedure was again slightly modified. For the apparatus and test conditions used in this study, approximately 30 g of dust is the maximum amount which can be dispersed through the nozzle and into the chamber. However, for a fixed coal dust concentration of 0.5 kg/m^3 (13 g in 26 L) and dolomite percentages greater than 60%, the total amount of solids (coal dust and dolomite) to be dispersed can be significantly greater than 30 g. Figure 2.3 gives a plot of the mass of dolomite required for various dolomite percentages. It was necessary, therefore, to adopt the procedure recommended by Cashdollar and Hertzberg (1985). Only that amount of dust which could easily be dispersed through the nozzle was placed in the curved-tube reservoir. The remainder was placed on top of the nozzle and was dispersed by the dust/air mixture flowing through the nozzle perforations.

2.3.3 Chemical ignitors

The 5-kJ chemical ignitors, manufactured by Fr. Sobbe G.m.b.H. in West Germany, were used as the ignition source for all tests. A good description of these ignitors has been given by Hertzberg et al. (1988). Briefly, each ignitor consists of a small plastic cup containing 1.2 g of explosive powder and a fuse wire for electrical activation. The powder is composed of 40% by mass zirconium, 30% by mass barium nitrate and 30% by mass barium peroxide. The plastic cup is capped with a thin paper diaphragm through which protrude two wire leads connected to the internal fuse wire. Ignition sources such as these are routinely used in dust explosion research (for example, Hertzberg et al., 1986a and Mintz, 1989).

2.3.4 Data acquisition and analysis

The IBM PC used to record pressure-time data was interfaced with the piezoelectric transducer through an external analog-to-digital converter. The analog

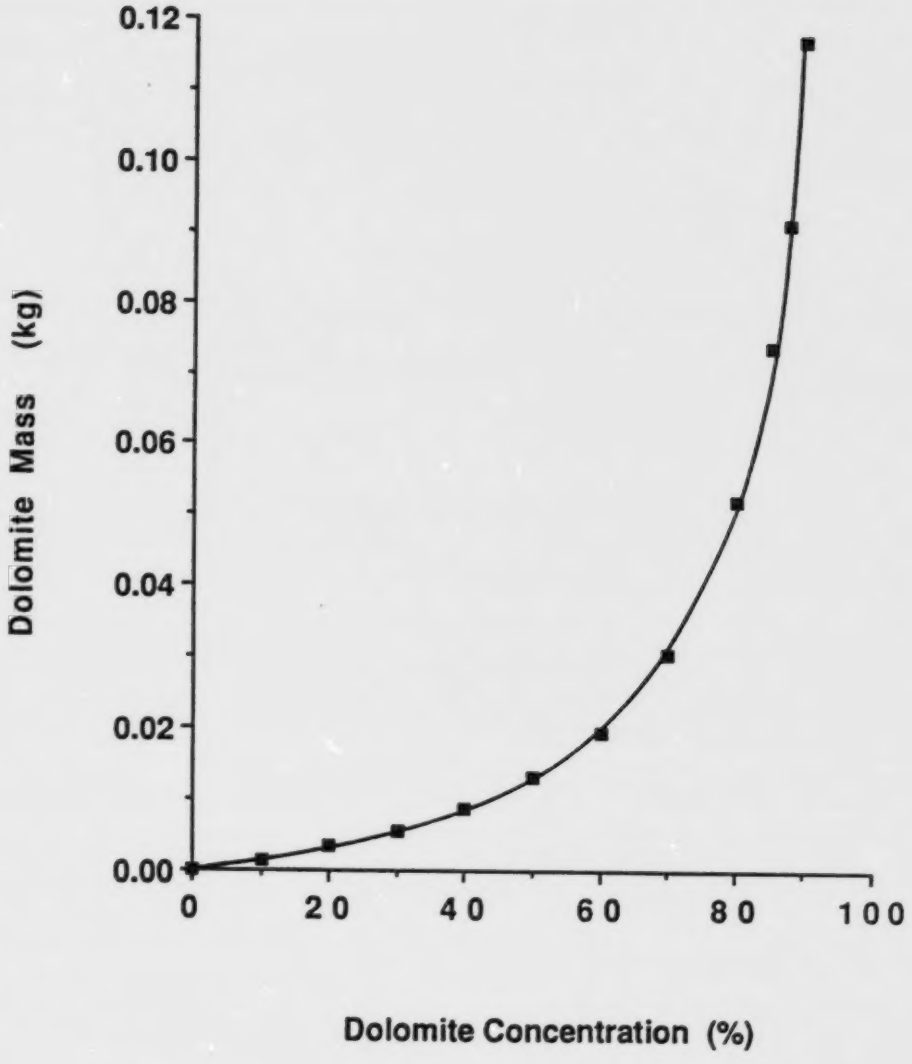

Fig. 2.3 Relationship between mass of dolomite and dolomite percentage.

signal from the transducer was sampled at a rate of 10 kHz for coal dust concentrations greater than 0.2 kg/m^3 and at 5 kHz for concentrations less than or equal to 0.2 kg/m^3. These sampling rates have previously been shown to be satisfactory by Swift (1982).

A sample pressure-time trace recorded by the PC is given in Fig. 2.4. An upper axis corresponding to real time and an absolute pressure axis on the right-hand side have been added to the computer printout. This has been done in an attempt to clarify the lower time axis and the pressure axis on the left-hand side, both of which are computer-generated.

At zero time on the lower axis in Fig. 2.4, the solenoid valve shown in Fig. 2.2 has just been closed. The corresponding real time is 400 ms since the opening of the solenoid valve. Ten ms later the chemical ignitor is fired and there is a rapid increase in pressure; in real time this corresponds to 410 ms after the solenoid valve opening.

Because the piezoelectric transducer is a dynamic device which measures pressure changes, zero pressure on the left-hand axis in Fig. 2.4 is actually the initial reduced pressure in the explosion chamber (0.53 bar on the right-hand axis). The pressure at time zero (or 400 ms in real time) in Fig. 2.4 is 0.45 bar; this is added to the initial reduced pressure of 0.53 bar to give the pressure in the vessel at the time of ignition. As indicated on the right-hand axis, this is 0.98 bar (a), or essentially one atmosphere.

The maximum explosion pressures given in this report are absolute pressures which have been corrected for the contribution due to the ignitor. This was determined in preliminary testing to be 0.48 bar. In calculating the maximum rate of pressure rise, the procedure recommended by Swift (1982) was followed. The slope at each point was calculated from the slope of a line through three points before and three points after. Thus the slope at each point was a best fit of the data over six time intervals; this derivative calculation procedure was done by the computer software. The solid line in

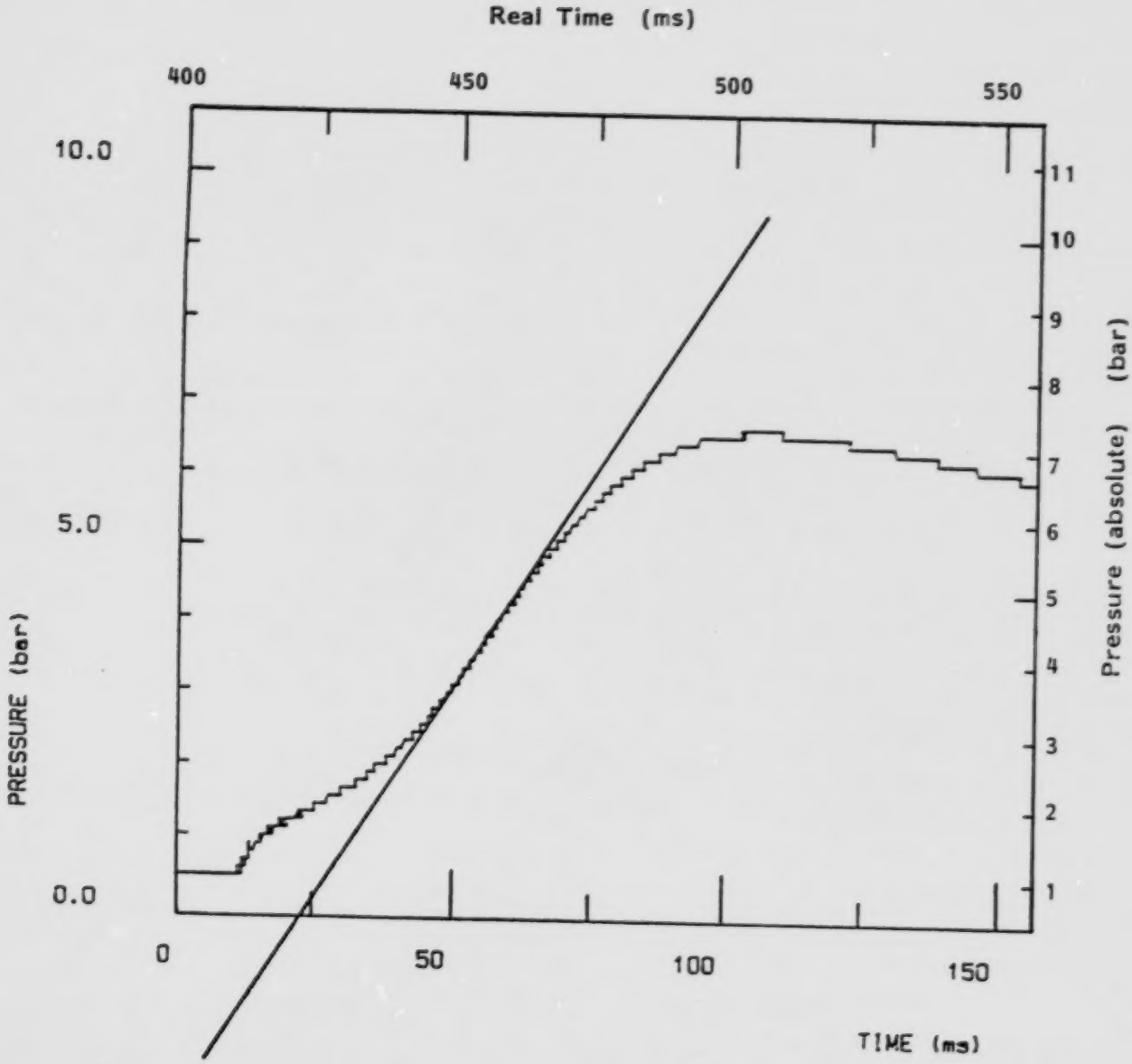

Fig. 2.4 Sample pressure-time trace.

Fig. 2.4, drawn tangent to the steepest portion of the pressure–time curve, offers a quick visual check on the location where $(dP/dt)_{max}$ occurs.

CHAPTER 3

RESULTS

In this chapter, the results from the explosion tests are presented. Discussion and interpretation of the results are given in the next chapter of the report.

Figures 3.1 to 3.18 present the phase I results (coal dust/air and methane/coal dust/air). Each figure gives two plots for a given coal type, particle size and methane concentration. One plot shows maximum explosion pressure (absolute), P_{max}, as a function of coal dust concentration; the other shows maximum rate of pressure rise, $(dP/dt)_{max}$, as a function of coal dust concentration.

Figures 3.19 to 3.36 present the phase II results (coal dust/dolomite/air and methane/coal dust/dolomite/air). Each figure gives two plots for a given coal type, particle size and methane concentration, and the fixed coal dust concentration of 0.5 kg/m^3. One plot shows P_{max} (absolute) as a function of dolomite concentration; the other shows $(dP/dt)_{max}$ as a function of dolomite concentration.

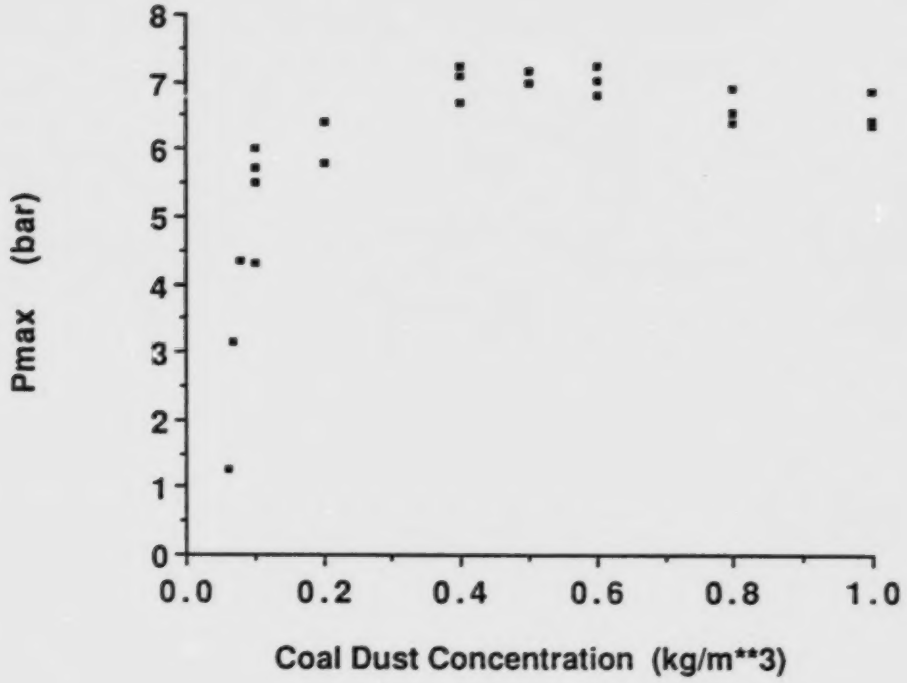

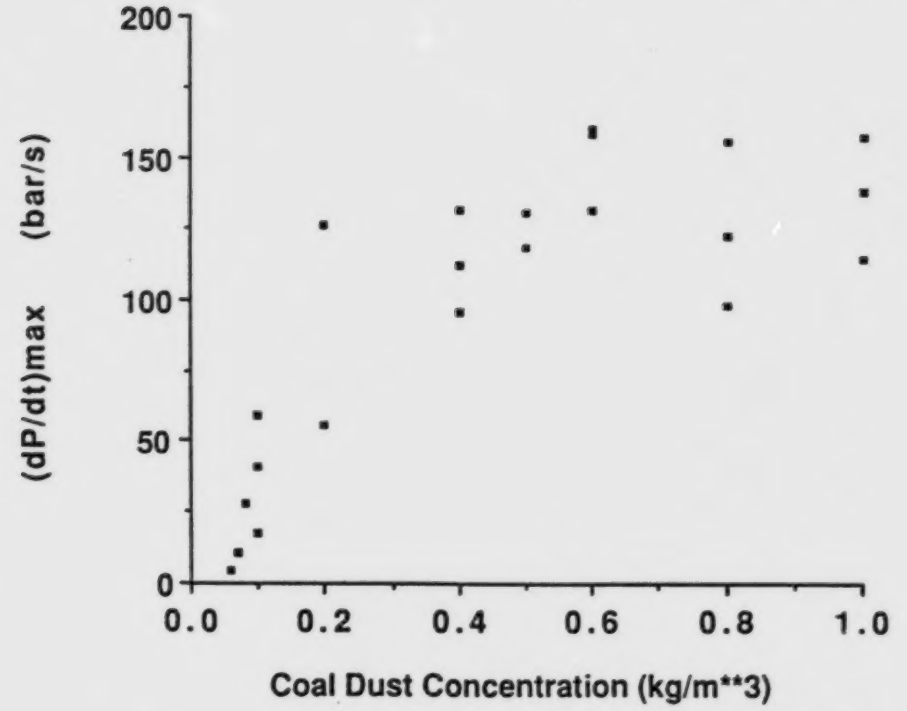

Fig. 3.1 P_{max} and $(dP/dt)_{max}$ at various coal dust concentrations (Prince 1, 0% methane).

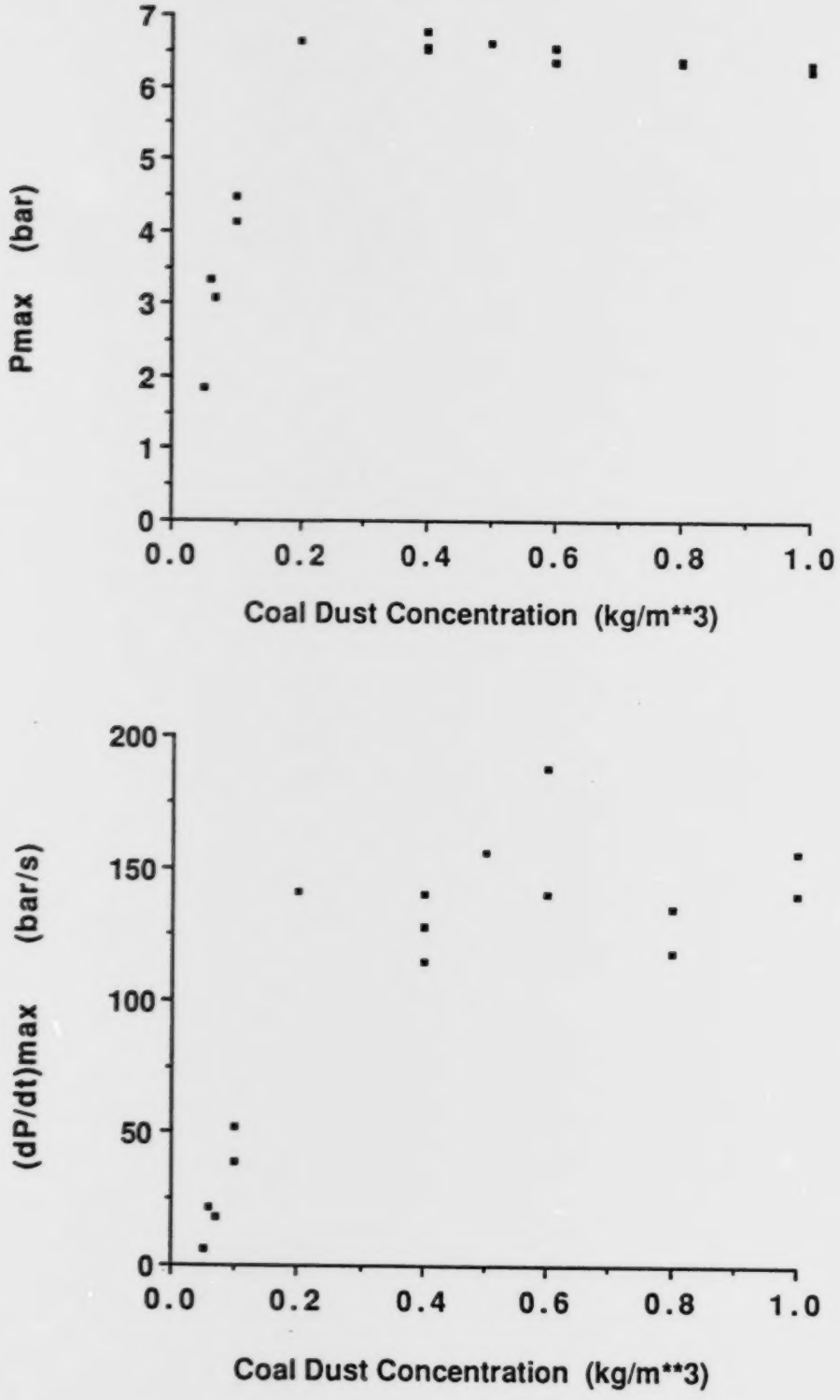

Fig. 3.2 P_{max} and $(dP/dt)_{max}$ at various coal dust concentrations (Prince 1, 1% methane).

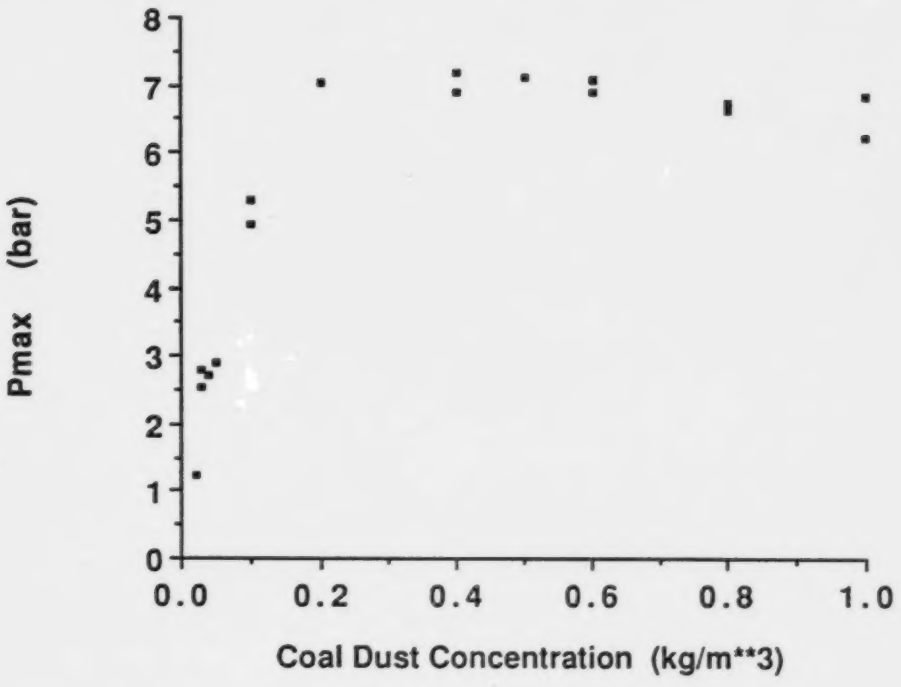

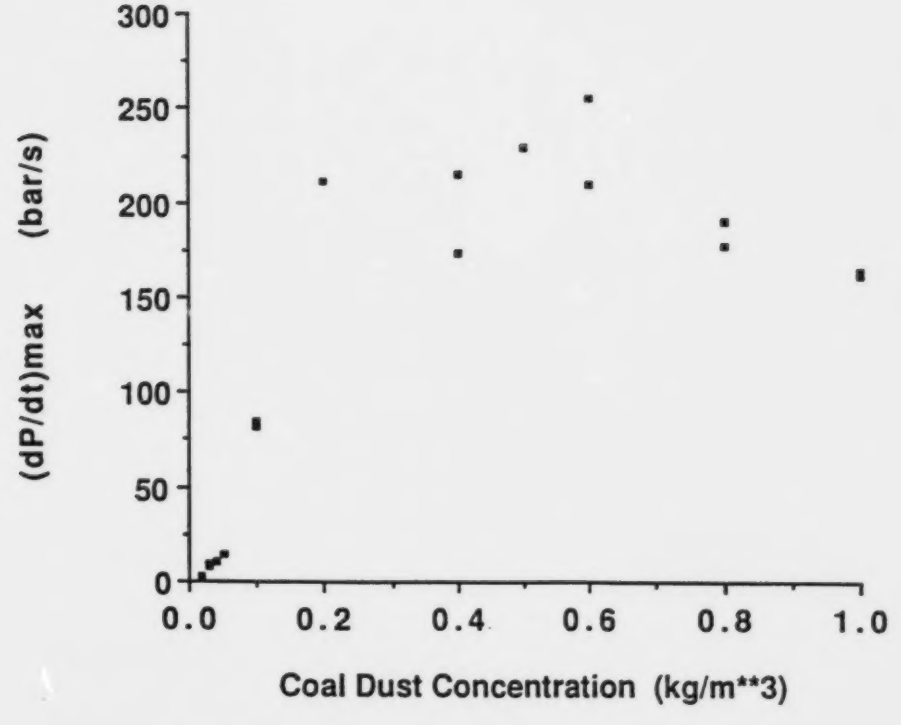

Fig. 3.3 P_{max} and $(dP/dt)_{max}$ at various coal dust concentrations (Prince 1, 2% methane).

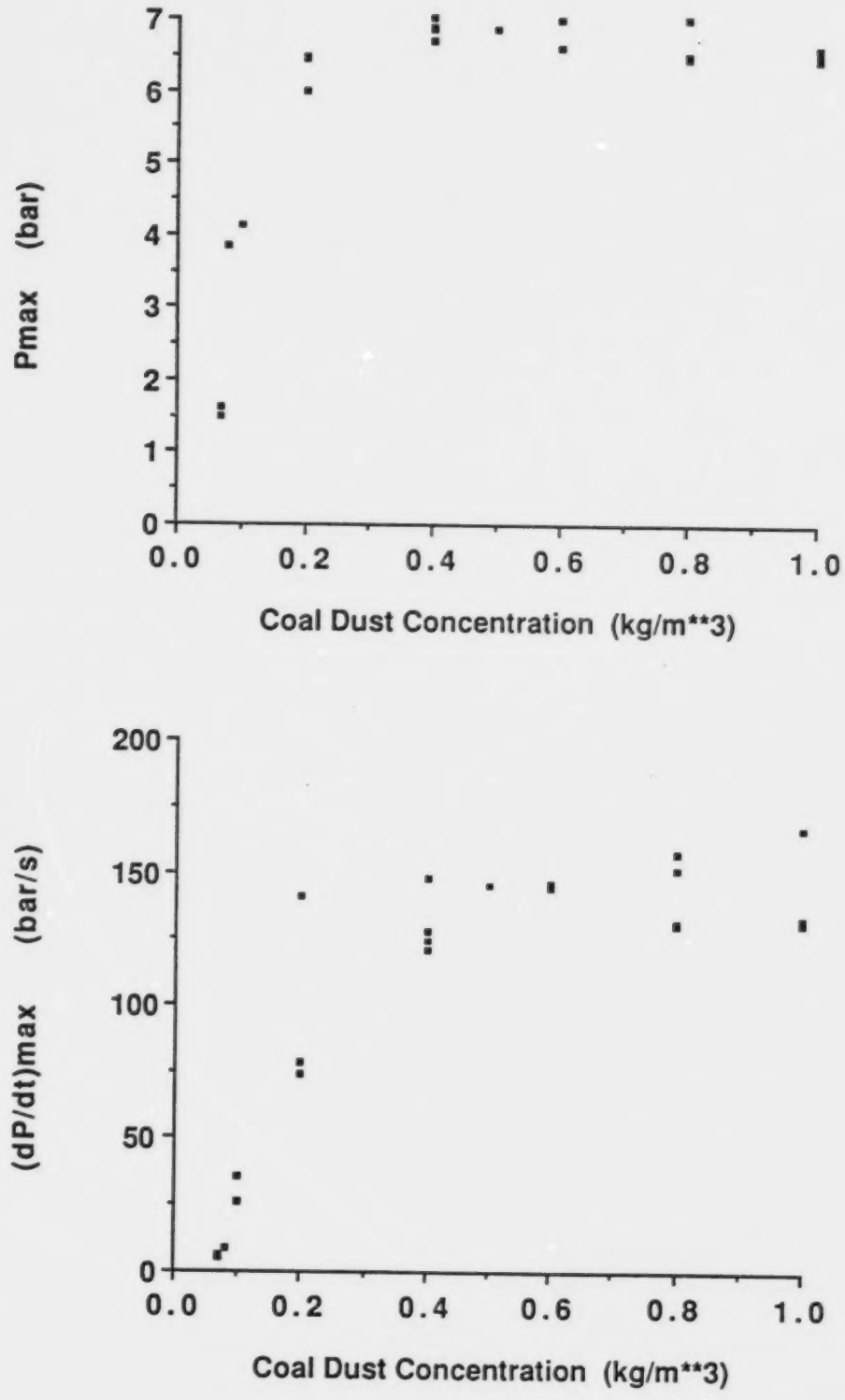

Fig. 3.4 P_{max} and $(dP/dt)_{max}$ at various coal dust concentrations (Prince 2, 0% methane).

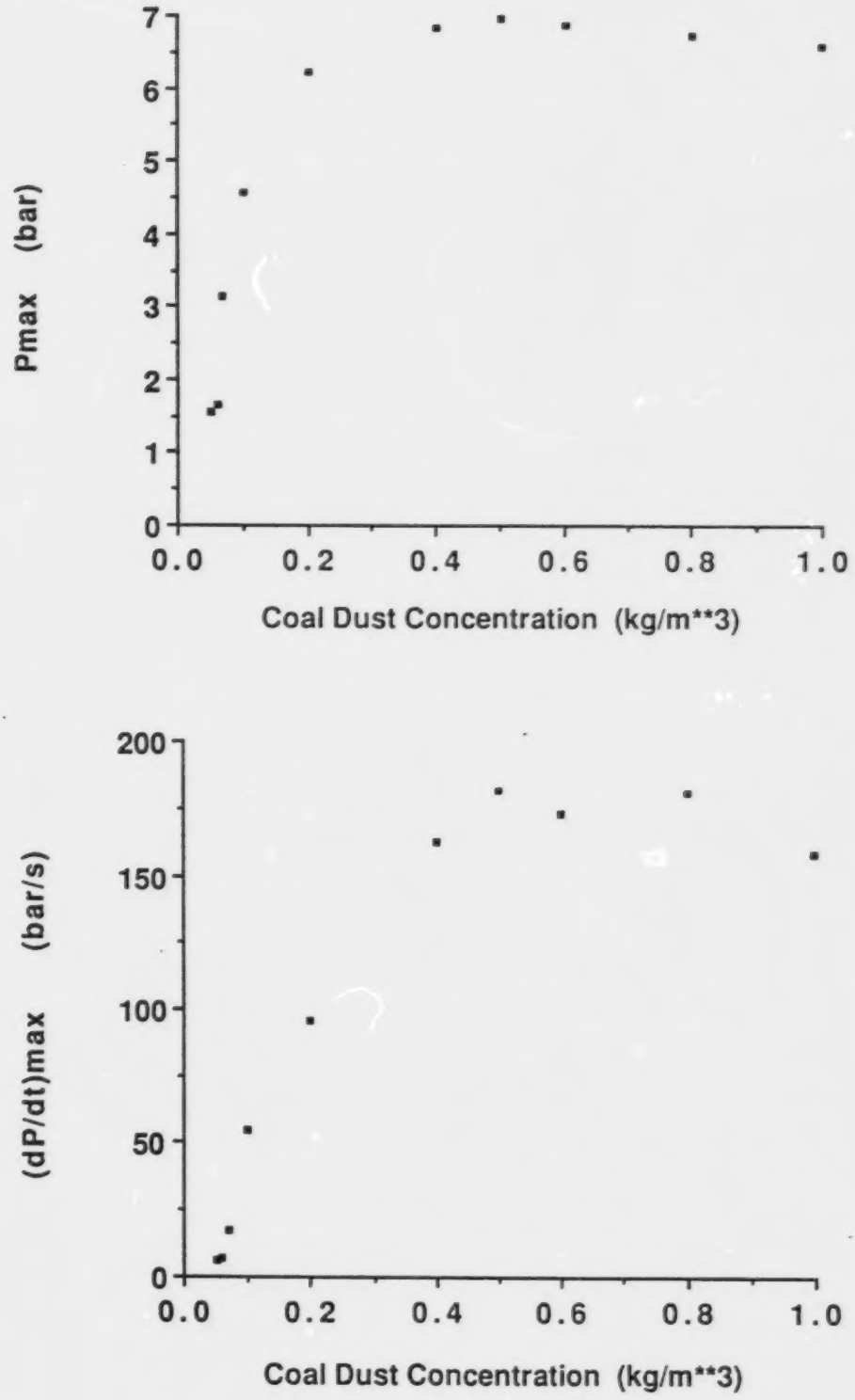

Fig. 3.5 P_{max} and $(dP/dt)_{max}$ at various coal dust concentrations (Prince 2, 1% methane).

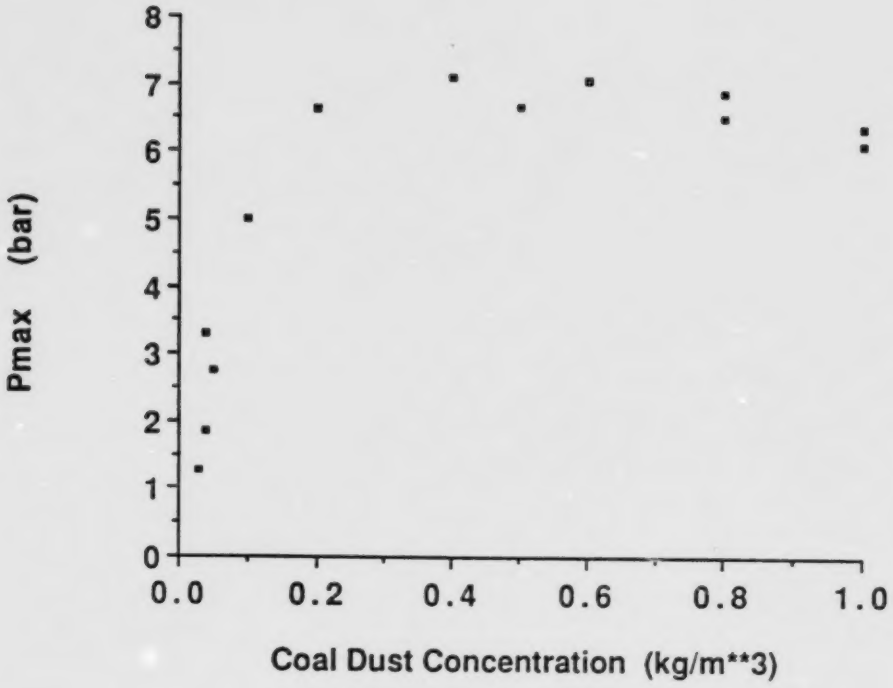

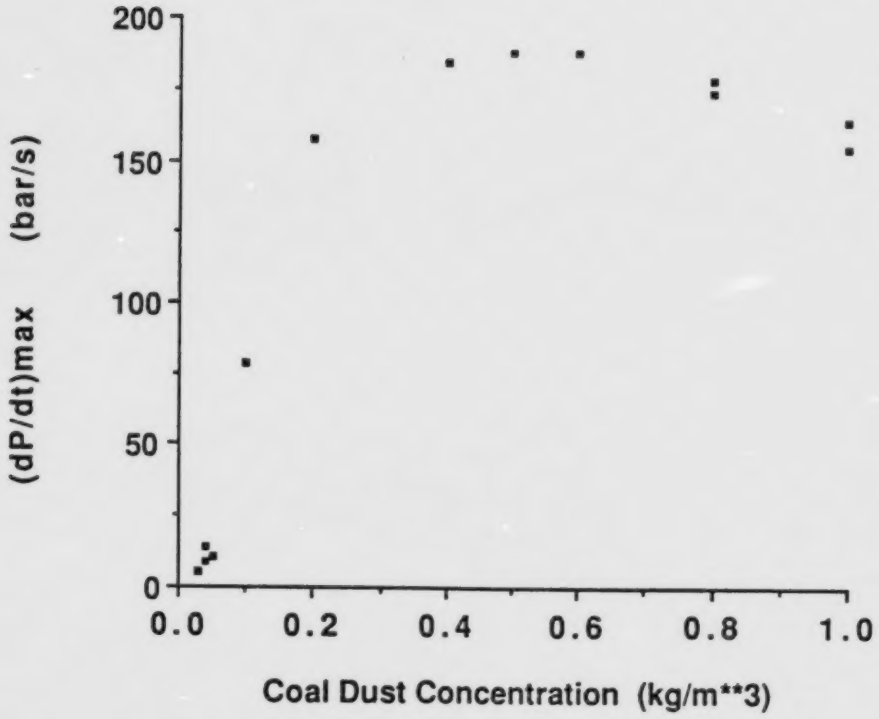

Fig. 3.6 P_{max} and $(dP/dt)_{max}$ at various coal dust concentrations (Prince 2, 2% methane).

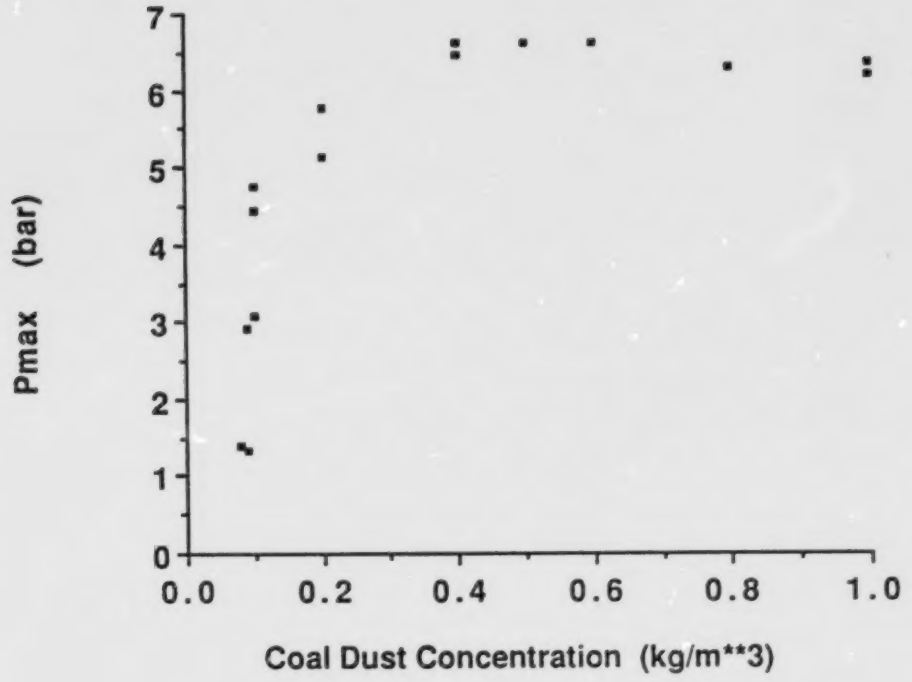

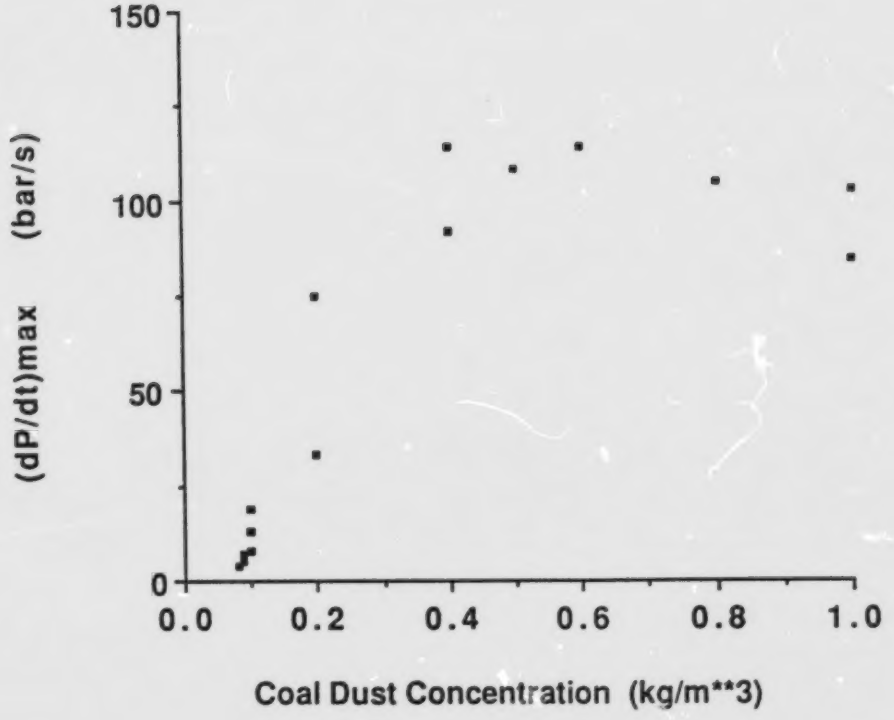

Fig. 3.7 P_{max} and $(dP/dt)_{max}$ at various coal dust concentrations (Lingan 1, 0% methane).

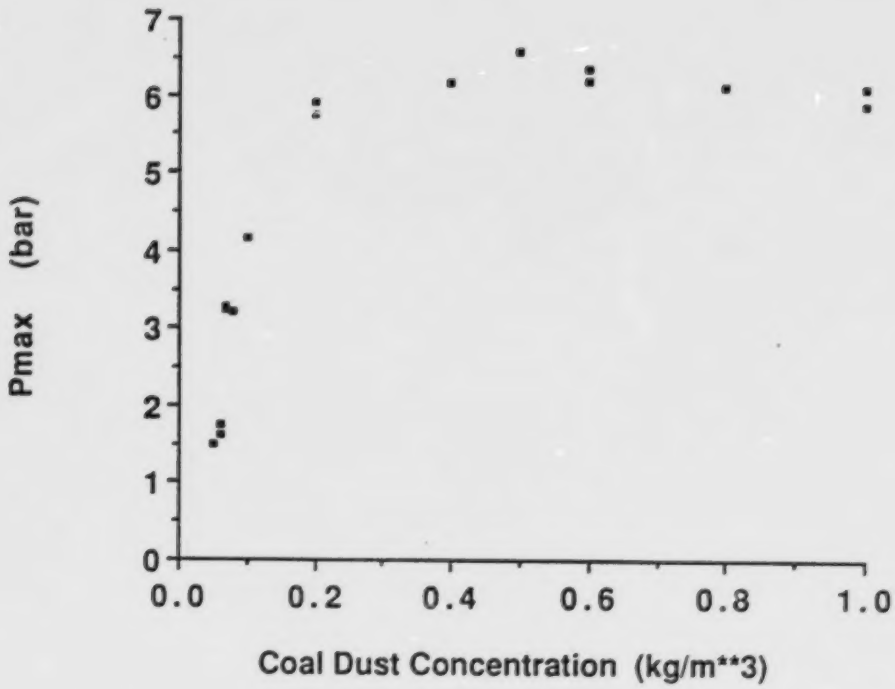

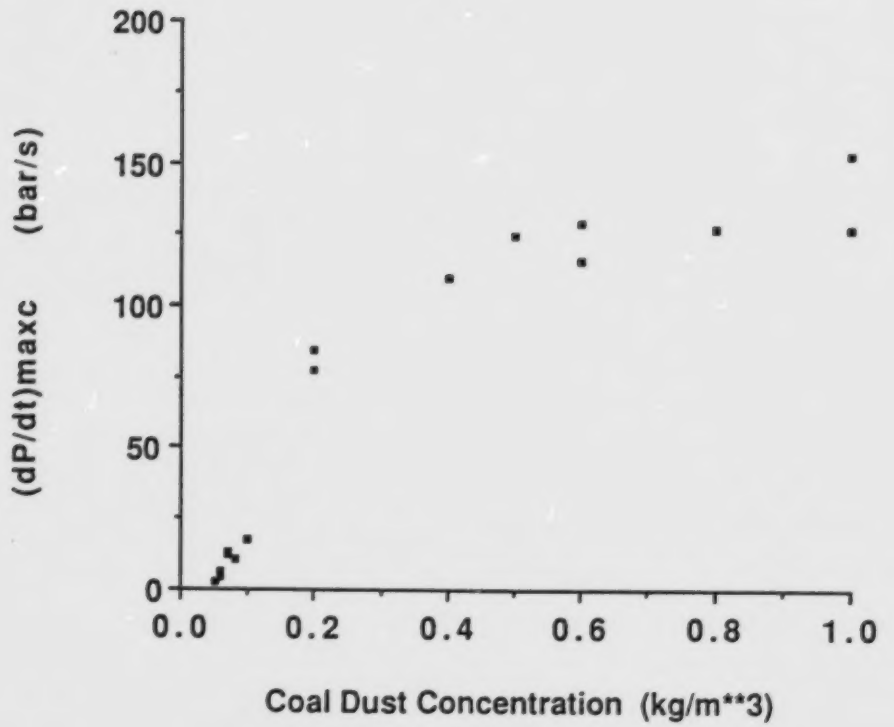

Fig. 3.8 P_{max} and $(dP/dt)_{max}$ at various coal dust concentrations (Lingan 1, 1% methane).

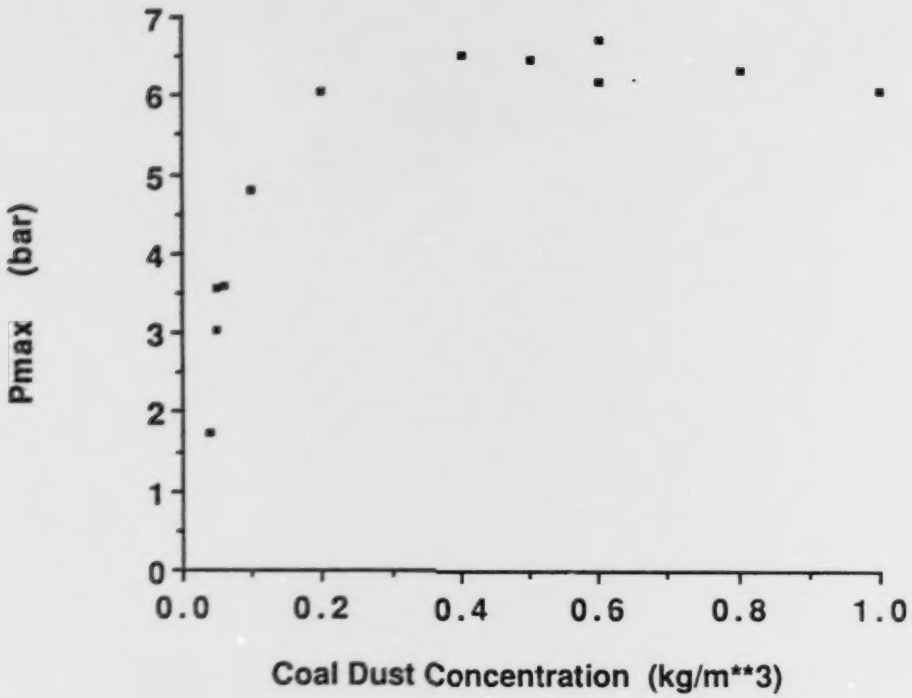

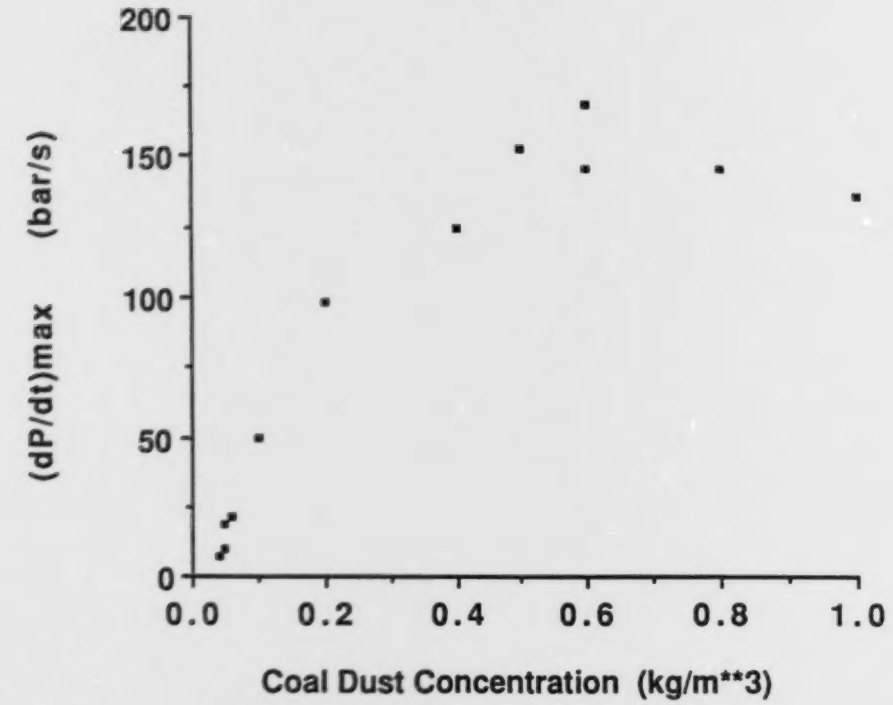

Fig. 3.9 P_{max} and $(dP/dt)_{max}$ at various coal dust concentrations (Lingan 1, 2% methane).

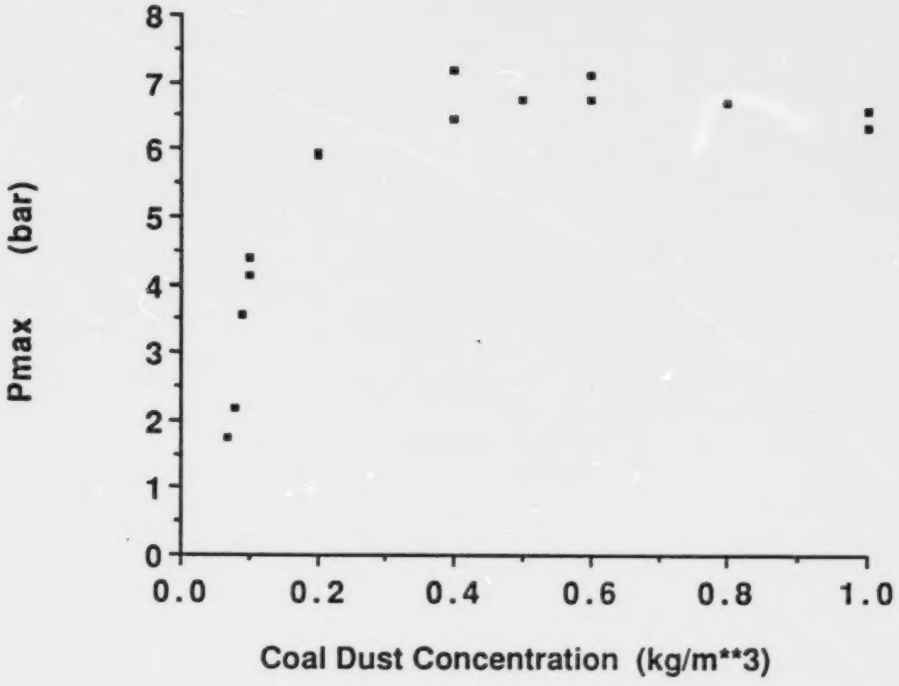

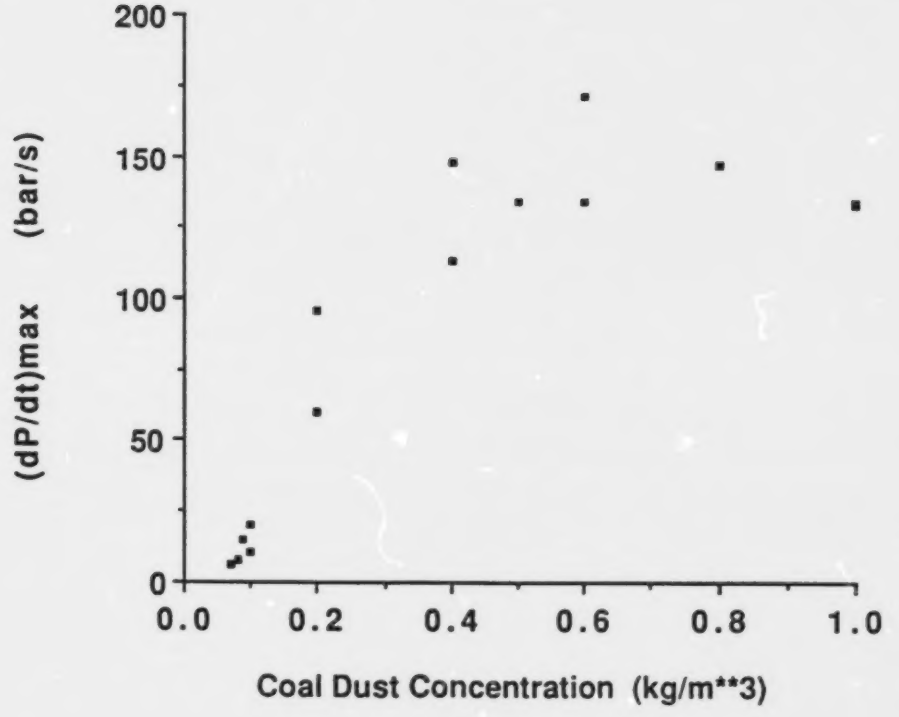

Fig. 3.10 P_{max} and $(dP/dt)_{max}$ at various coal dust concentrations (Lingan 2, 0% methane).

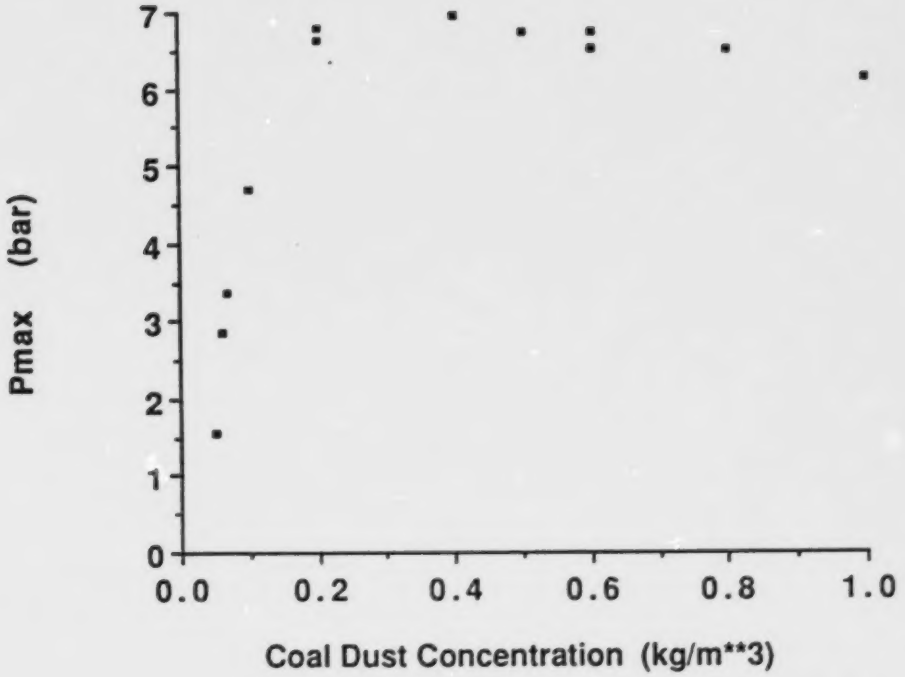

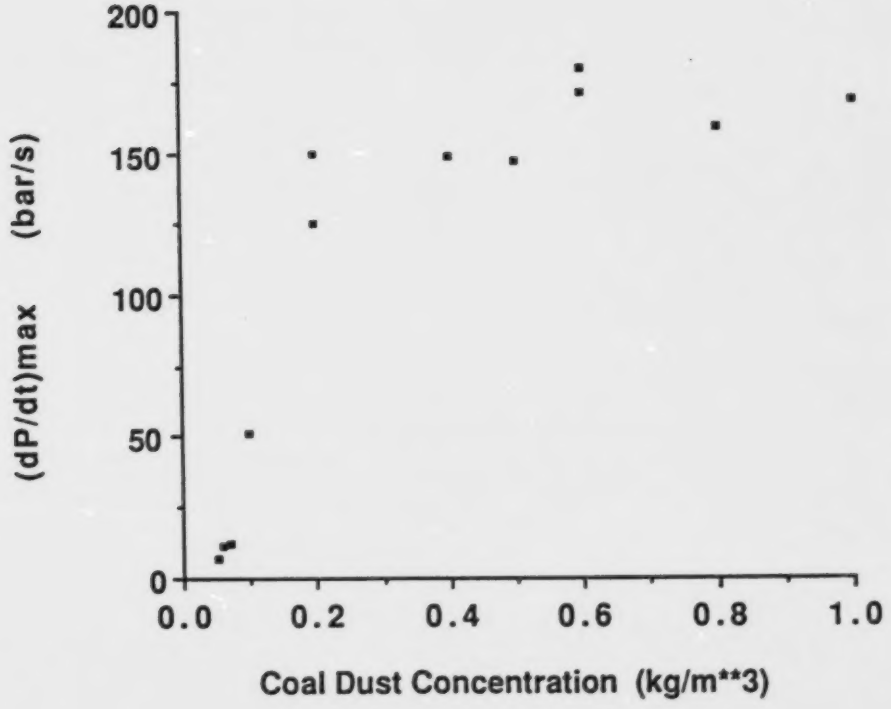

Fig. 3.11 P_{max} and $(dP/dt)_{max}$ at various coal dust concentrations (Lingan 2, 1% methane).

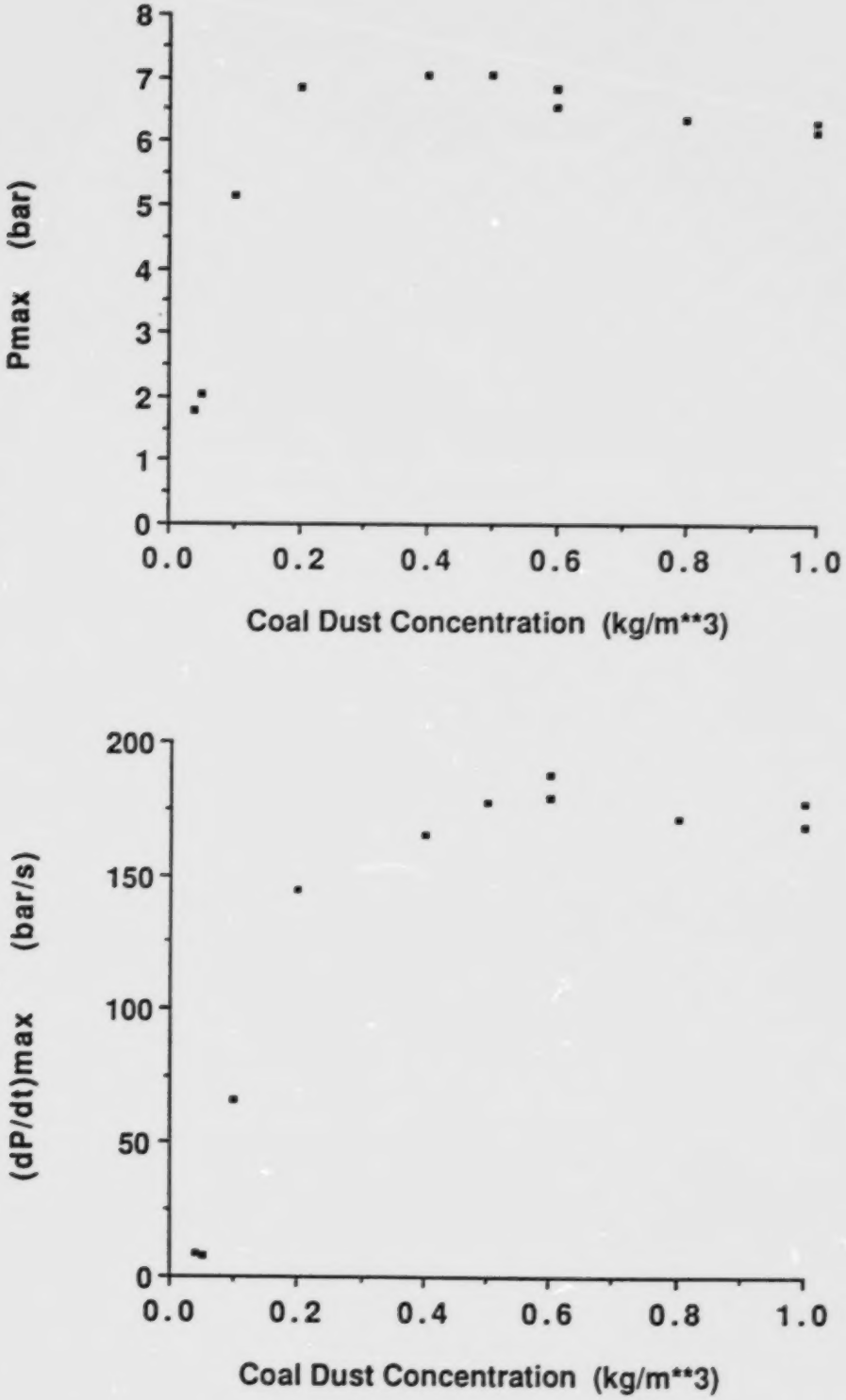

Fig. 3.12 P_{max} and $(dP/dt)_{max}$ at various coal dust concentrations (Lingan 2, 2% methane).

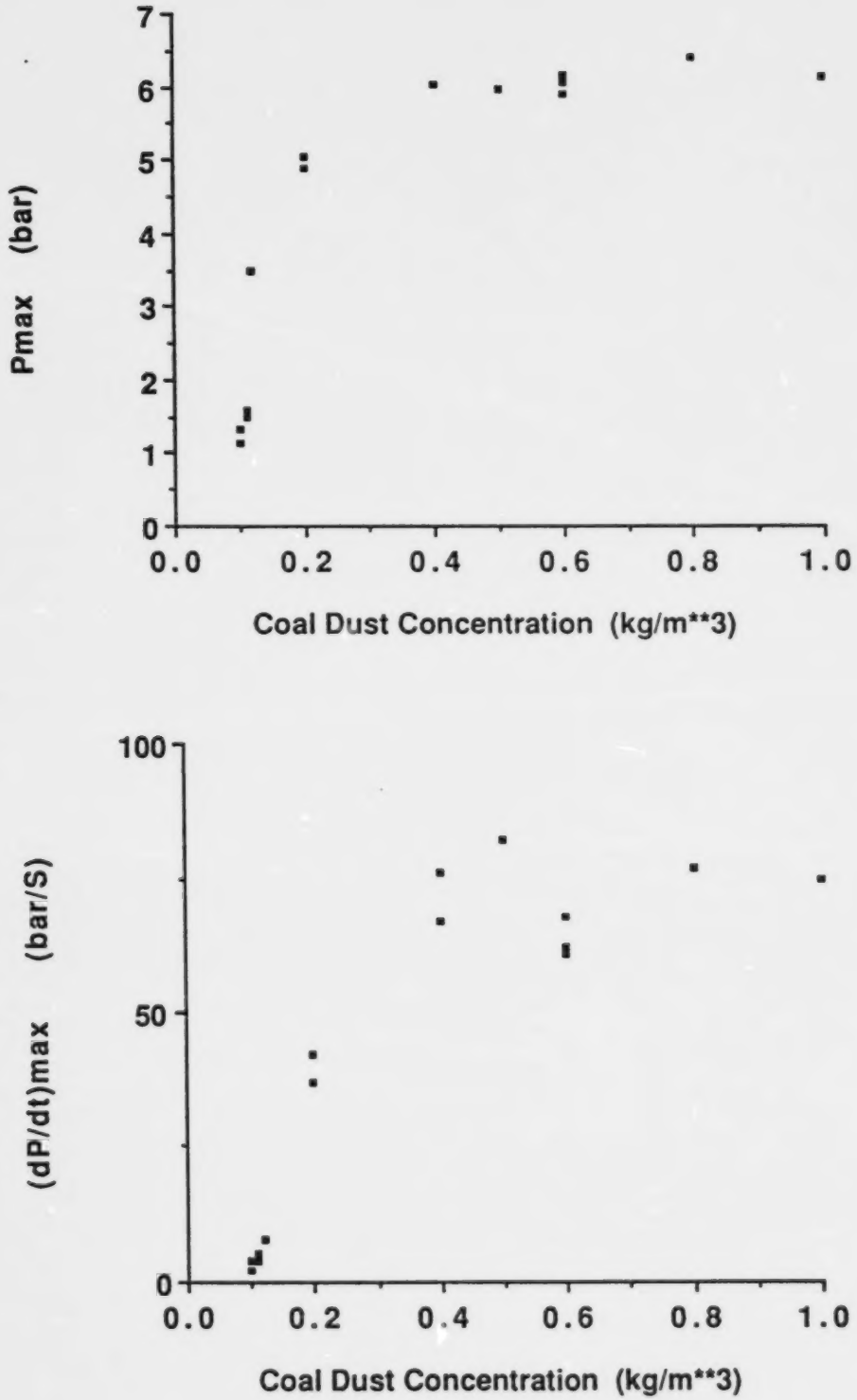

Fig. 3.13 P_{max} and $(dP/dt)_{max}$ at various coal dust concentrations (Phalen 1, 0% methane).

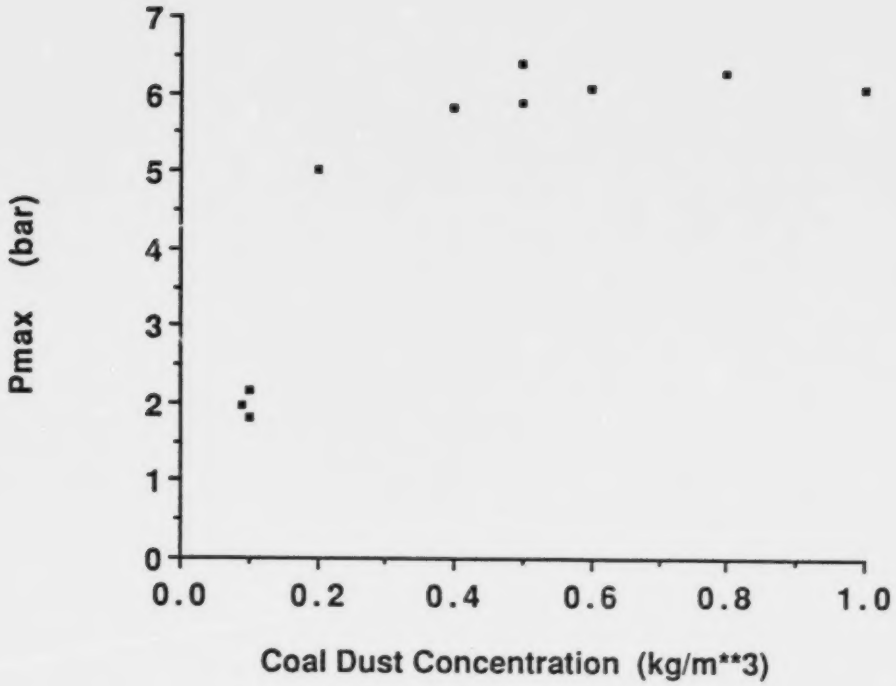

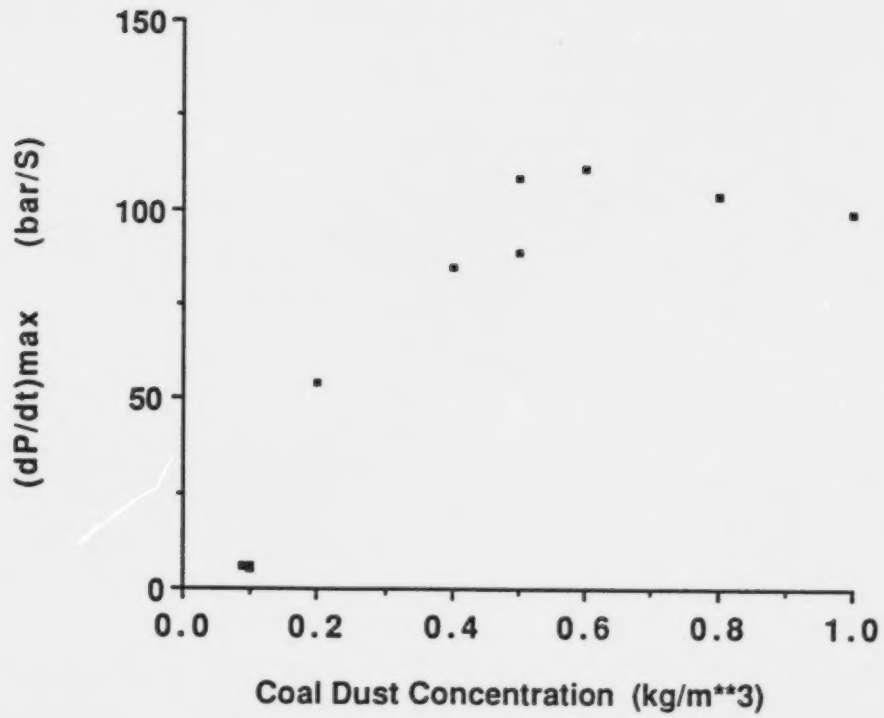

Fig. 3.14 P_{max} and $(dP/dt)_{max}$ at various coal dust concentrations (Phalen 1, 1% methane).

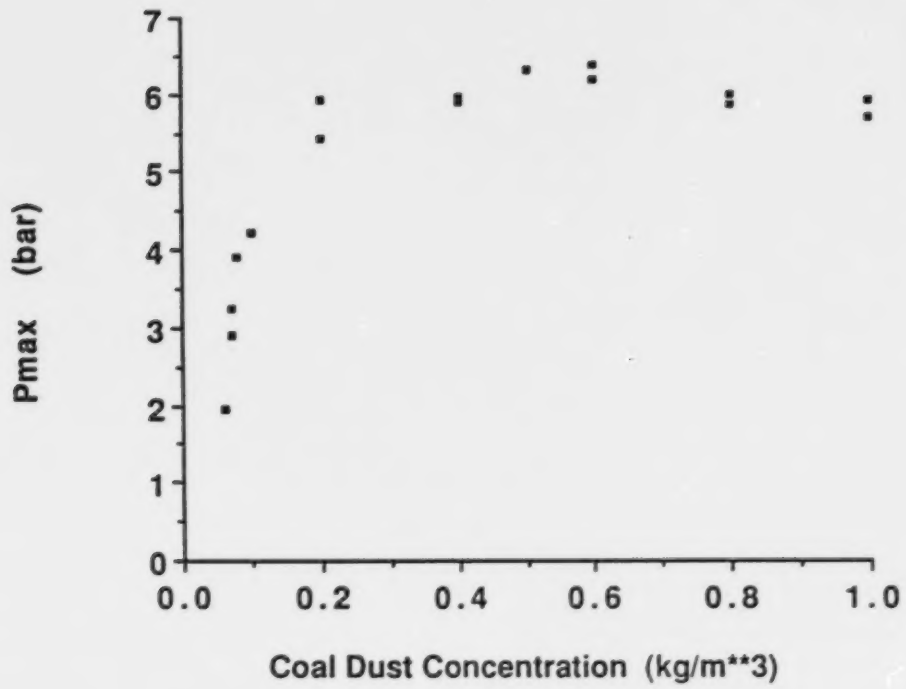

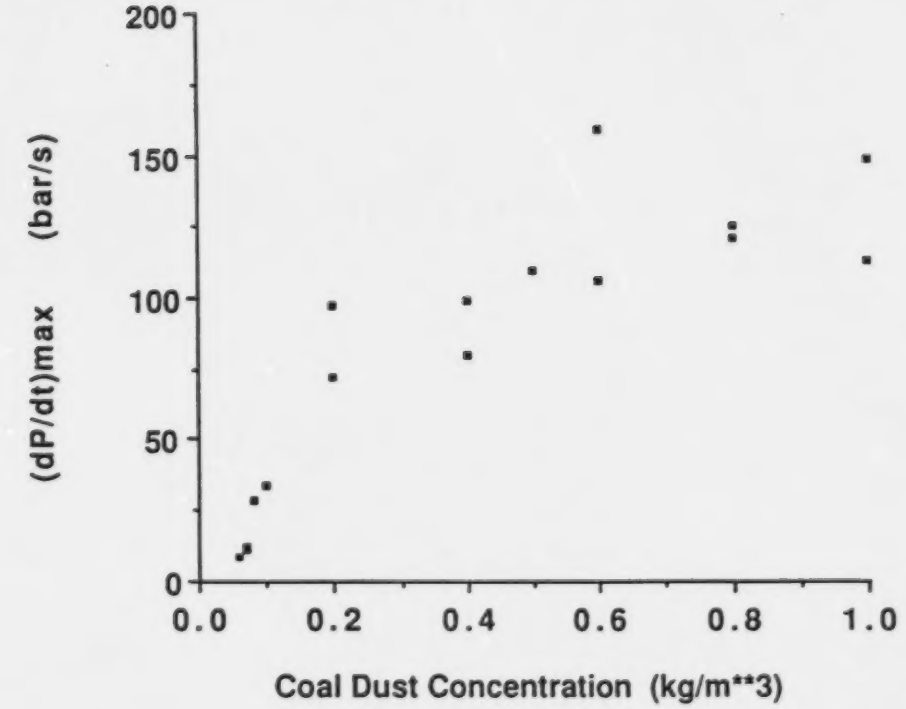

Fig. 3.15 P_{max} and $(dP/dt)_{max}$ at various coal dust concentrations (Phalen 1, 2% methane).

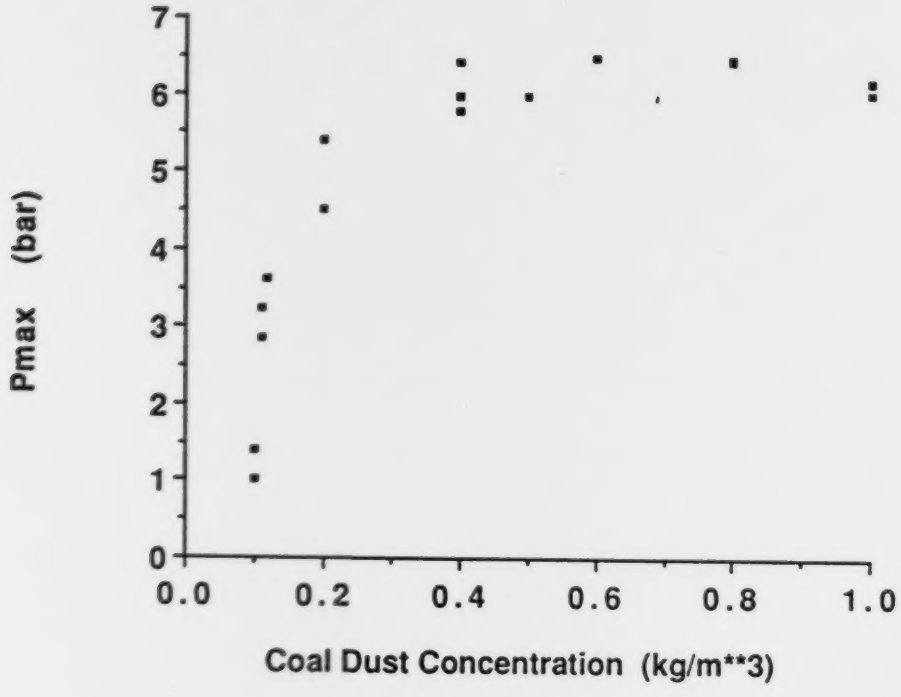

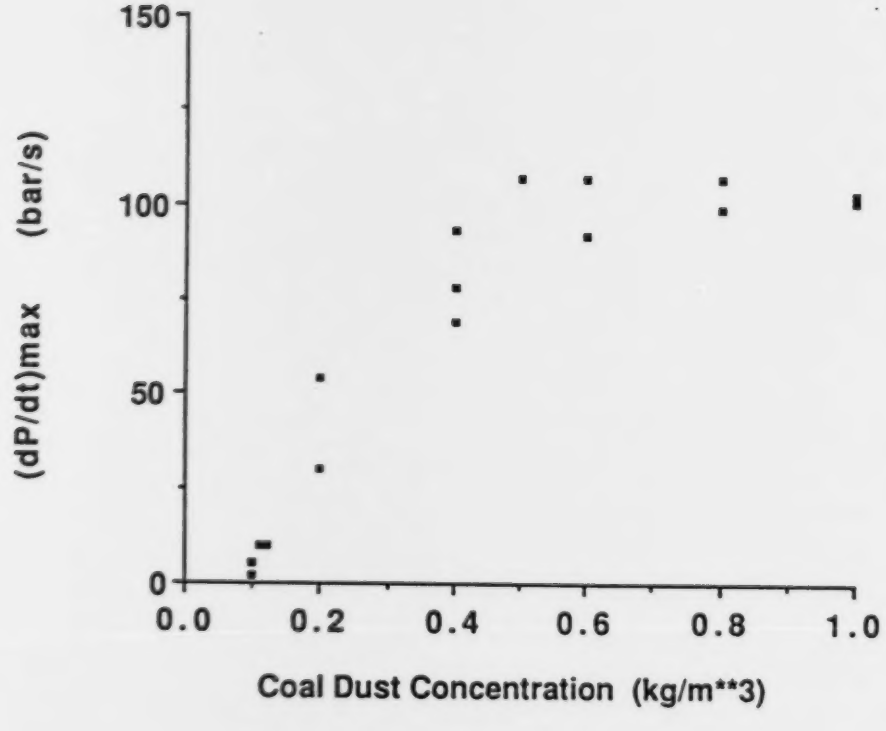

Fig. 3.16 P_{max} and $(dP/dt)_{max}$ at various coal dust concentrations (Phalen 2, 0% methane).

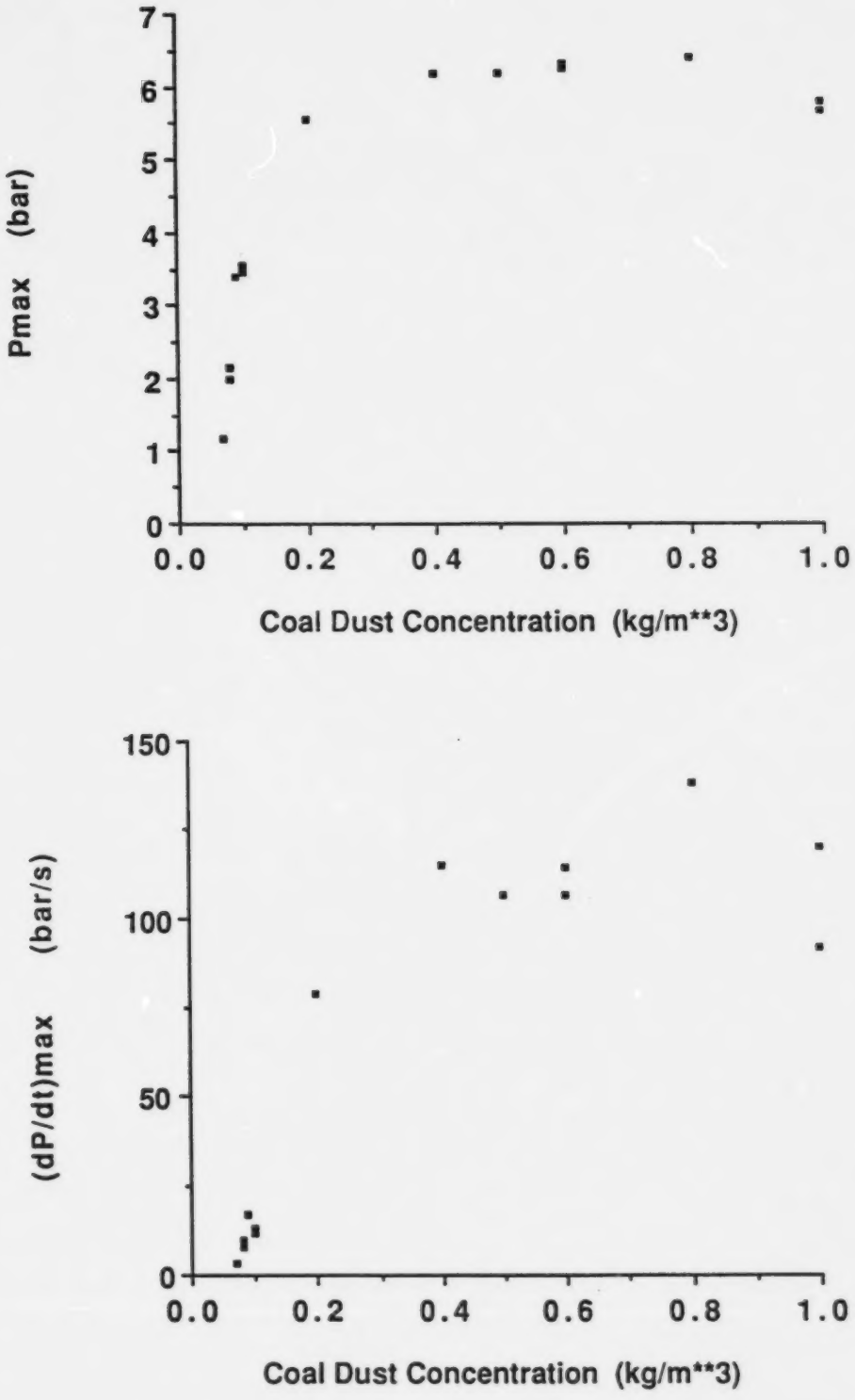

Fig. 3.17 P_{max} and $(dP/dt)_{max}$ at various coal dust concentrations (Phalen 2, 1% methane).

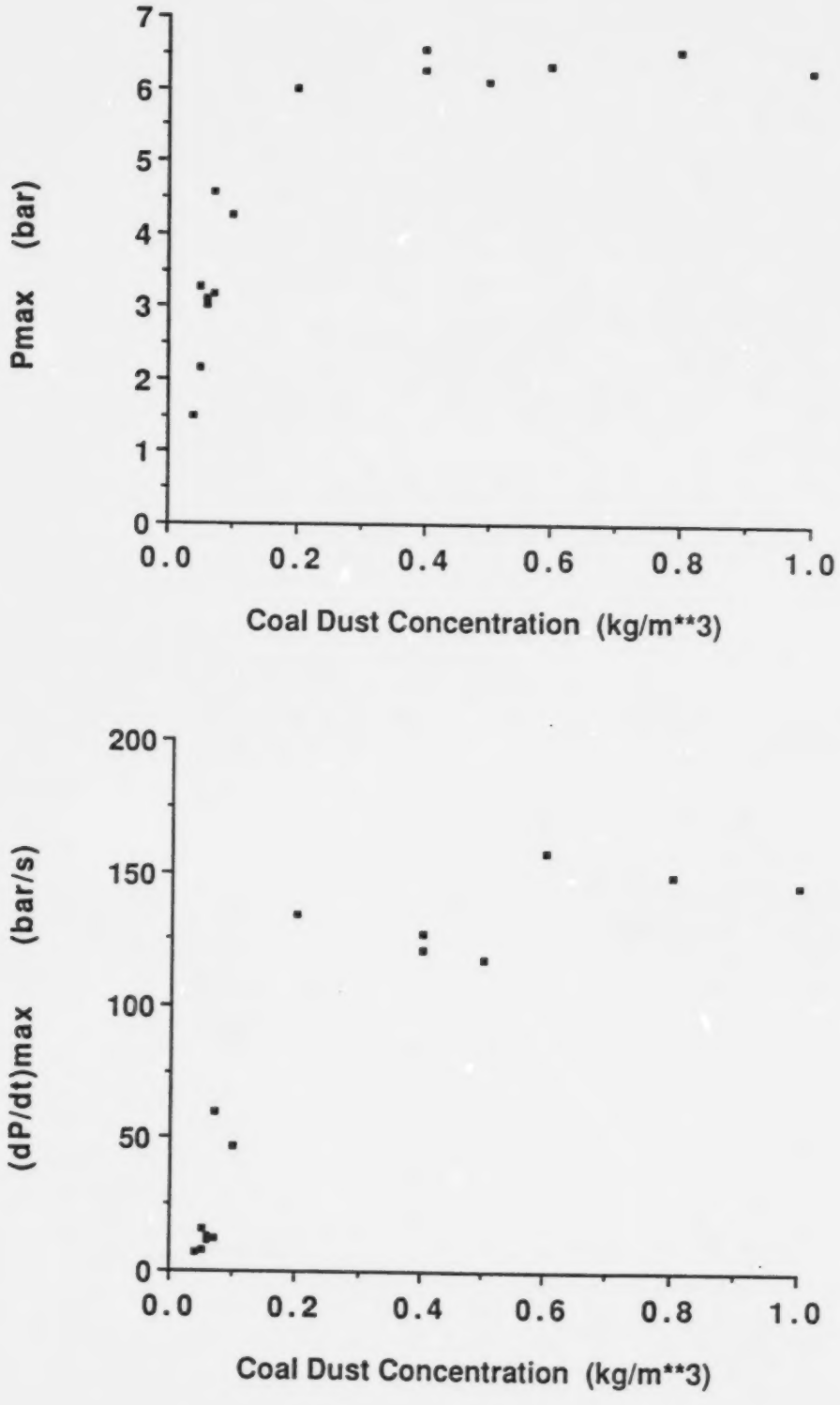

Fig. 3.18 P_{max} and $(dP/dt)_{max}$ at various coal dust concentrations (Phalen 2, 2% methane).

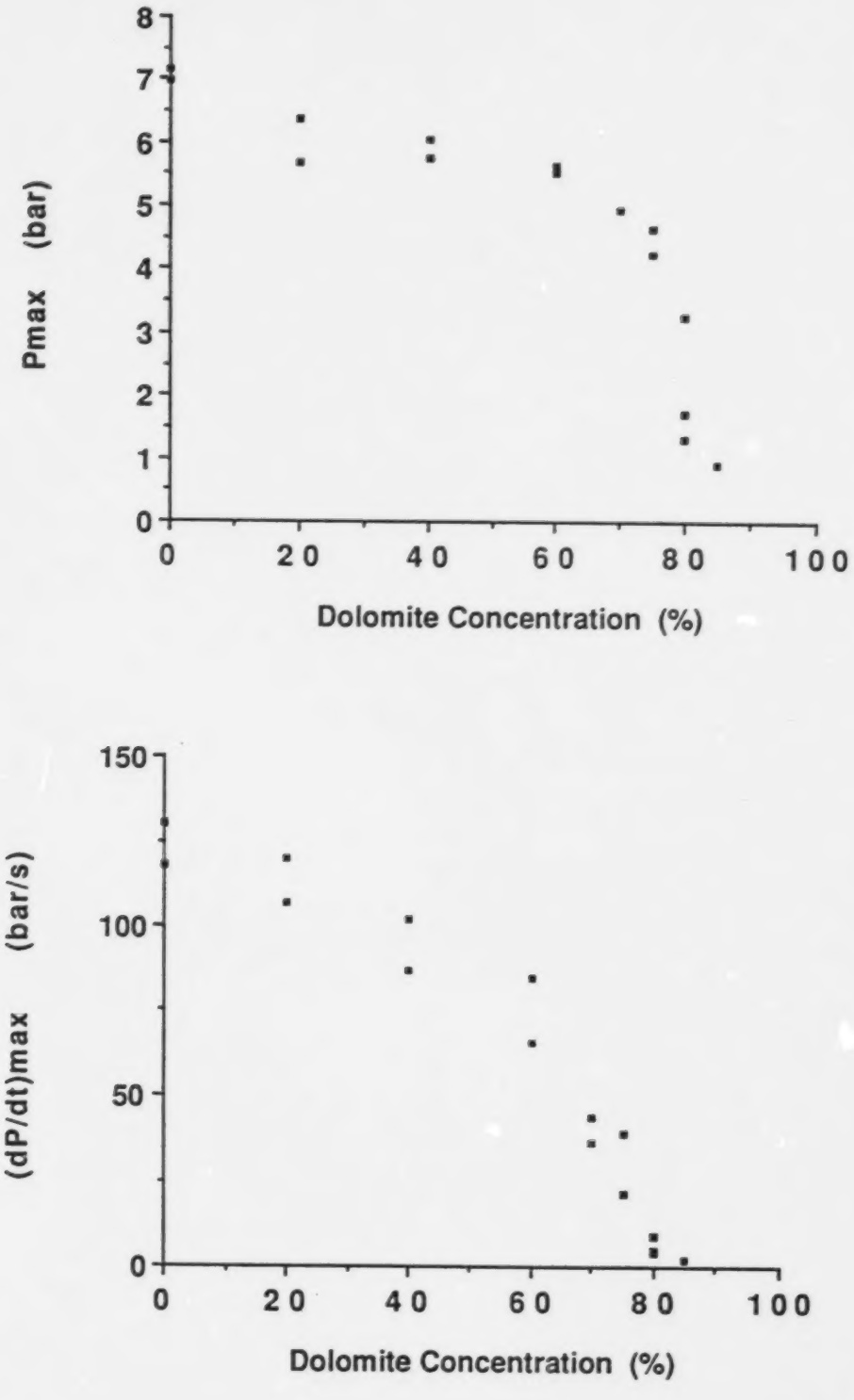

Fig. 3.19 P_{max} and $(dP/dt)_{max}$ at various dolomite concentrations (Prince 1, 0.5 kg/m^3 coal dust, 0% methane).

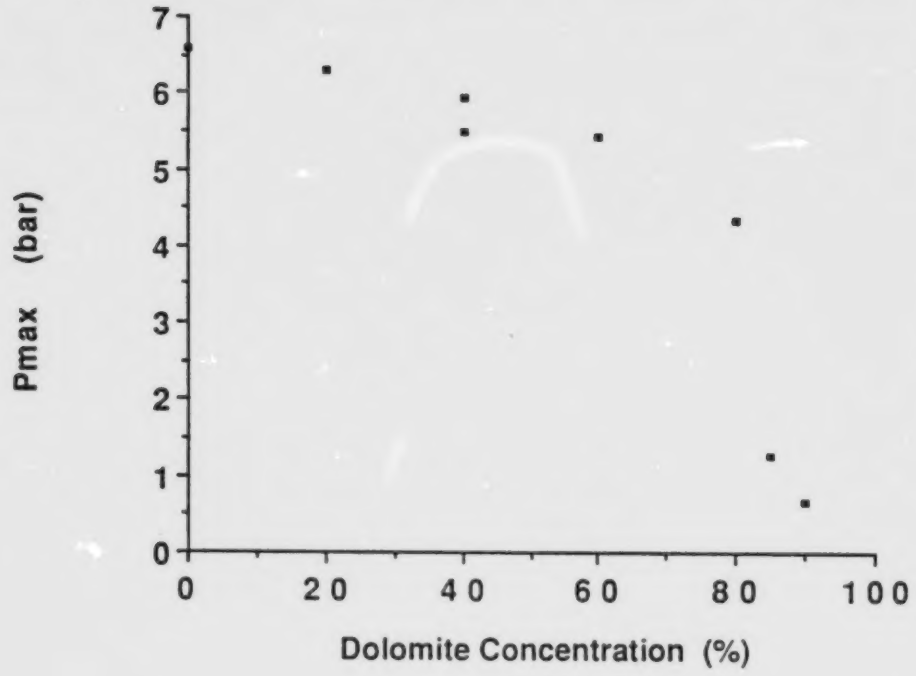

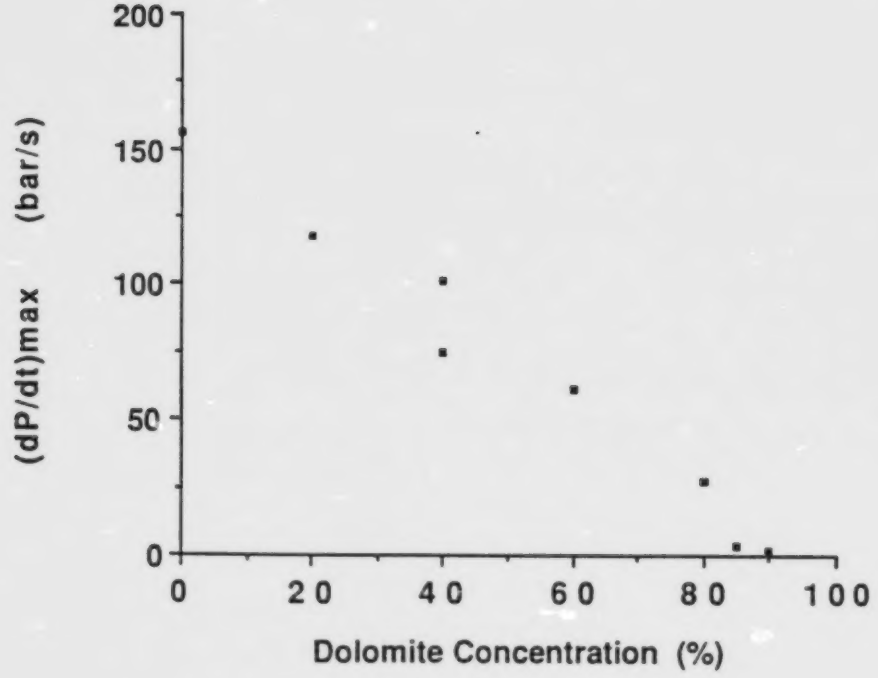

Fig. 3.20 P_{max} and $(dP/dt)_{max}$ at various dolomite concentrations (Prince 1, 0.5 kg/m^3 coal dust, 1% methane).

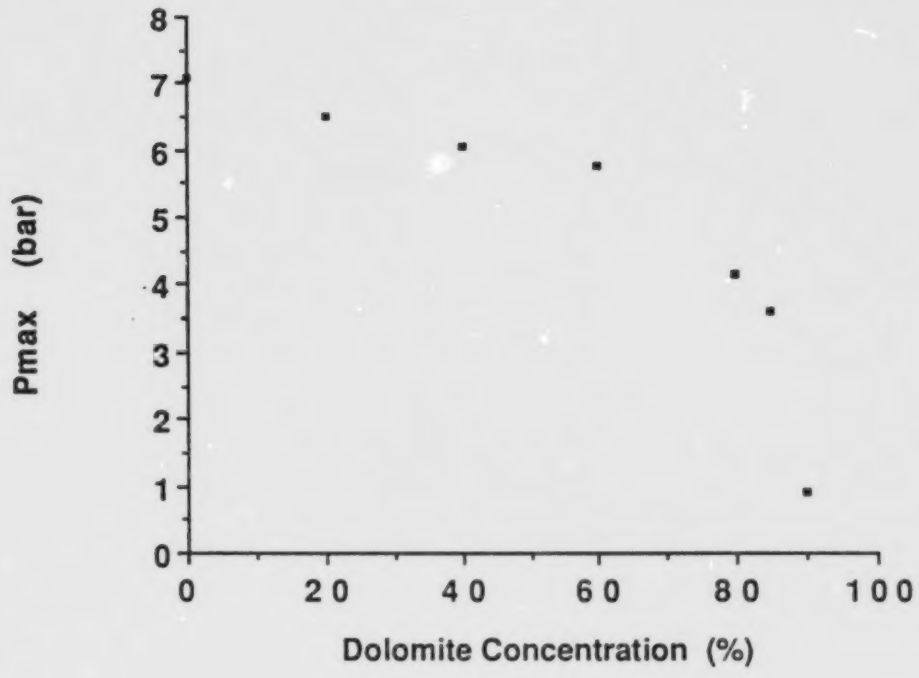

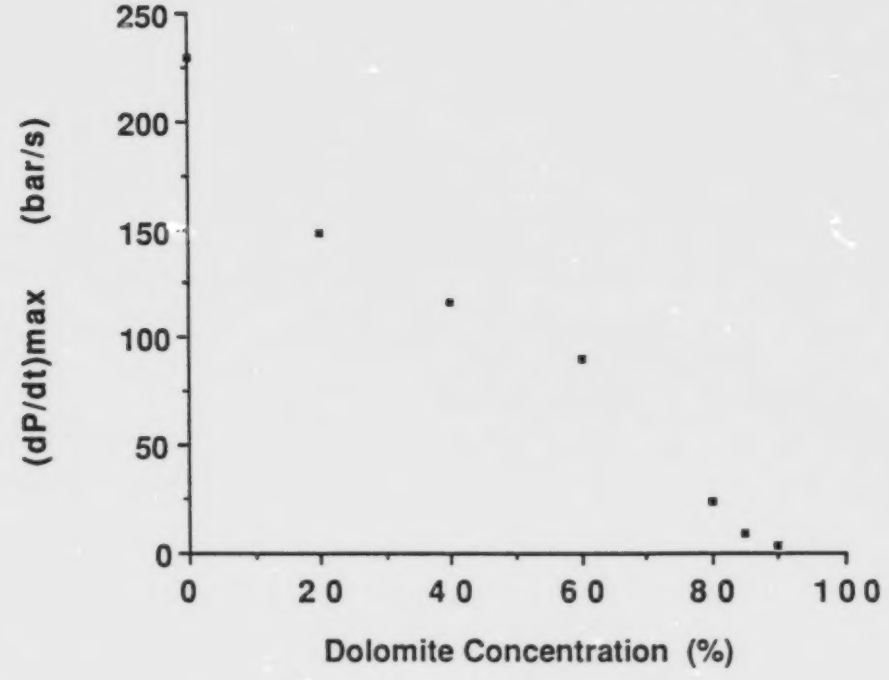

Fig. 3.21 P_{max} and $(dP/dt)_{max}$ at various dolomite concentrations (Prince 1, 0.5 kg/m^3 coal dust, 2% methane).

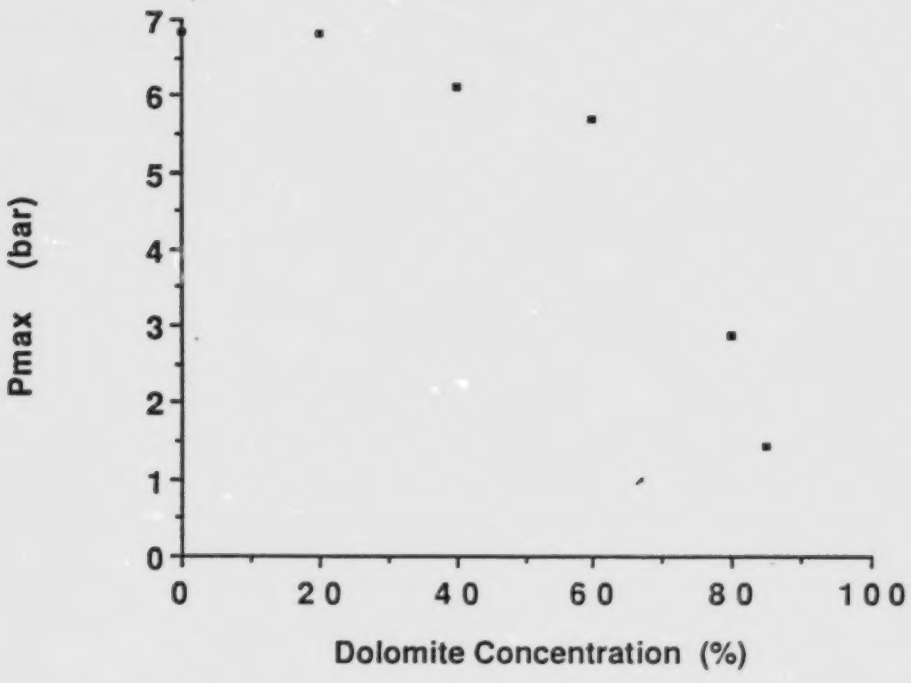

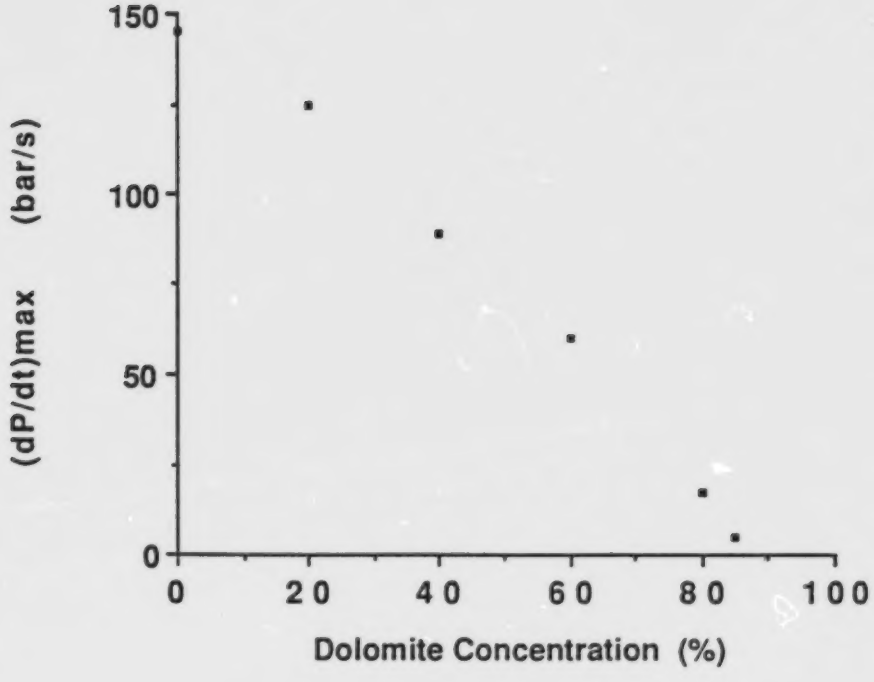

Fig. 3.22 P_{max} and $(dP/dt)_{max}$ at various dolomite concentrations (Prince 2, 0.5 kg/m^3 coal dust, 0% methane).

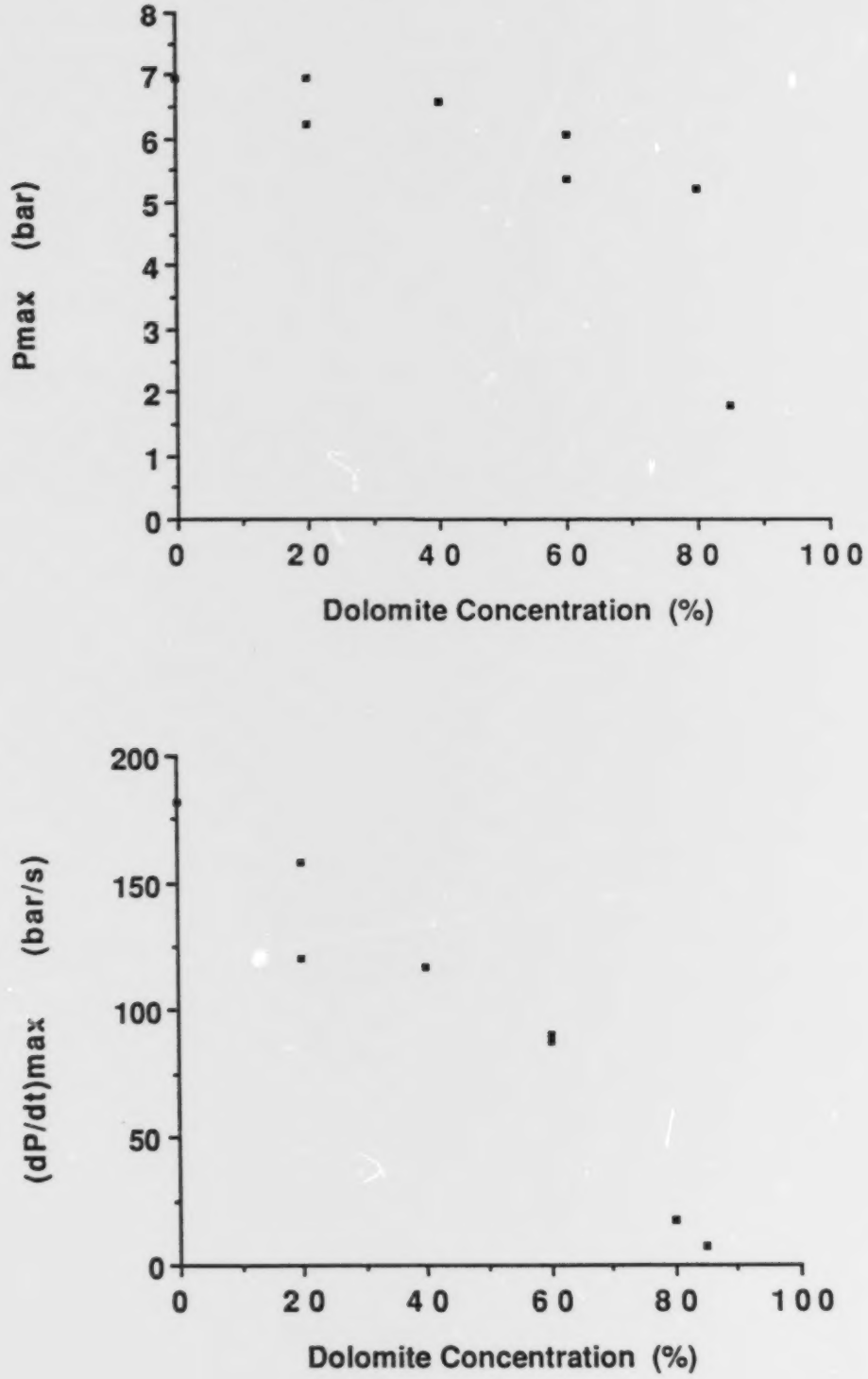

Fig. 3.23 P_{max} and $(dP/dt)_{max}$ at various dolomite concentrations (Prince 2, 0.5 kg/m^3 coal dust, 1% methane).

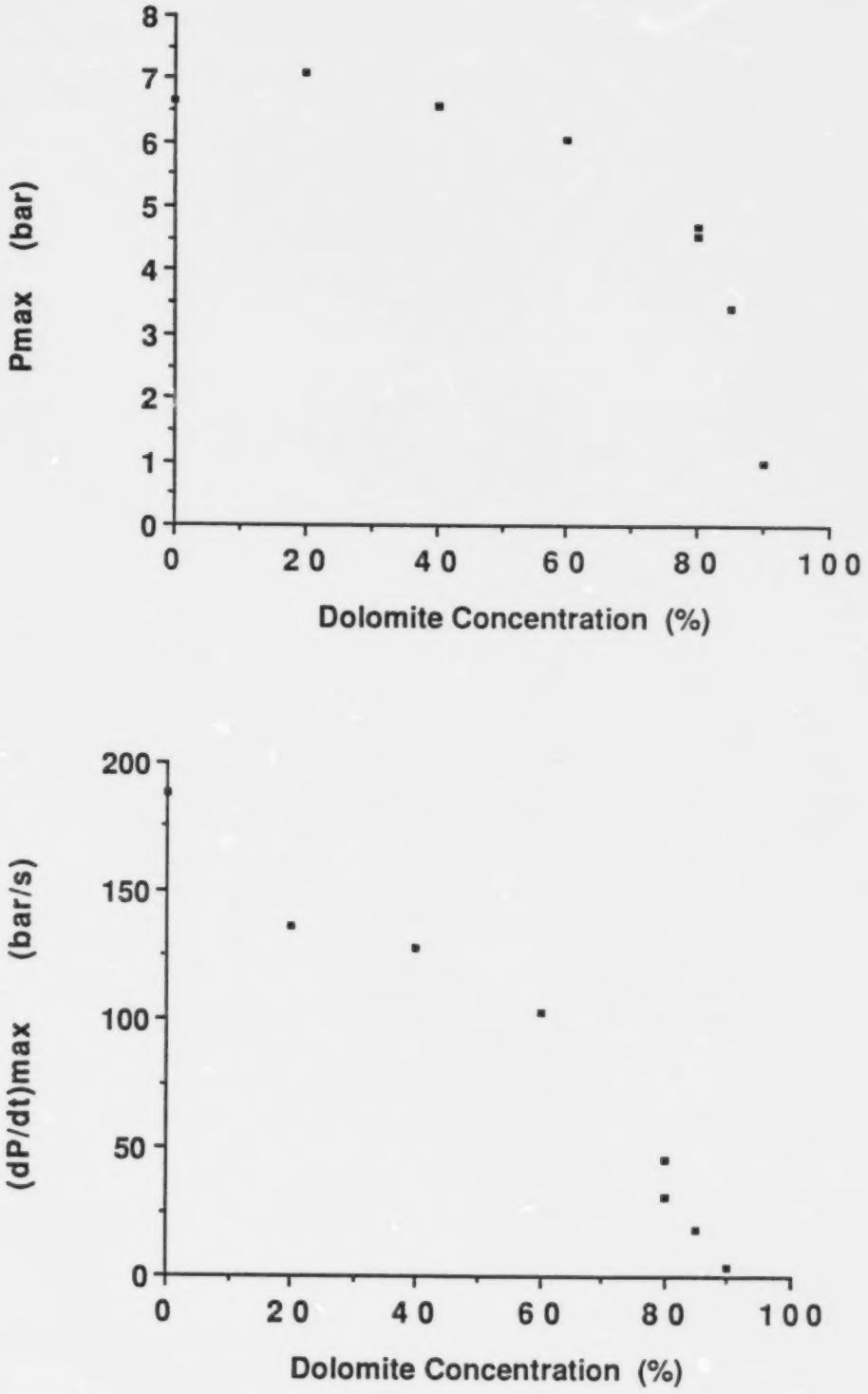

Fig. 3.24 P_{max} and $(dP/dt)_{max}$ at various dolomite concentrations (Prince 2, 0.5 kg/m^3 coal dust, 2% methane).

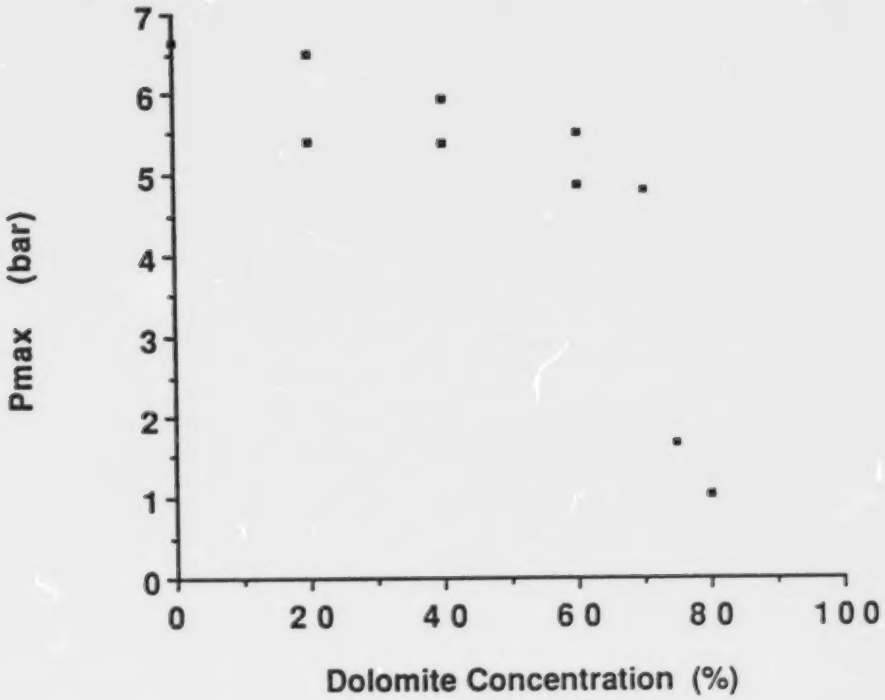

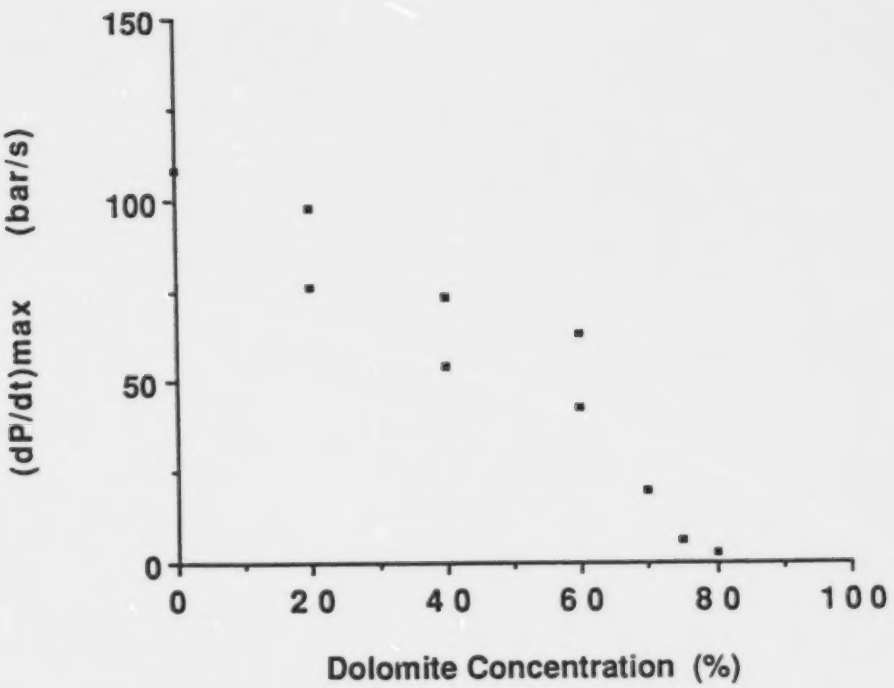

Fig. 3.25 P_{max} and $(dP/dt)_{max}$ at various dolomite concentrations (Lingan 1, 0.5 kg/m^3 coal dust, 0% methane).

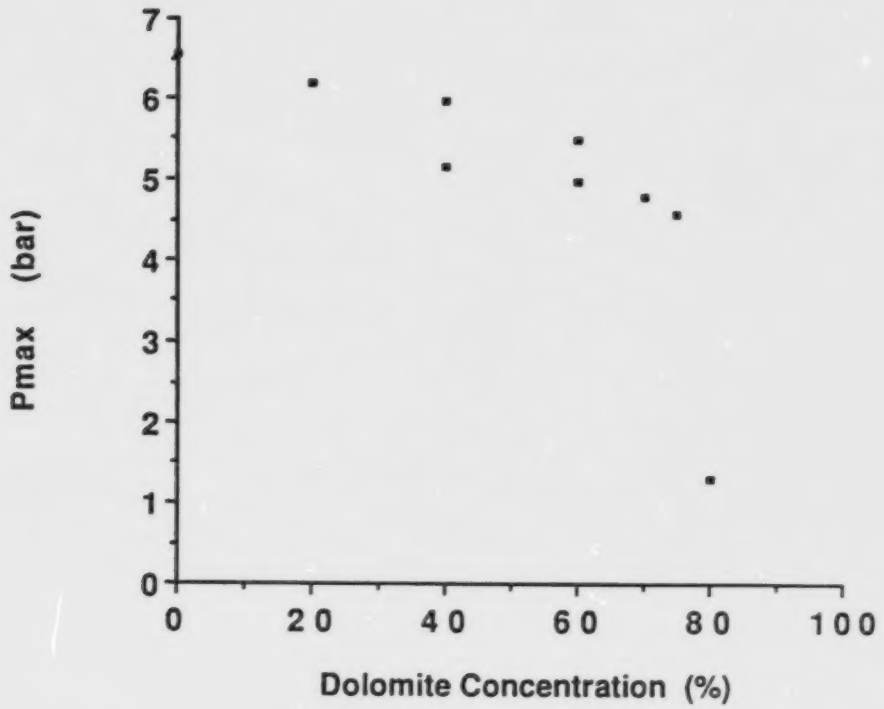

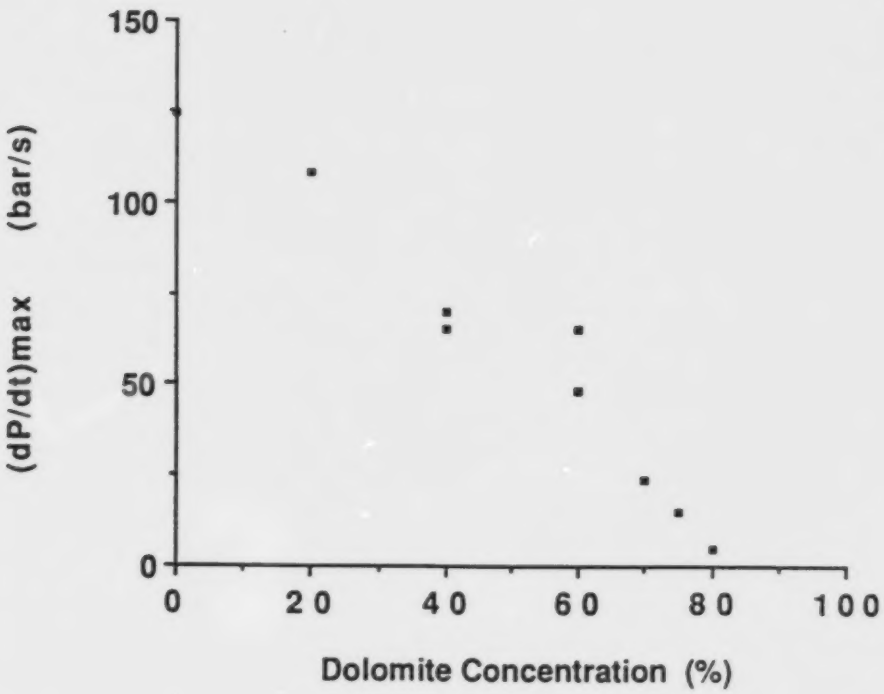

Fig. 3.26 P_{max} and $(dP/dt)_{max}$ at various dolomite concentrations (Lingan 1, 0.5 kg/m^3 coal dust, 1% methane).

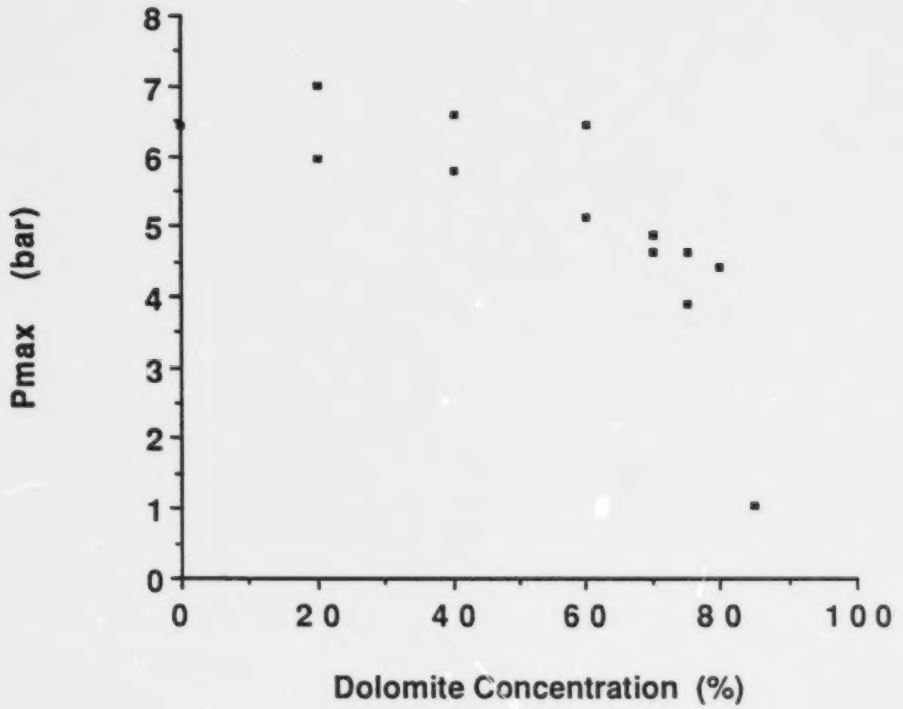

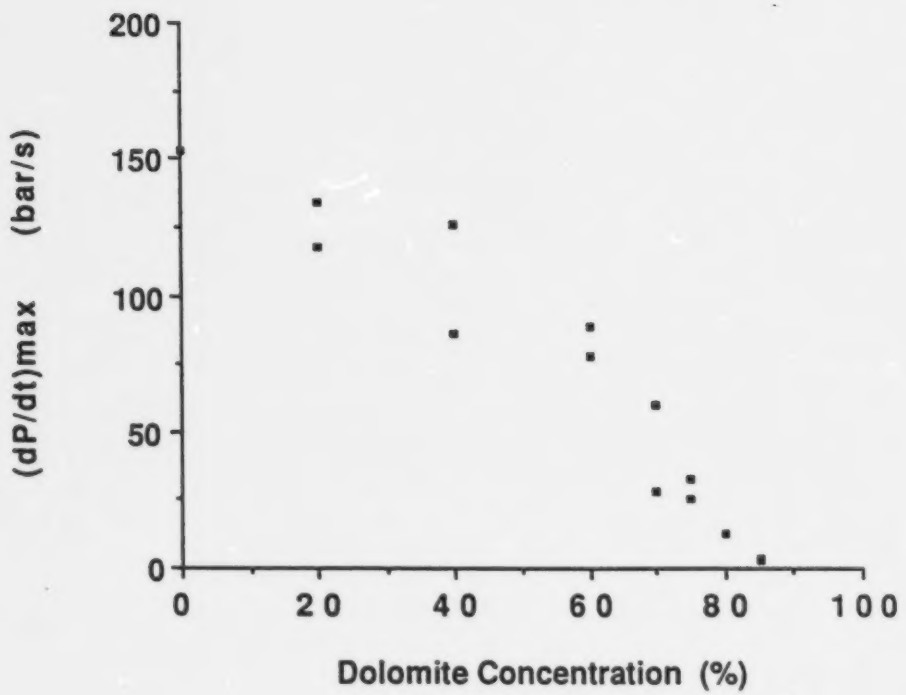

Fig. 3.27 P_{max} and $(dP/dt)_{max}$ at various dolomite concentrations (Lingan 1, 0.5 kg/m^3 coal dust, 2% methane).

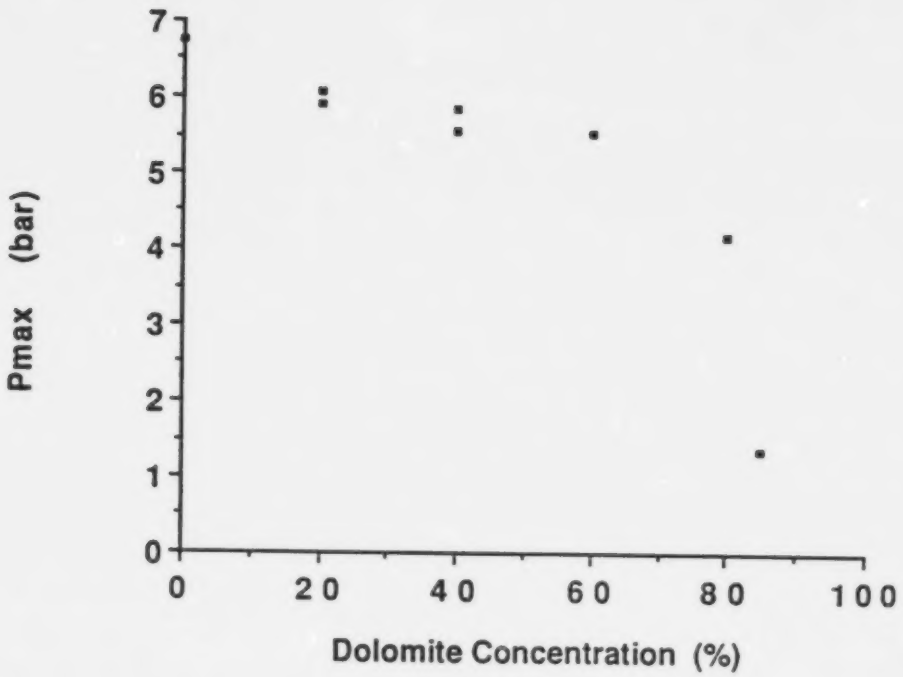

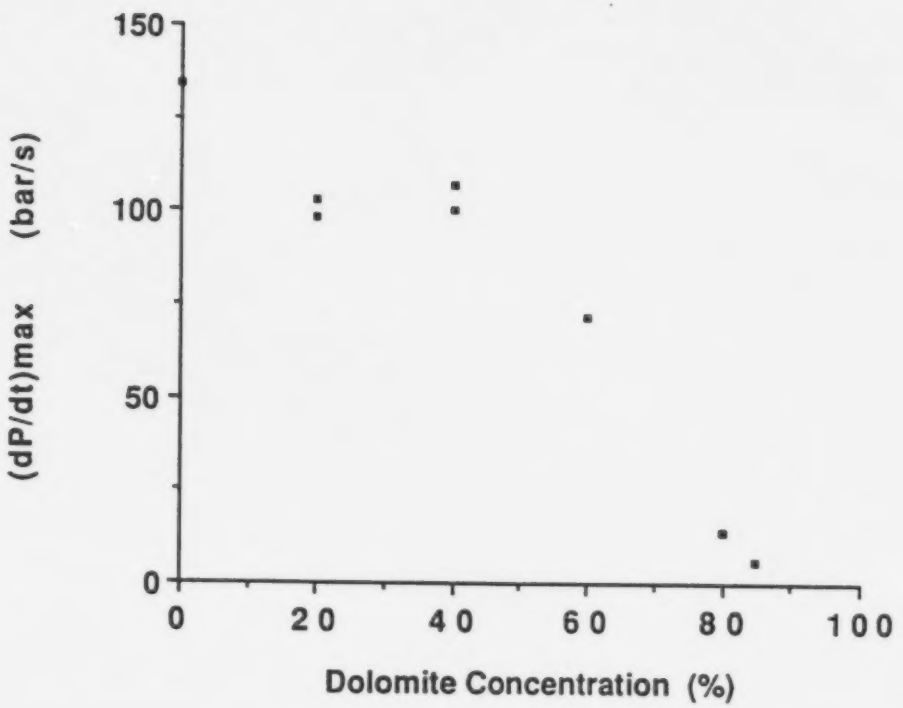

Fig. 3.28 P_{max} and $(dP/dt)_{max}$ at various dolomite concentrations (Lingan 2, 0.5 kg/m^3 coal dust, 0% methane).

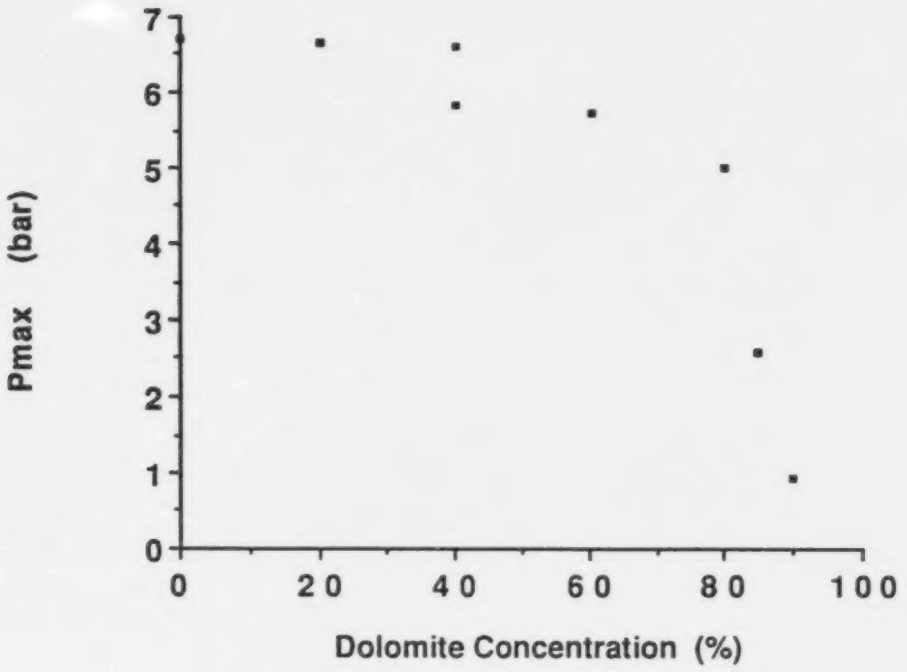

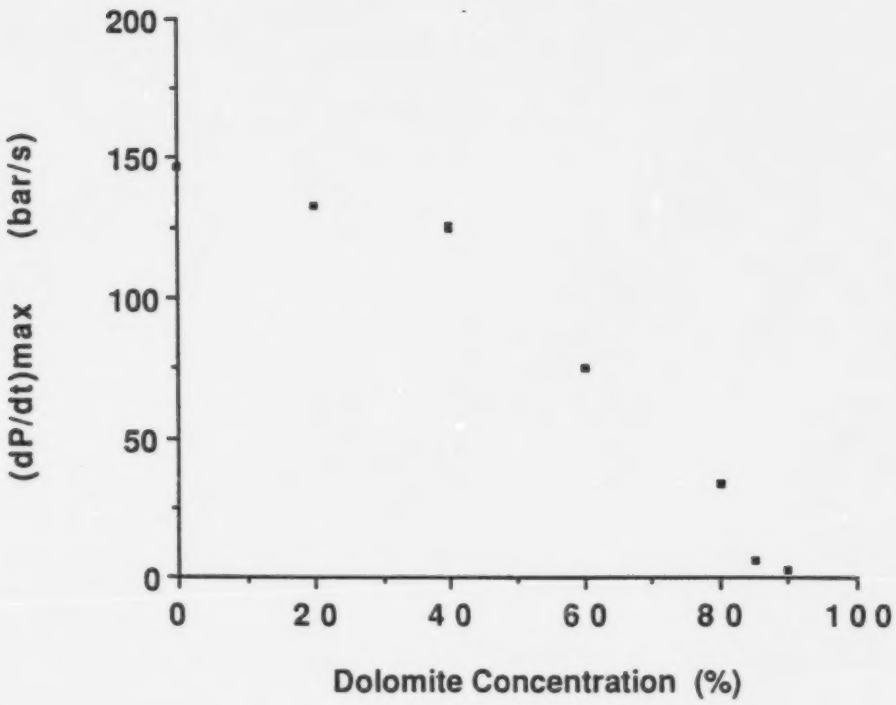

Fig. 3.29 P_{max} and $(dP/dt)_{max}$ at various dolomite concentrations (Lingan 2, 0.5 kg/m^3 coal dust, 1% methane).

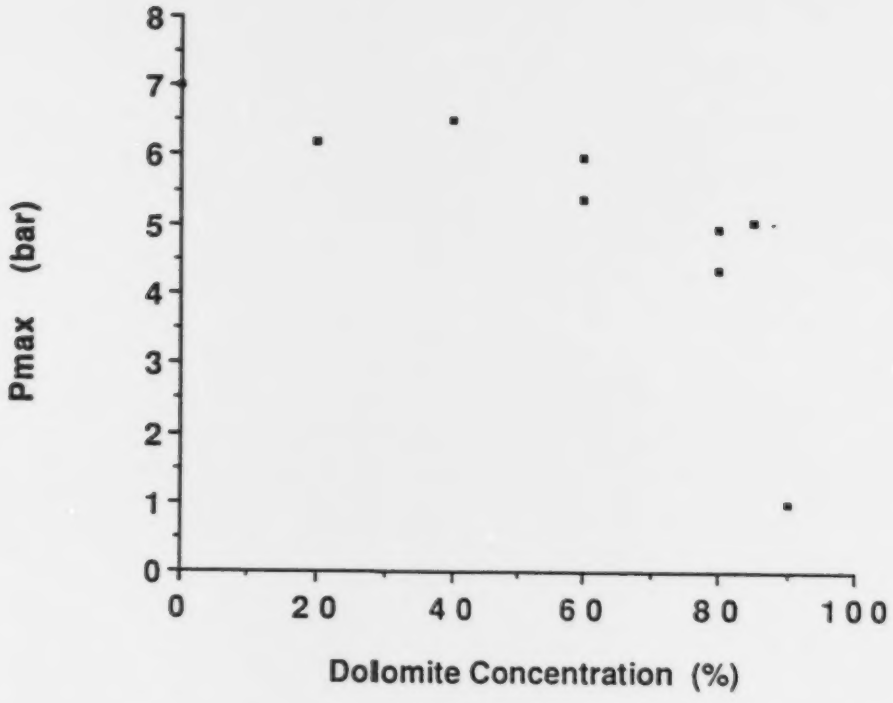

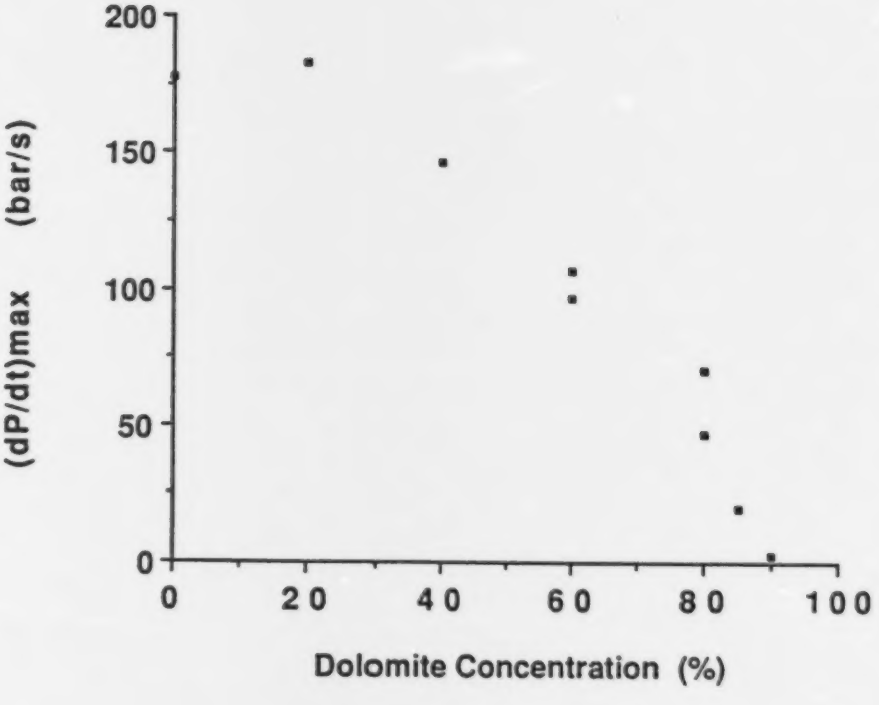

Fig. 3.30 P_{max} and $(dP/dt)_{max}$ at various dolomite concentrations (Lingan 2, 0.5 kg/m^3 coal dust, 2% methane).

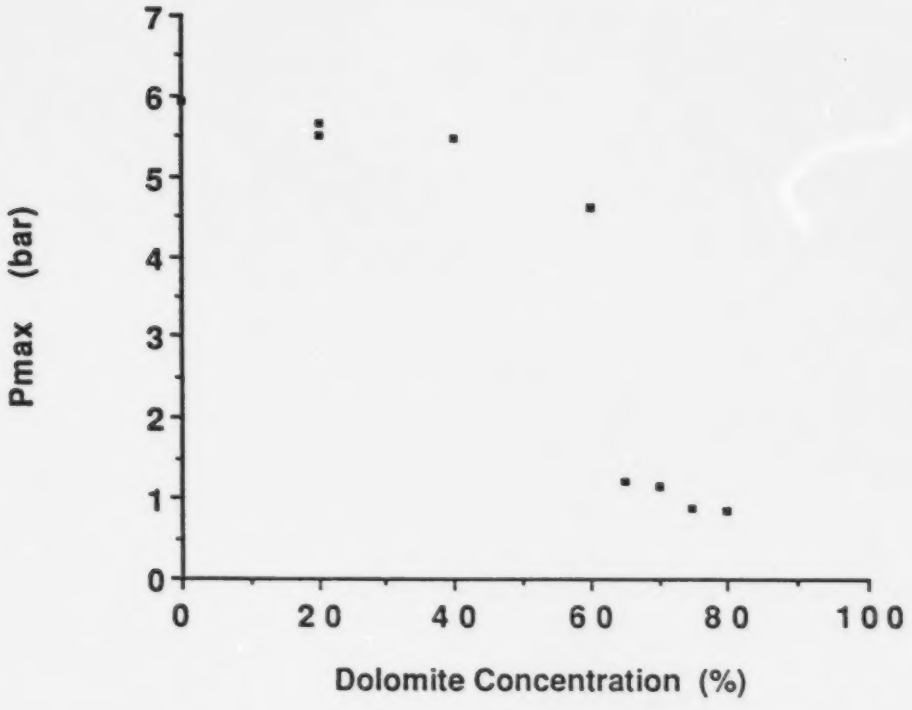

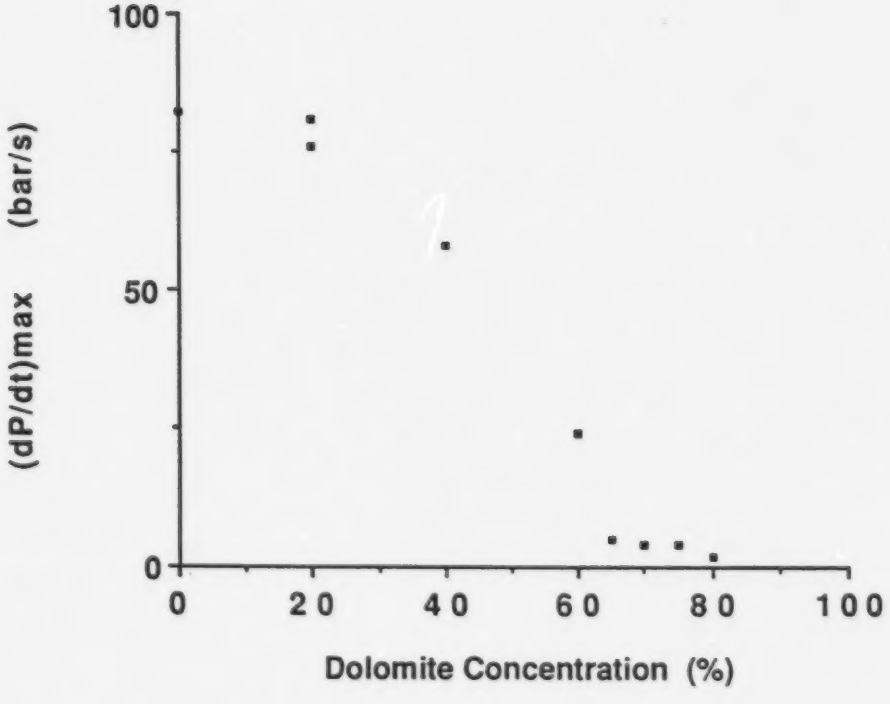

Fig. 3.31 P_{max} and $(dP/dt)_{max}$ at various dolomite concentrations (Phalen 1, 0.5 kg/m^3 coal dust, 0% methane).

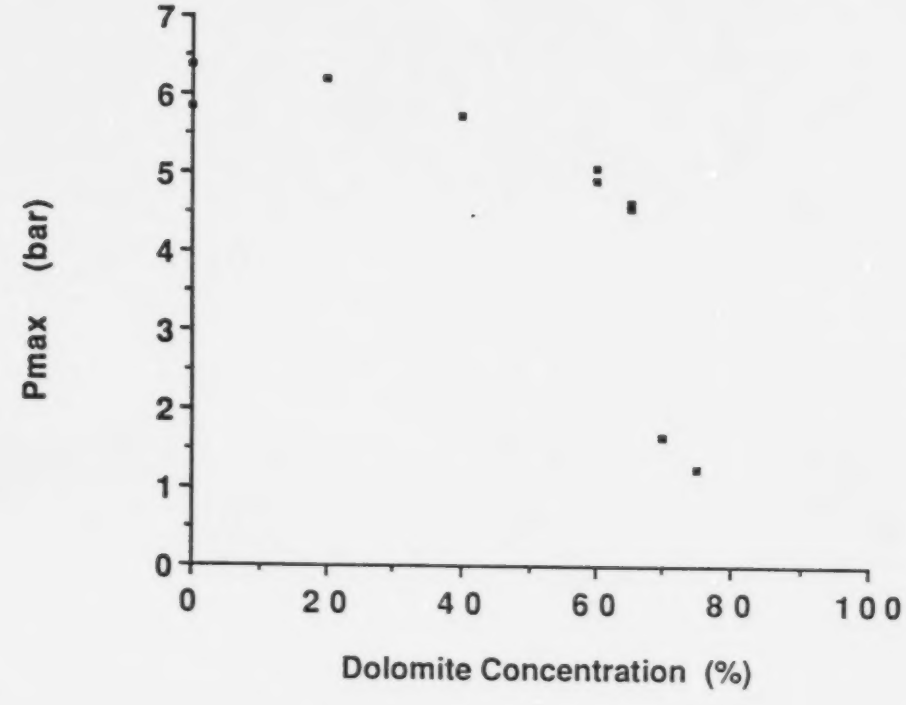

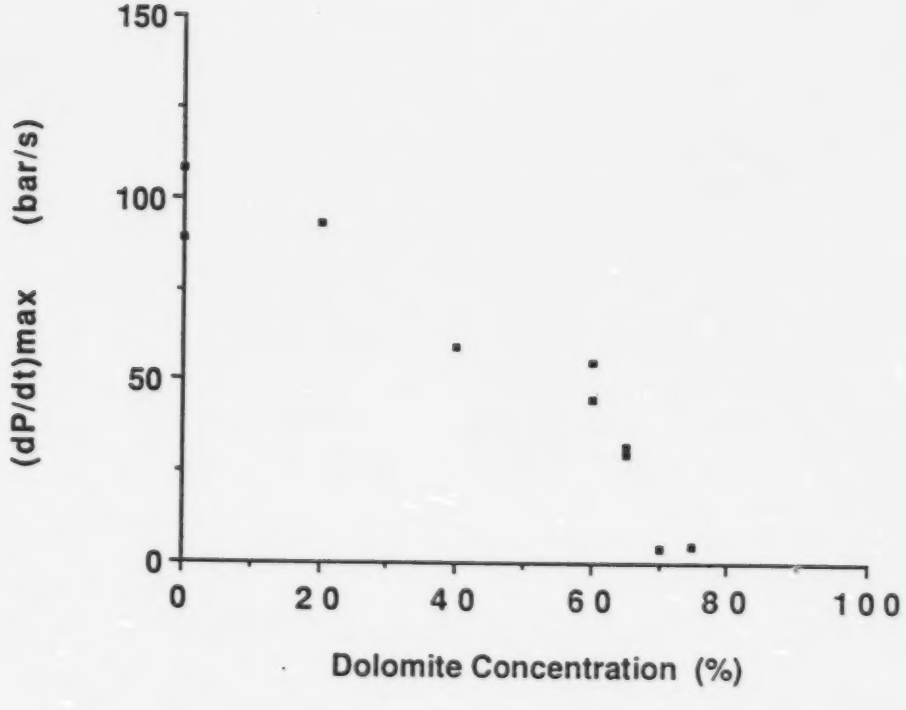

Fig. 3.32 P_{max} and $(dP/dt)_{max}$ at various dolomite concentrations (Phalen 1, 0.5 kg/m^3 coal dust, 1% methane).

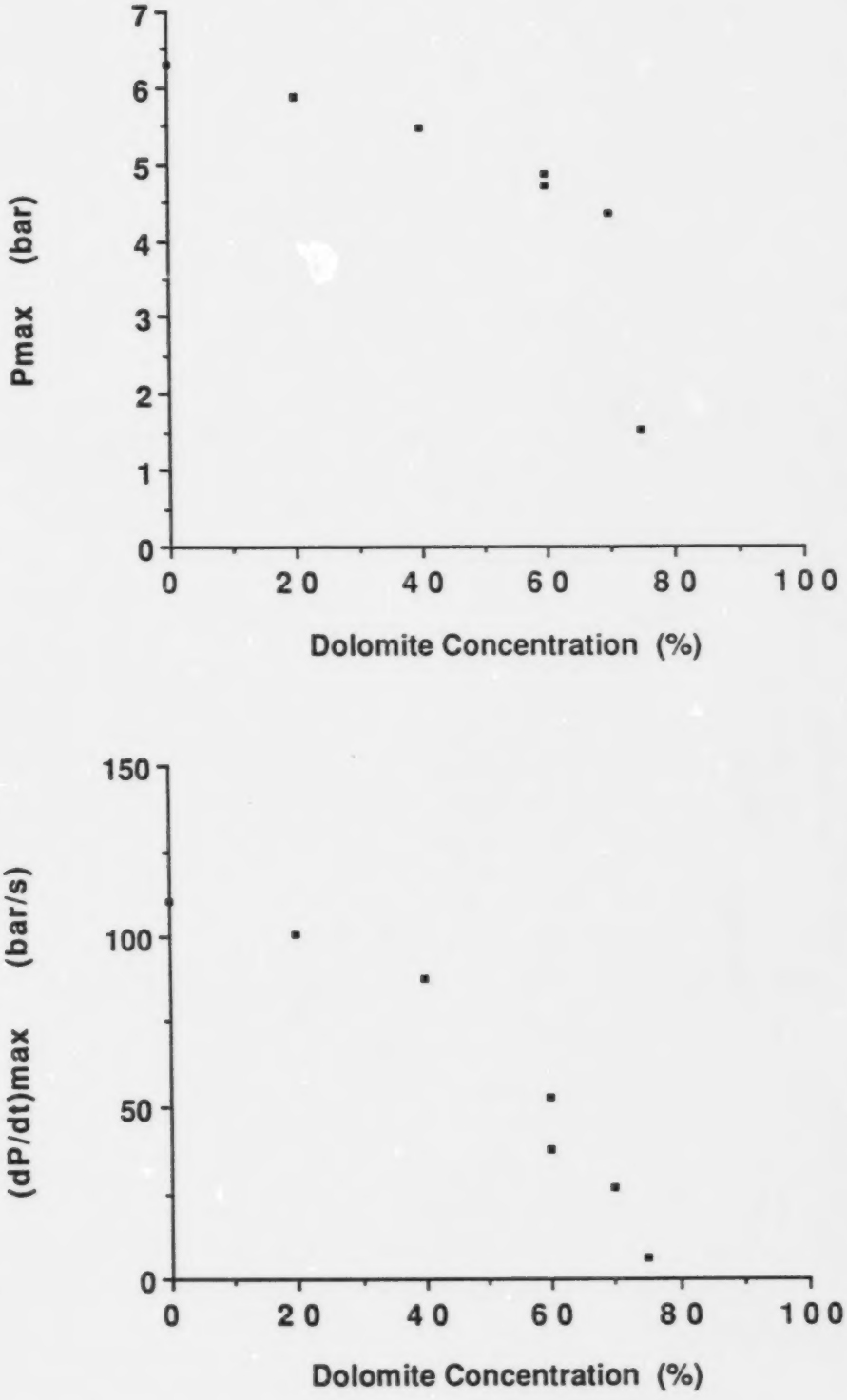

Fig. 3.33 P_{max} and $(dP/dt)_{max}$ at various dolomite concentrations (Phalen 1, 0.5 kg/m^3 coal dust, 2% methane).

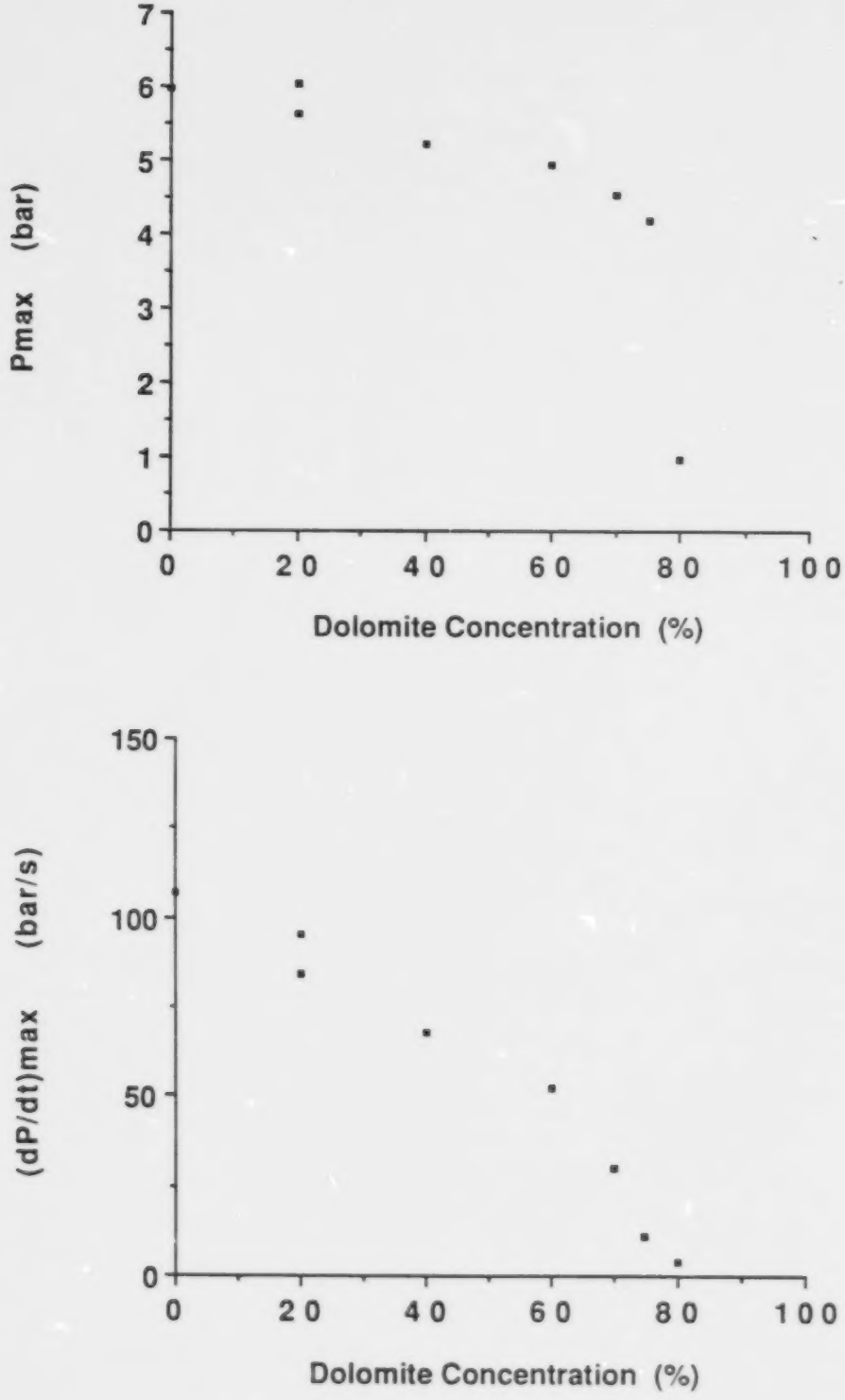

Fig. 3.34 P_{max} and $(dP/dt)_{max}$ at various dolomite concentrations (Phalen 2, 0.5 kg/m^3 coal dust, 0% methane).

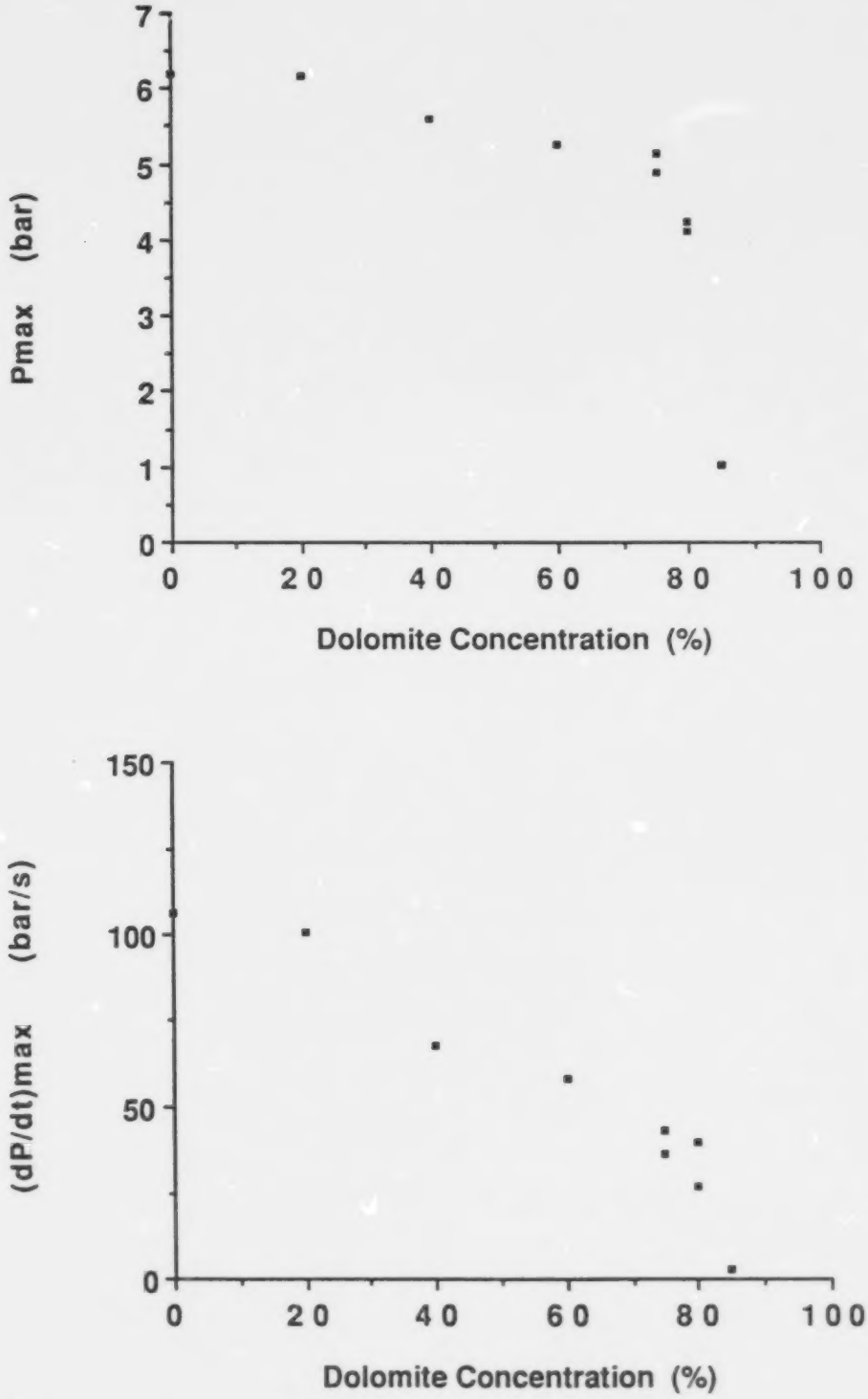

Fig. 3.35 P_{max} and $(dP/dt)_{max}$ at various dolomite concentrations (Phalen 2, 0.5 kg/m^3 coal dust, 1% methane).

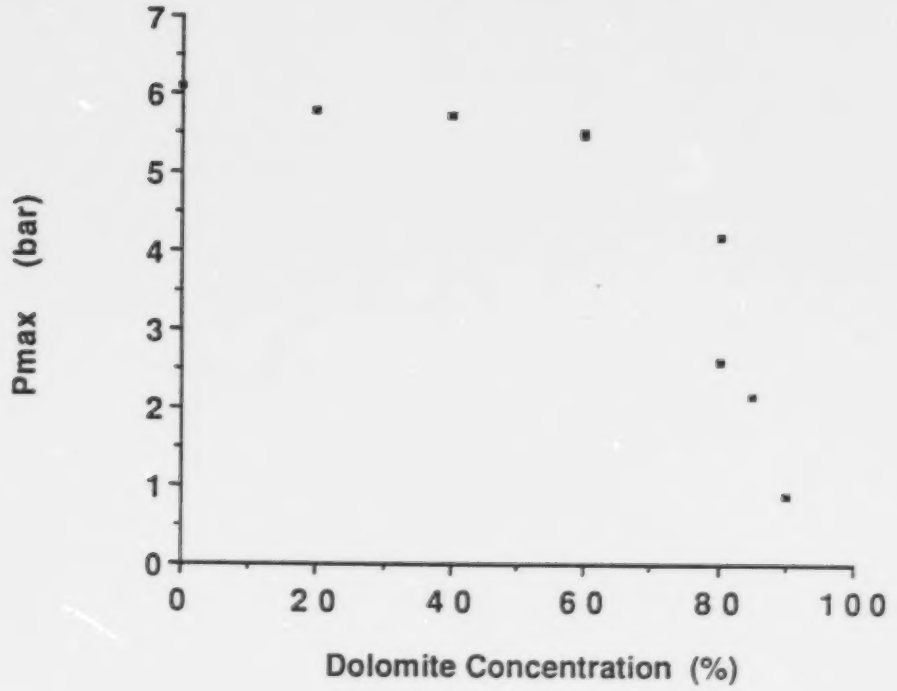

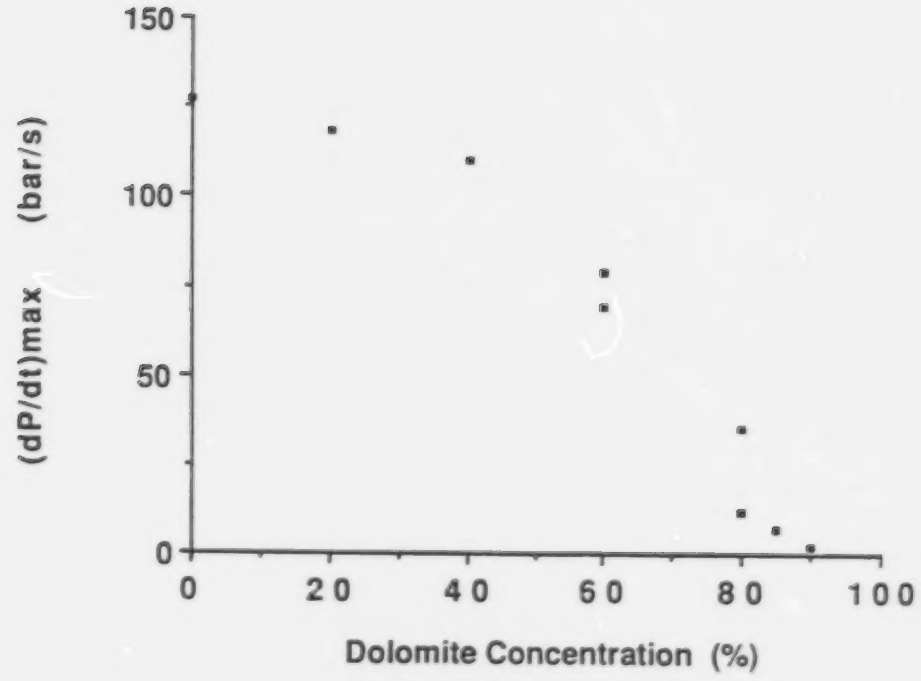

Fig. 3.36 P_{max} and $(dP/dt)_{max}$ at various dolomite concentrations (Phalen 2, 0.5 kg/m^3 coal dust, 2% methane).

CHAPTER 4

DISCUSSION

The purpose of this chapter is to propose explanations for the results obtained from the experimental work. The results from the phase I tests are considered first. This is followed by a discussion of the phase II results. The final section of this chapter examines the applicability of the results to the coal mining industry.

4.1 Phase I Results

Phase I of the experimental program involved coal dust/air and methane/coal dust/air mixtures. The results given in Figs. 3.1 to 3.18 show that the repeatability of the maximum explosion pressure is, as expected, much better than that for the maximum rate of pressure rise. Values of P_{max} from repeat runs generally agreed to within less than 10%, whereas $(dP/dt)_{max}$ values from duplicate tests occasionally differed by as much as a factor of two (although the difference was usually much less than this). Multiple testing at a given set of conditions was therefore carried out; some coals were examined more intensively than others in terms of repeat tests. These points on repeatability of P_{max} and $(dP/dt)_{max}$ are consistent with our previous experience (Amyotte and Pegg, 1989) and also that of other workers (Cashdollar and Hertzberg, 1985 and Mintz, 1989).

In the discussion which follows, comparisons are made to illustrate the effects of methane admixture and particle size and volatile content of the coal. To facilitate the discussion, mean values of P_{max} and $(dP/dt)_{max}$ from duplicate runs, with a smooth curve drawn through them, have been used. This procedure is illustrated in Figs. 4.1 and 4.2 for the Prince 2 coal with no methane present.

The data for coal dust alone shown in Figs. 4.1 and 4.2 display the same trend as that observed for Pittsburgh seam bituminous coal in tests conducted by the U.S.

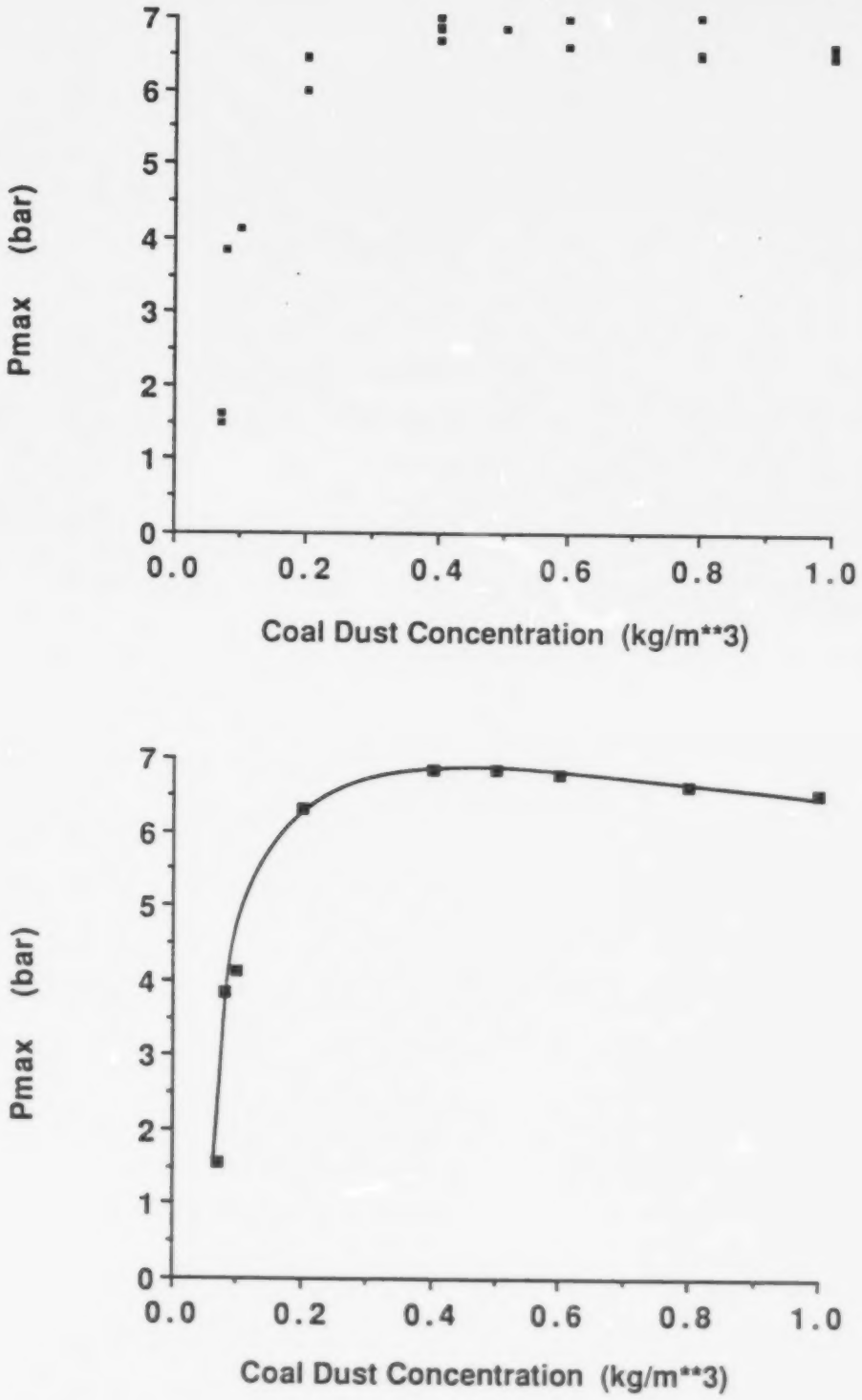

Fig. 4.1 Actual values (upper plot) and mean values (lower plot) of P_{max} as a function of coal dust concentration (Prince 2, 0% methane).

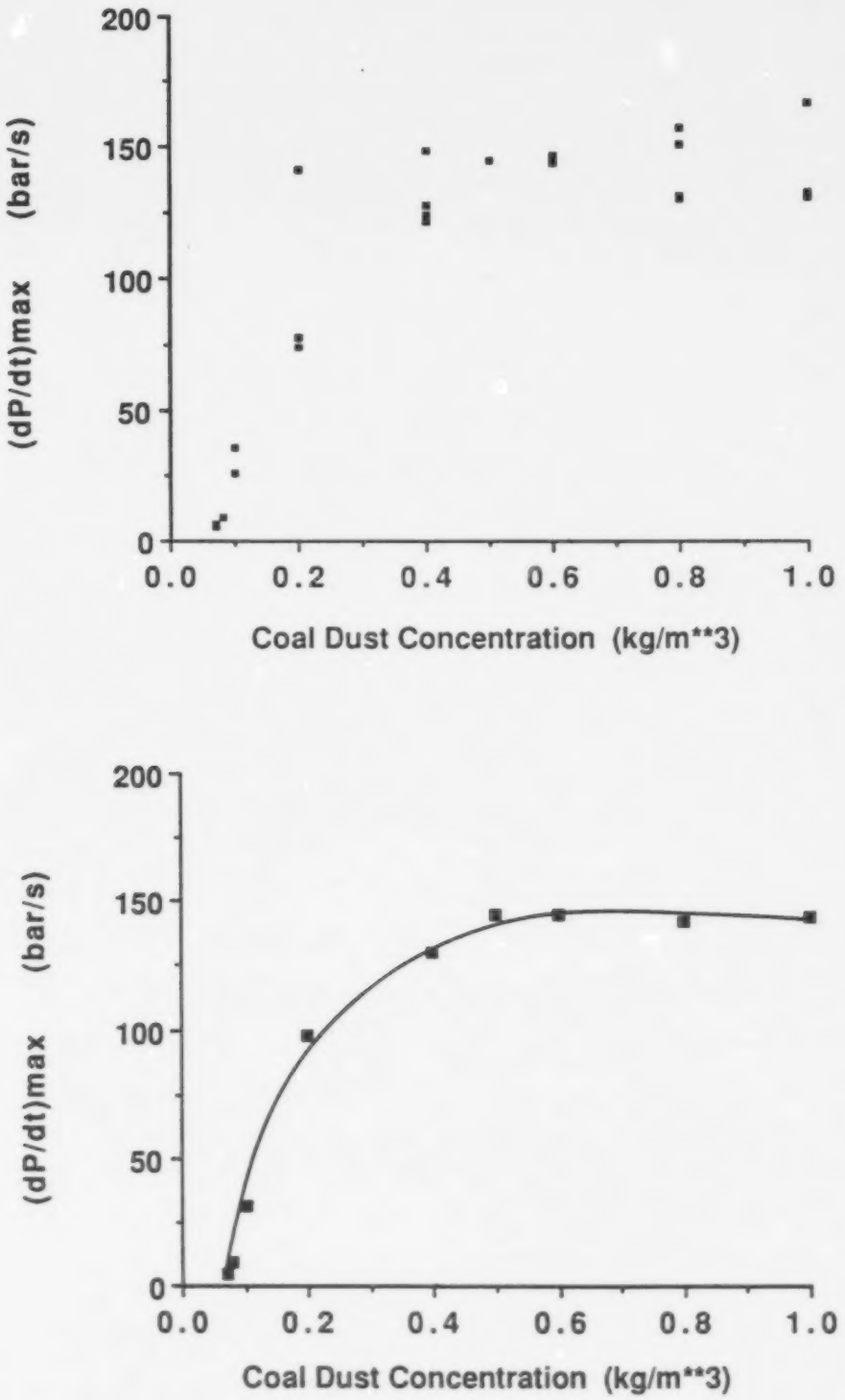

Fig. 4.2 Actual values (upper plot) and mean values (lower plot) of $(dP/dt)_{max}$ as a function of coal dust concentration (Prince 2, 0% methane).

Bureau of Mines (Cashdollar and Hertzberg, 1985 and Cashdollar et al., 1987). As dust concentration is increased, both P_{max} and $(dP/dt)_{max}$ rise to a maximum and then level off. The increase in maximum rate of pressure rise is a reflection of the increase in burning velocity of the dust/air mixture, with the peak value corresponding to the burning of a near-stoichiometric concentration of combustible volatiles (Hertzberg and Cashdollar, 1987) This does not occur, however, until the coal dust concentration is three to four times its stoichiometric concentration (about 0.14 kg/m^3 for the Prince 2 coal). This demonstrates one of the fundamental differences between gas-phase and dust explosions. While optimum explosion effects are observed at approximately stoichiometric concentrations for flammable gases, the same is not true for dusts. Another characteristic of dust explosions which is evident in Figs. 4.1 and 4.2 is the absence of a rich flammability limit up to a coal dust concentration of 1.0 kg/m^3. The occurrence of a lean flammability limit and the factors influencing this parameter are discussed in section 4.1.4.

4.1.1 Methane admixture

The effects of adding small amounts of methane (1% and 2%) to the oxidizing atmosphere are shown in Fig. 4.3. These results are for the Phalen 2 coal, but are typical of those obtained for all the coals tested. The upper plot in Fig. 4.3 shows that for dust concentrations up to about 0.5 kg/m^3, the maximum explosion pressure is increased by the addition of methane. The influence of added methane becomes less significant at high dust concentrations, perhaps due to the excess dust in these rich mixtures acting as a thermal sink (Lee et al., 1984). As seen in the lower plot in Fig. 4.3, the maximum rate of pressure rise is also increased by the addition of methane; this occurred at all dust concentrations tested. The explanation here may lie in the fact that gases (such as methane) generally produce greater maximum rates of pressure rise than dusts (such as coal dust). It appears then that an additive effect occurs,

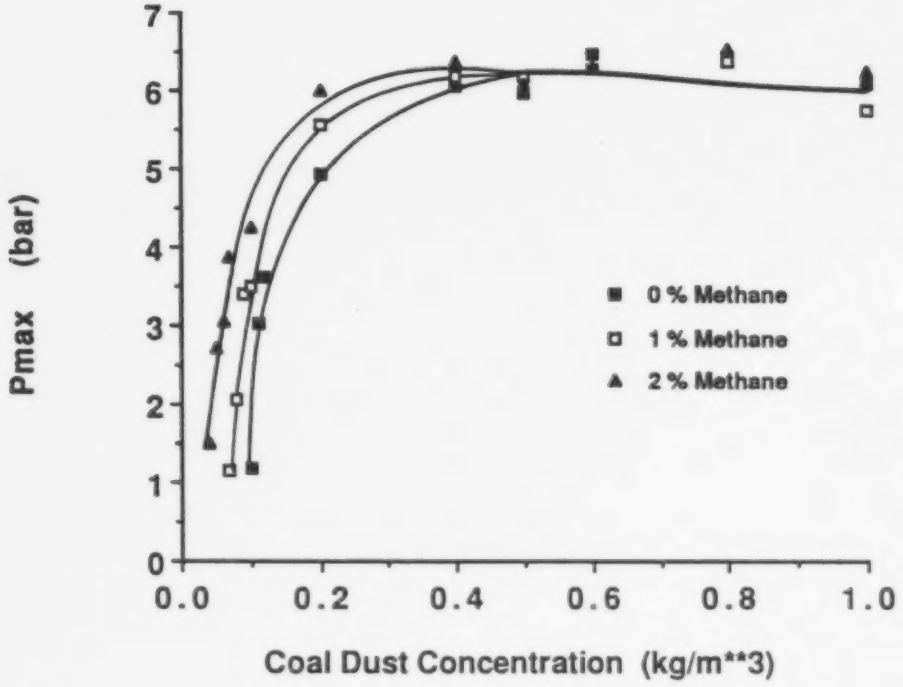

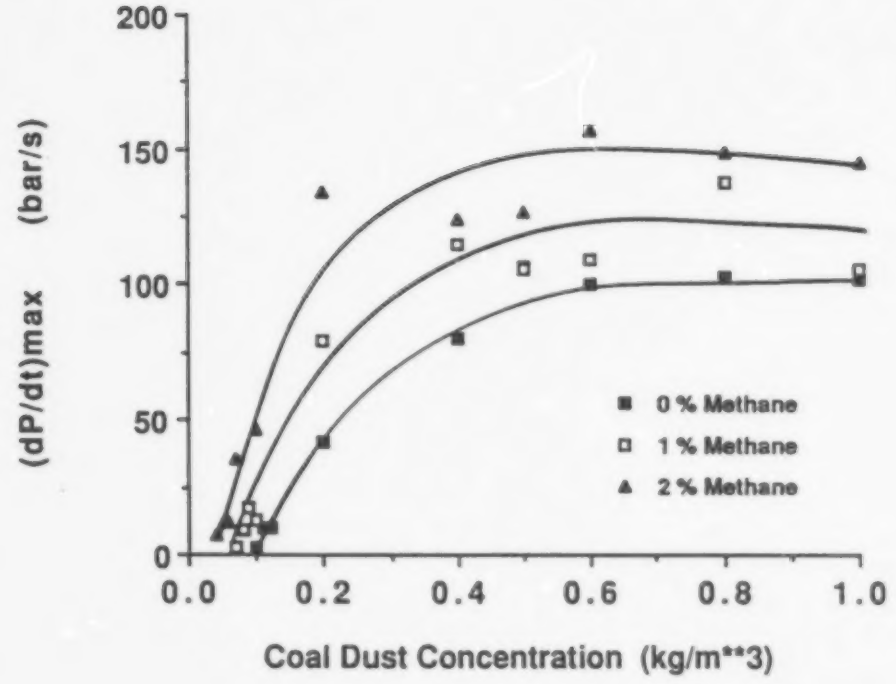

Fig. 4.3 Effect of methane admixture on P_{max} and $(dP/dt)_{max}$ of Phalen 2 coal.

whereby the methane contribution to $(dP/dt)_{max}$ is summed with the coal dust contribution.

Data for the Prince 1 and Prince 2 coals are given in Fig. 4.4. Again, the effect of methane admixture is to increase the maximum rate of pressure rise. For the high-volatile Prince 1 and Prince 2 coals, there is a slight drop in $(dP/dt)_{max}$ at high dust concentrations for the 2% methane level. This may be caused by a reduction in the burning velocity brought about by the thermal sink effect previously described.

The data in Figs. 4.3 and 4.4 indicate that with methane addition, the peak values of P_{max} and $(dP/dt)_{max}$ occur at dust concentrations which are slightly less than those for coal dust alone. This observation is consistent with the methane/cornstarch/air studies of Lee et al. (1984). Additionally, the peak values of $(dP/dt)_{max}$ for coal dust alone are exceeded by methane/coal dust mixtures at leaner dust concentrations. The main effect of methane admixture, therefore, is to enable the fuel/air mixture to attain a stoichiometric or near-stoichiometric concentration of combustible volatiles at lower dust concentrations. This can have serious implications for the design and operation of explosion relief venting and explosion suppression equipment, both of which rely on an accurate knowledge of $(dP/dt)_{max}$.

4.1.2 Coal particle size

The effect of a change in coal particle size (or more properly, particle size distribution) is shown in Fig. 4.5 for the Lingan coals at the 1% methane level. At all dust concentrations, both P_{max} and $(dP/dt)_{max}$ are increased as the mass mean diameter is decreased from 27 μm for the Lingan 1 coal to 18 μm for the Lingan 2 coal. As was the case with methane admixture, the influence of particle size on P_{max} becomes less significant at higher dust concentrations. These are typical results for the Lingan and Phalen coals, for which the volatile content remained relatively constant as

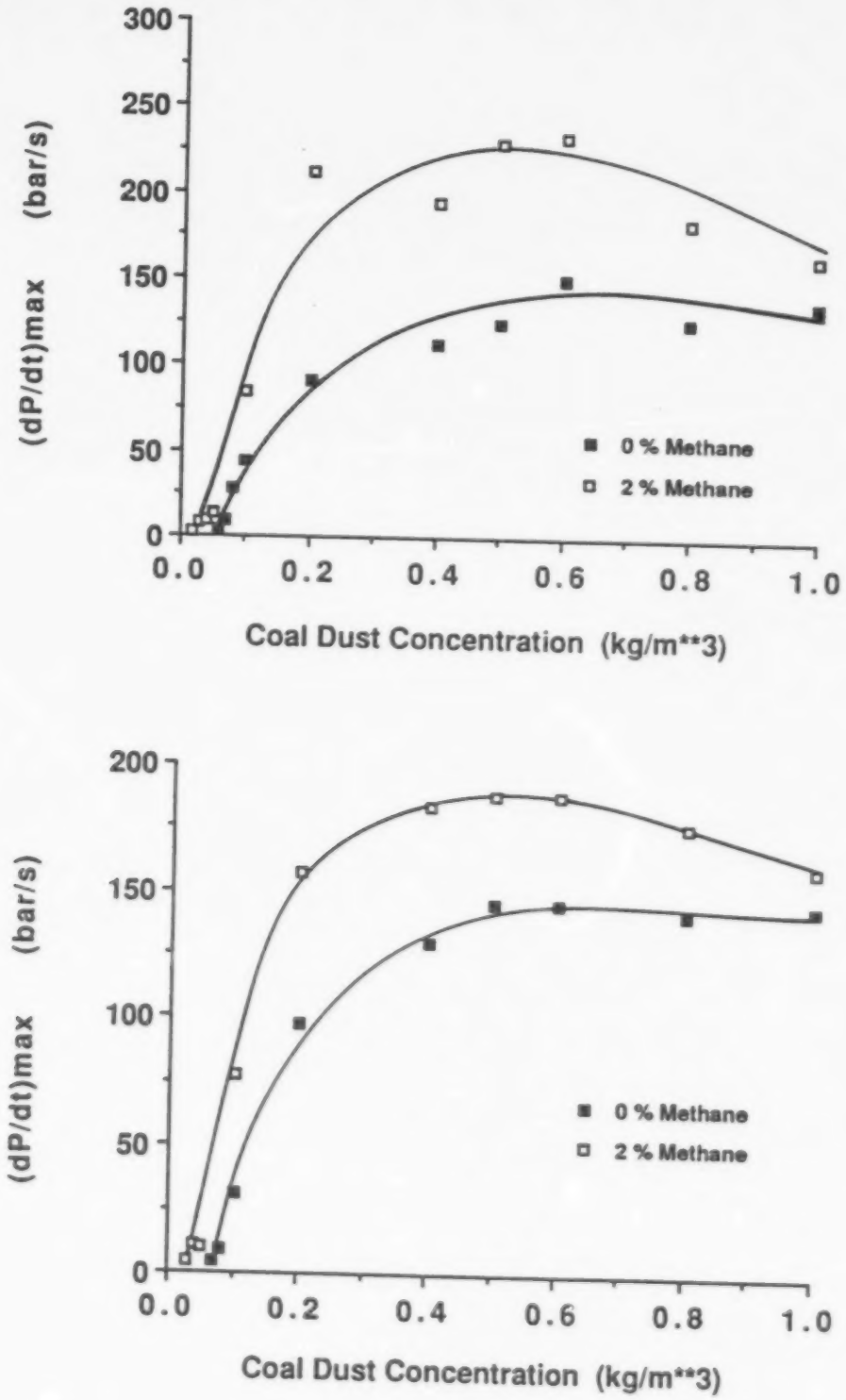

Fig. 4.4 Effect of methane admixture on $(dP/dt)_{max}$ of Prince 1 coal (upper plot) and Prince 2 coal (lower plot).

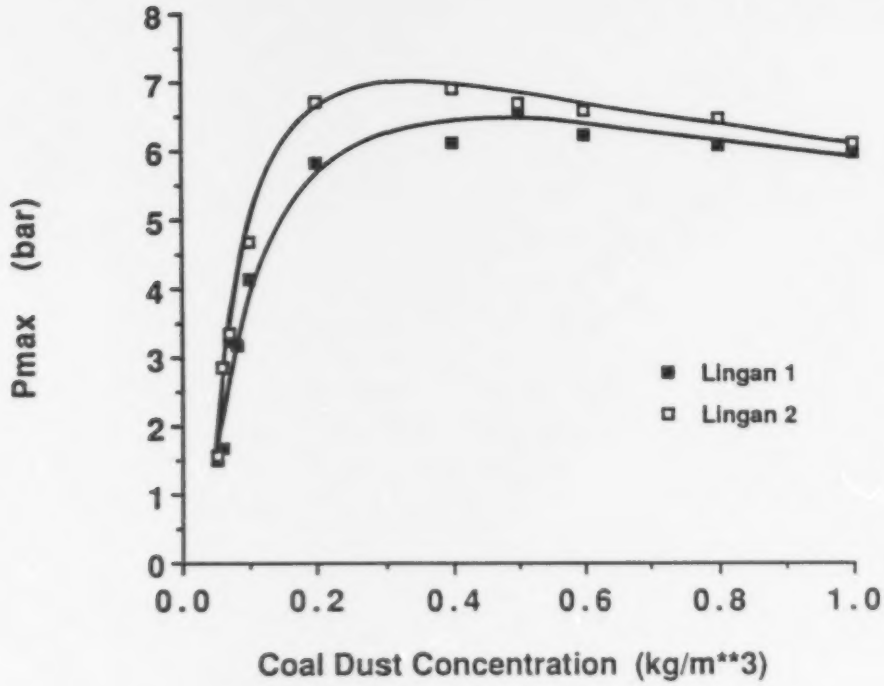

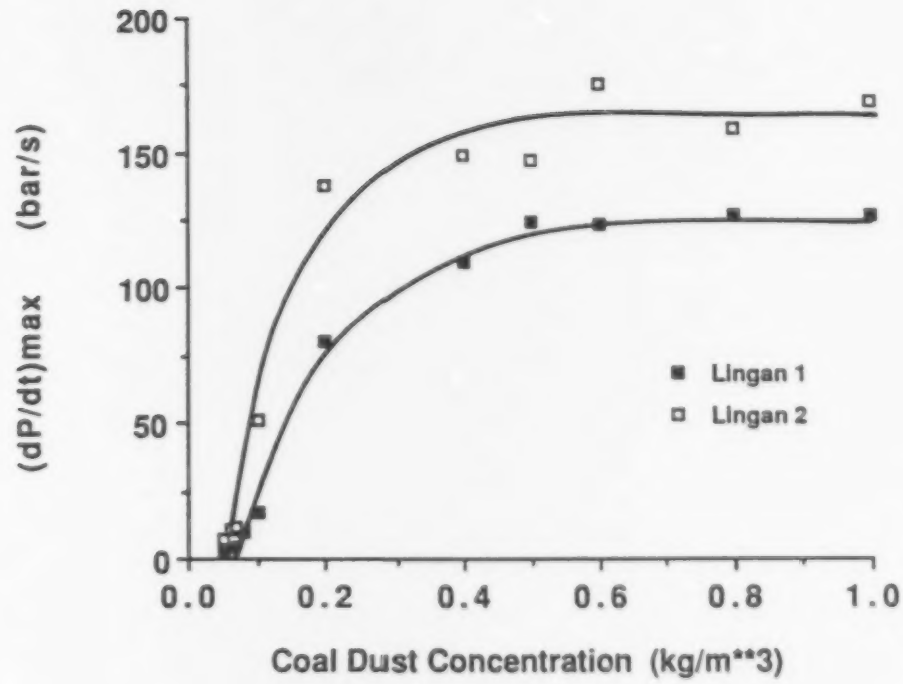

Fig. 4.5 Effect of coal particle size on P_{max} and $(dP/dt)_{max}$ of Lingan coals (1% methane).

the particle size changed. From Table 2.2, the volatile content of the Lingan coals is about 32% and that of the Phalen coals about 26%.

For the Prince coals, however, there is substantial overlap in the values of P_{max} and $(dP/dt)_{max}$ at the two different particle sizes. There are two reasons for this. First, the difference in size distributions of the Prince 1 and Prince 2 coals is not great, especially when compared with the difference in size between the Lingan coals and between the Phalen coals (Table 2.1). Second, there is a slight drop in volatile content with a decrease in particle size, from 36% for the Prince 1 coal to about 34% for the Prince 2 coal (Table 2.2). Although not a large difference in volatile content, it is expected to have some effect on the explosion parameters, as indicated by the discussion in the next section of this report.

The combustion of volatile dusts is usually viewed as a stepwise process in which devolatilization occurs followed by burning of the gaseous volatiles. In other words, once devolatilization of a sufficient number of particles occurs, the flame characteristics are dominated by the volatiles with combustion taking place primarily in the gas phase (Hertzberg et al., 1986b and Dixon-Lewis et al., 1987). This is the reasoning previously used when commenting that the peak value of maximum rate of pressure rise occurs at a coal dust concentration which is three to four times the stoichiometric concentration of the dust, but which also yields a near-stoichiometric concentration of combustible volatiles.

With fine dusts, devolatilization can occur so rapidly that the behaviour of such materials can be adequately described by considering them essentially as gases. However, many of the dusts handled in industry, such as the coal dusts considered here, have a broad particle size distribution. In this case, the devolatilization process cannot be considered independently from the volatiles combustion. The small particles will undergo rapid devolatilization and can be described by gas-phase considerations, but the larger particles will undergo devolatilization more slowly.

One implication of this is that volatile dusts with a broad particle size distribution behave as hybrid mixtures of flammable gas and combustible dust. The present work supports this interpretation of dust explosions. The upper plot in Fig. 4.6 shows the effect of methane addition on the maximum rate of pressure rise of the Lingan 1 coal. As expected from the discussion in the previous section, $(dP/dt)_{max}$ is significantly increased at all dust concentrations by the addition of 2% methane. The lower plot in Fig. 4.6 shows the effect of particle size on the maximum rate of pressure rise of the Lingan coals with no methane present. Decreasing the mass mean diameter from 27 μm to 18 μm increases $(dP/dt)_{max}$ significantly at all dust concentrations.

An additional point to note is that decreasing the mass mean diameter increases the number of fine particles, which is equivalent to adding a combustible gas because of their rapid rate of devolatilization. Inspection of both plots in Fig. 4.6 shows that reducing the mass mean diameter from 27 μm to 18 μm is almost equivalent to adding 2% methane to the oxidizing atmosphere for the parent coal having a mass mean diameter of 27 μm. At low dust concentrations, the effect of particle size does not appear to be quite as significant as the effect of methane admixture. Although the devolatilization process for fine particles is rapid, this process is completely eliminated by direct addition of volatile gases.

Further evidence of flame propagation by volatiles combustion was gained by examining the Prince 1 coal dust particles before testing and the residue remaining after several representative explosion tests. This was done with the aid of a scanning electron microscope; the microscopy work was performed by the Mining and Metallurgical Engineering Department, TUNS. The scanning electron micrographs (SEM's) shown in Figs. 4.7 to 4.9 are similar to those given by Hertzberg et al. (1982b) for Pittsburgh seam bituminous coal. The SEM's of the unburned coal (Fig. 4.7) show that the particles had a clearly defined shape with sharp edges and features. Examination of the char residue (Figs. 4.8 and 4.9), however, indicates that the burned

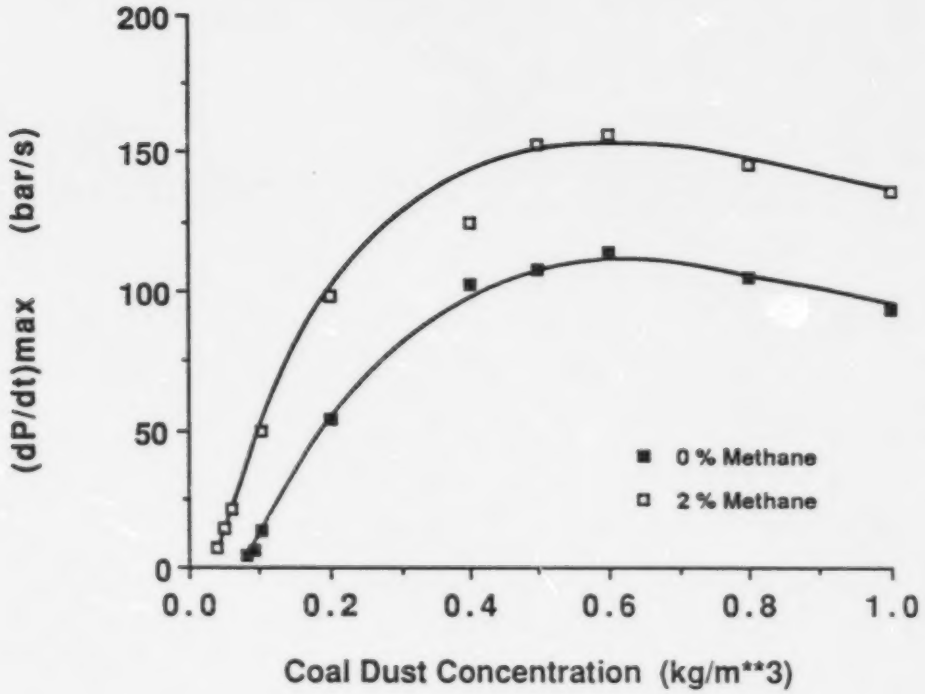

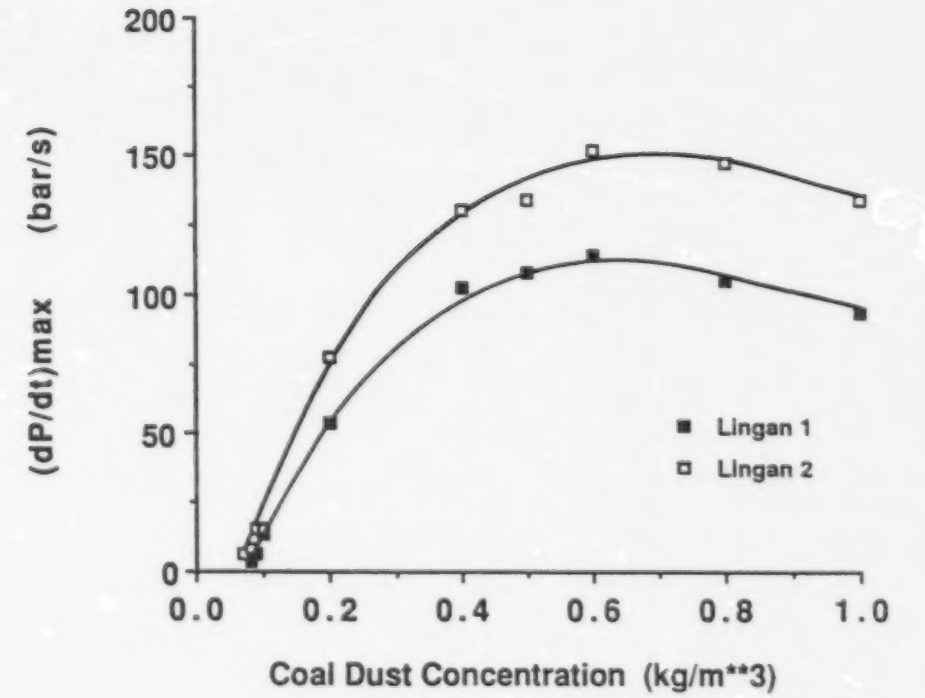

Fig. 4.6 Comparison of effect of methane admixture on $(dP/dt)_{max}$ of Lingan 1 coal with effect of coal particle size on $(dP/dt)_{max}$ of Lingan coals (0% methane).

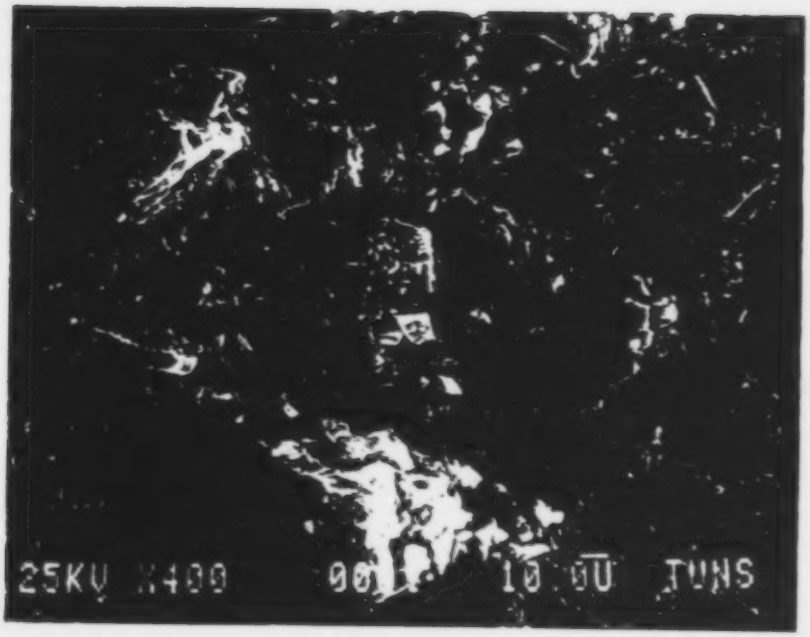

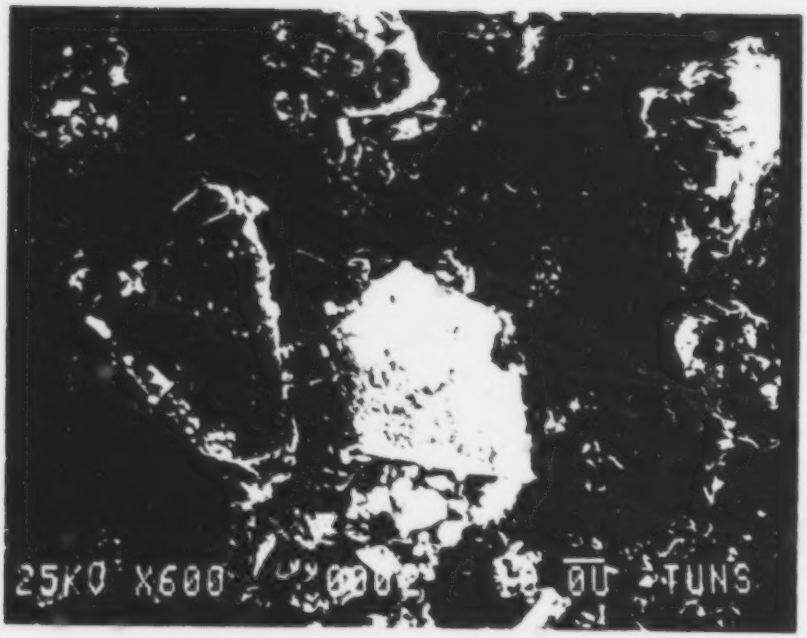

Fig. 4.7 Scanning electron micrographs of unburned Prince 1 coal dust.

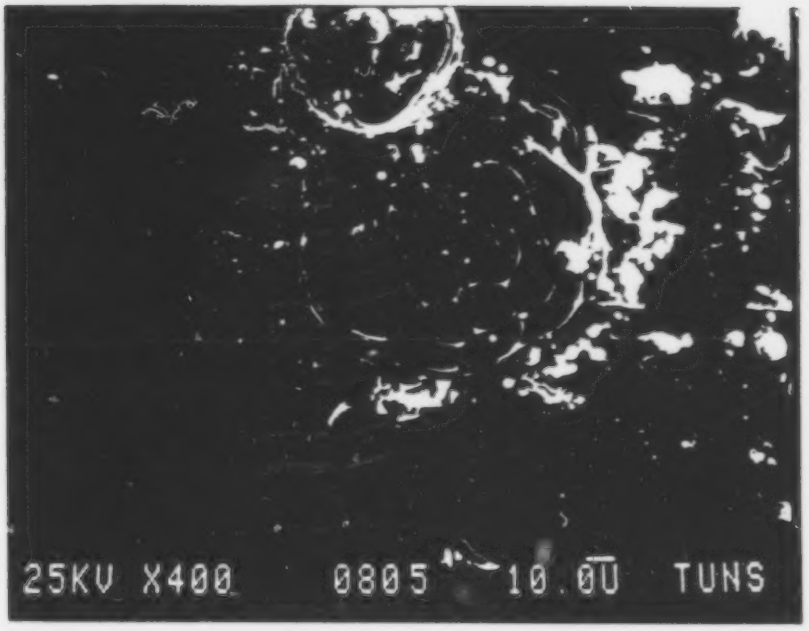

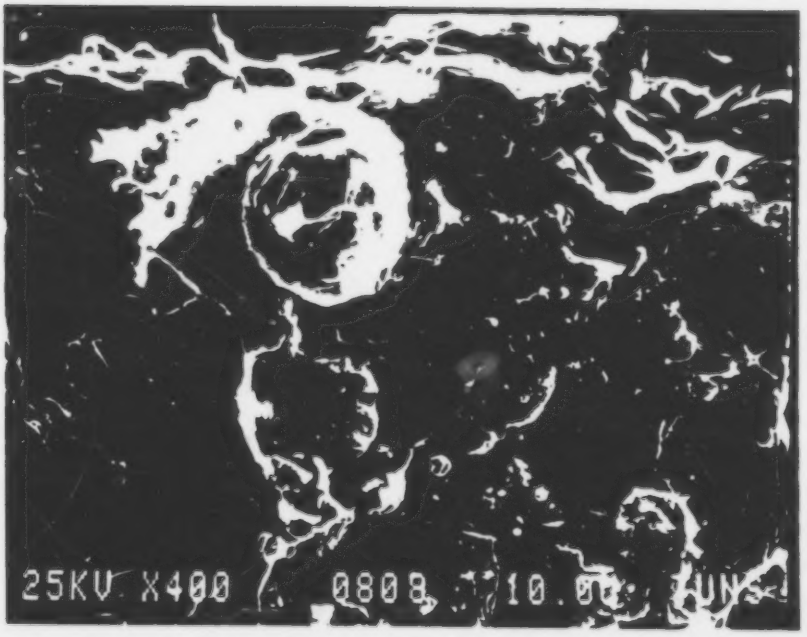

Fig. 4.8 Scanning electron micrographs of Prince 1 char residue at 0% methane, 0.1 kg/m^3 coal dust (upper plot) and 0% methane, 0.4 kg/m^3 coal dust (lower plot).

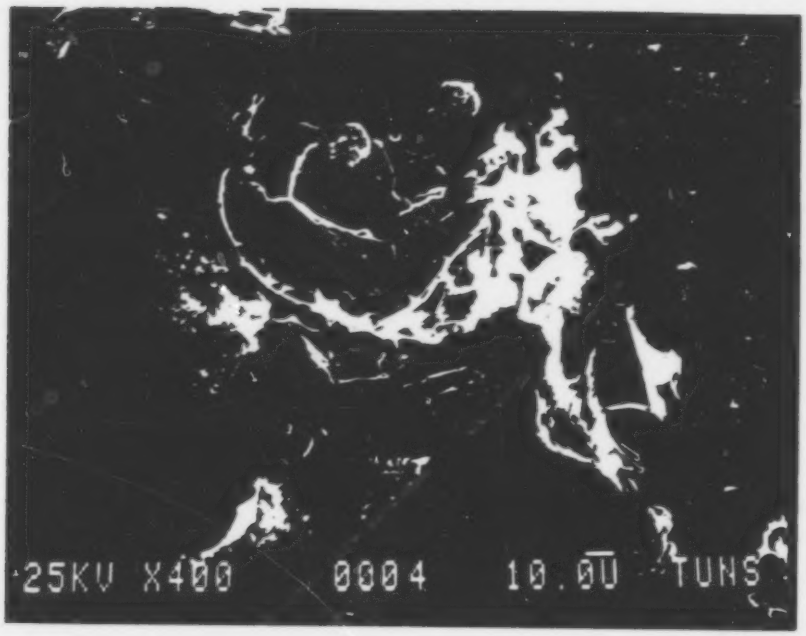

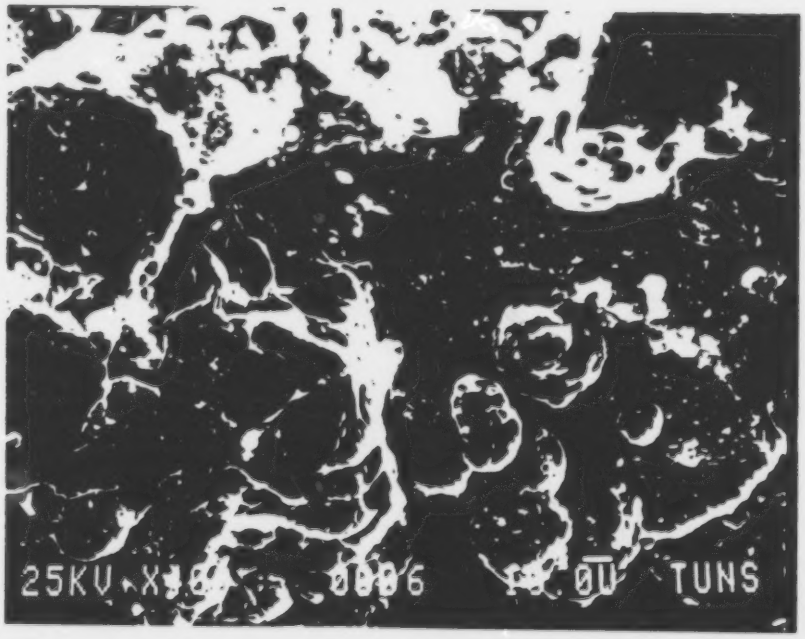

Fig. 4.9 Scanning electron micrographs of Prince 1 char residue at 1% methane, 1.0 kg/m^3 coal dust (upper plot) and 2% methane, 0.1 kg/m^3 coal dust (lower plot).

coal particles were more rounded in shape and were often fused together. There is also clear evidence of the existence of blow holes through which the volatiles had been emitted.

4.1.3 Coal volatile content

The discussion thus far has concentrated primarily on the dominant role of combustion of the devolatilization products. It would therefore be expected that the volatile content of the parent coal has a significant effect on the explosion behaviour of that coal. This is shown in Fig. 4.10 for the Prince 1, Lingan 1 and Phalen 1 coals, having volatile contents of approximately 36%, 32% and 26%, respectively. The size distributions for the three coals are not identical, but are approximately the same. Thus, the changes in P_{max} and $(dP/dt)_{max}$ illustrated in Fig. 4.10 should be caused mainly by differences in volatile content, not particle size. These results are consistent with data published by Hertzberg and Cashdollar (1987) for a high-volatile bituminous coal and a low-volatile bituminous coal.

4.1.4 Lean flammability limit

The lean flammability limit is the concentration boundary above which a fuel/oxidant mixture will react explosively in the presence of an adequate ignition source. For dusts, the lean limit, or minimum explosible concentration, is defined as the minimum concentration of dust in a cloud required for sustained flame propagation. Different criteria have been proposed by researchers to quantify the phrase "sustained flame propagation" and hence judge the limit concentration for lean dust/air mixtures. The criteria used here to specify the occurrence of a lean limit were those proposed by Hertzberg et al. (1986a). These are a pressure ratio (P_{max} divided by the initial vessel pressure) greater than or equal to 2 and a K_{St} value greater than or equal to 1.5 bar • m/s. The parameter K_{St} is obtained by multiplying the maximum

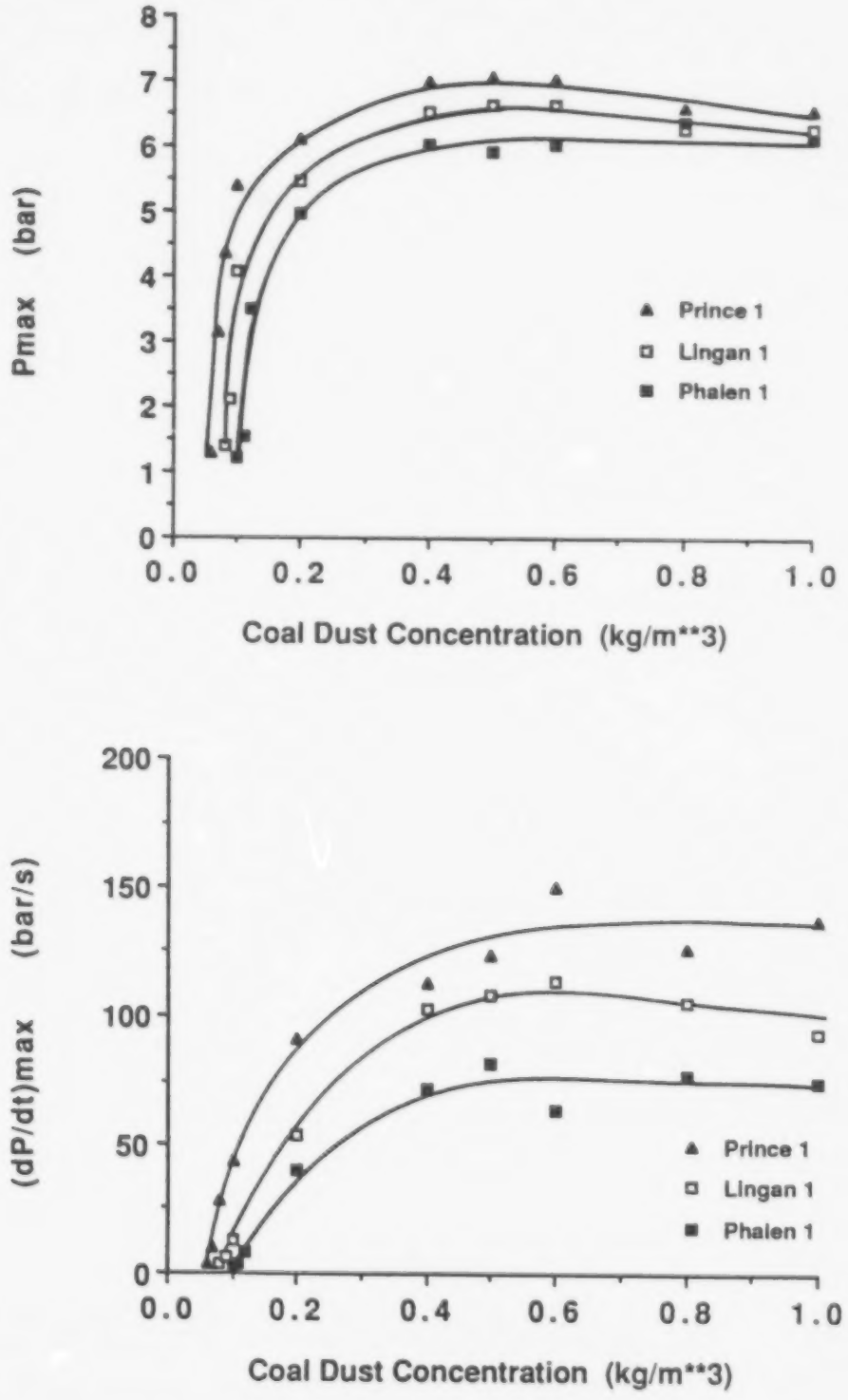

Fig. 4.10 Effect of coal volatile content on P_{max} and $(dP/dt)_{max}$ (0% methane).

rate of pressure rise by the cube root of the vessel volume; this is done in an attempt to size-normalize $(dP/dt)_{max}$.

In this work, the initial vessel pressure was 1 bar, so the pressure ratio is essentially equal to the absolute maximum explosion pressure. Also, the volume is 0.026 m^3, so K_{St} is equal to $(dP/dt)_{max}$ multiplied by 0.296 m; to satisfy the requirement of $K_{St} \geq 1.5$ bar • m/s, the maximum rate of pressure rise must be at least 5 bar/s in the vessel used in this study. The experimental procedure used was to approach the lean limit from the upper end by decreasing the coal dust concentration in increments of 0.01 kg/m^3. This resulted in a situation where the limit criteria were satisfied at a particular coal dust concentration, but then were not satisfied upon reduction of the dust concentration by 0.01 kg/m^3. The value selected as the lean limit was the last concentration at which the limit criteria were met.

The lean flammability limits obtained with this approach are given in Table 4.1. A direct comparison of the lean limits of the coal dust/air mixtures with values reported by other workers is difficult to make. This is because the coals tested in the present study are somewhat unique in terms of particle size distribution and proximate analysis. An order-of-magnitude comparison can be made, however, and this reveals that the lean limits reported here are consistent with the value of 0.09 kg/m^3 determined by Hertzberg et al. (1986a) for Pittsburgh seam bituminous coal dust. It must be remembered, though, that the Pittsburgh coal had a much lower ash content (6%) and a higher mass mean diameter (50 μm) than the coals used here. Similarly, the lean limits in Table 4.1 are consistent with the values reported by Mintz (1989) for various coal dusts when factors such as particle size distribution are considered.

Inspection of the data in Table 4.1 shows that the lean flammability limit is a function of coal volatile content, with the lean limit being lower for higher volatile containing coals. For example, the limit decreases from 0.12 kg/m^3 to 0.09 kg/m^3 to 0.07 kg/m^3 as one moves from Phalen 1 (26% volatiles) to Lingan 1 (32% volatiles) to

Table 4.1 Lean flammability limits for coal dust/air and methane/coal dust/air mixtures.

Coal Type and Size	Methane Concentration [%]	Lean Flammability Limit [kg/m^3]
Prince 1	0	0.07
Prince 1	1	0.06
Prince 1	2	0.03
Prince 2	0	0.08
Prince 2	1	0.07
Prince 2	2	0.04
Lingan 1	0	0.09
Lingan 1	1	0.07
Lingan 1	2	0.05
Lingan 2	0	0.08
Lingan 2	1	0.06
Lingan 2	2	0.05
Phalen 1	0	0.12
Phalen 1	1	0.09
Phalen 1	2	0.06
Phalen 2	0	0.11
Phalen 2	1	0.08
Phalen 2	2	0.05

Prince 1 (36% volatiles). There is also a particle size effect, with the lean limit being slightly lower for Lingan 2 than for Lingan 1, and for Phalen 2 than for Phalen 1. The reverse occurs for the Prince coals, and is explained by the two reasons cited previously; namely, the comparatively small difference in particle size and the lower volatility of the Prince 2 coal.

The particle size dependence of the lean limits of the Lingan and Phalen coals appears, at first glance, to contradict the work of Hertzberg et al. (1982b). They found that for Pittsburgh seam coal dust (36% volatiles), the lean limit was independent of particle size for mass mean diameters less then approximately 50 μm. The equivalent diameter determined for Pocahontas seam coal dust (16% volatiles) was about 15 μm. Their work was carried out, however, with coal dusts having very narrow size distributions.

Broad particle size distributions, such as those used here, can be thought of as a series of narrow size distributions, each of which makes a contribution to the lean flammability limit. The contribution will be independent of particle size up to some characteristic particle diameter. Particles larger than this characteristic diameter can then influence the lean limit depending on their relative abundance. For the Lingan coals, this diameter should be about 50 μm since the Lingan volatility (34%) is nearly the same as that of the Pittsburgh coal (36%) used by Hertzberg et al. (1982b). Following a similar argument, the diameter of interest should be between 15 μm and 50 μm for the Phalen coals (26% volatility). Table 2.1 indicates that particles in the appropriate size ranges are present for both the Lingan and Phalen coals.

Table 2.1 also shows that methane admixture has a significant effect on the lean flammability limit. The limit data for the hybrid mixtures are shown graphically in Figs. 4.11, 4.12 and 4.13 for the Prince, Lingan and Phalen coals, respectively. A linear relationship predicted by Le Chatelier's law exists in all cases, with the straight lines separating each graph into two regions: a flammable zone to the right of the line

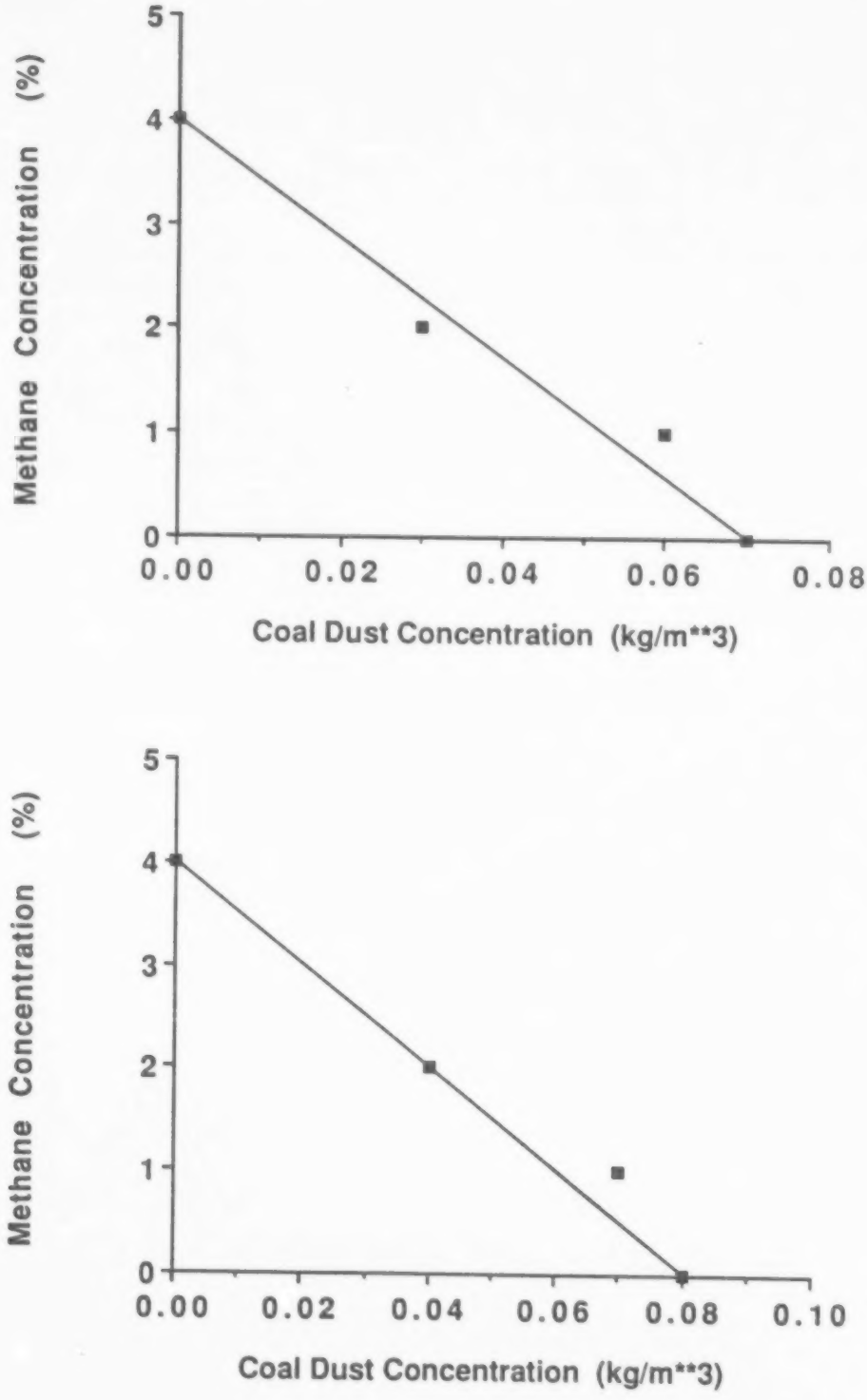

Fig. 4.11 Lean flammability limits of Prince 1 coal (upper plot) and Prince 2 coal (lower plot).

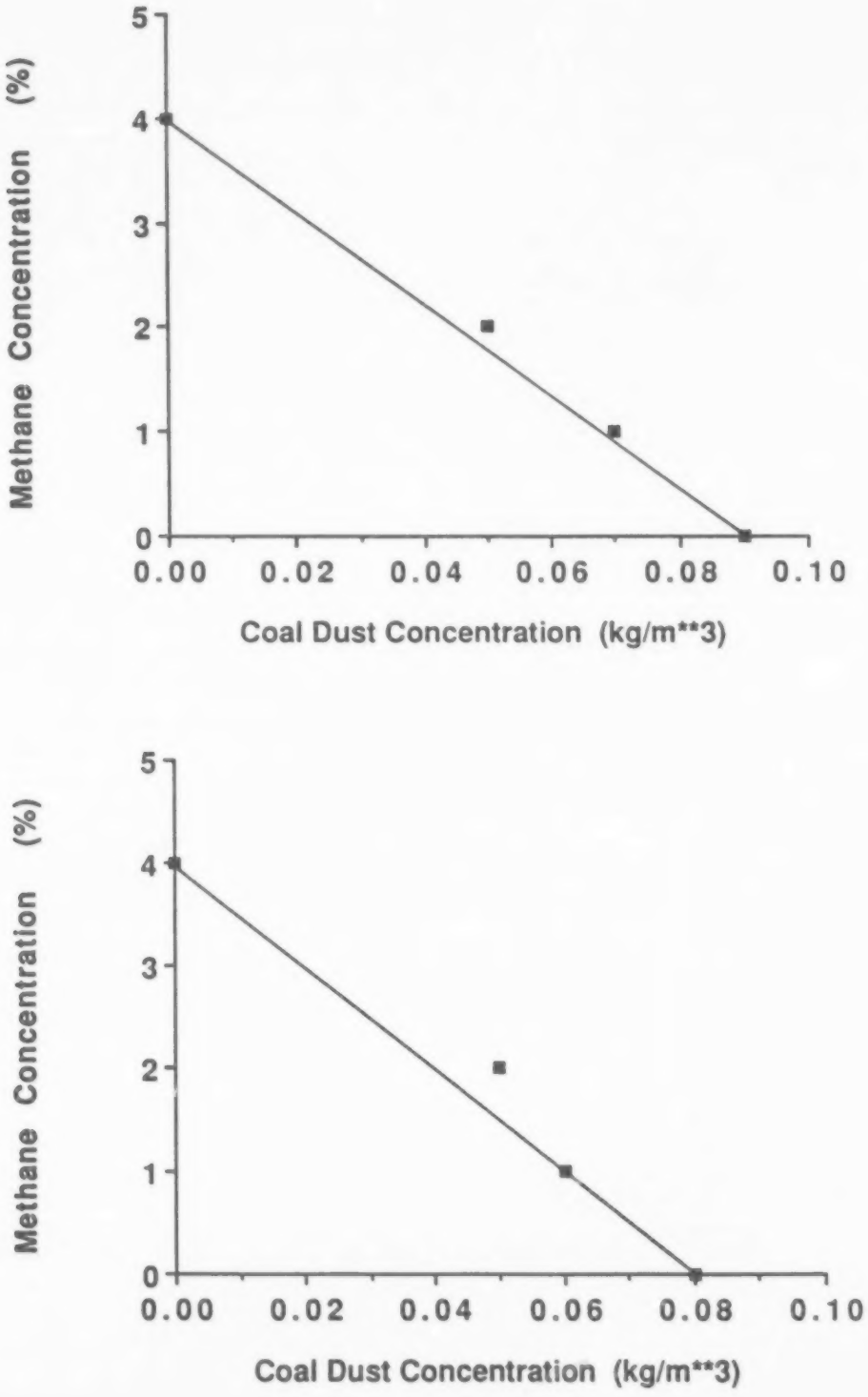

Fig. 4.12 Lean flammability limits of Lingan 1 coal (upper plot) and Lingan 2 coal (lower plot).

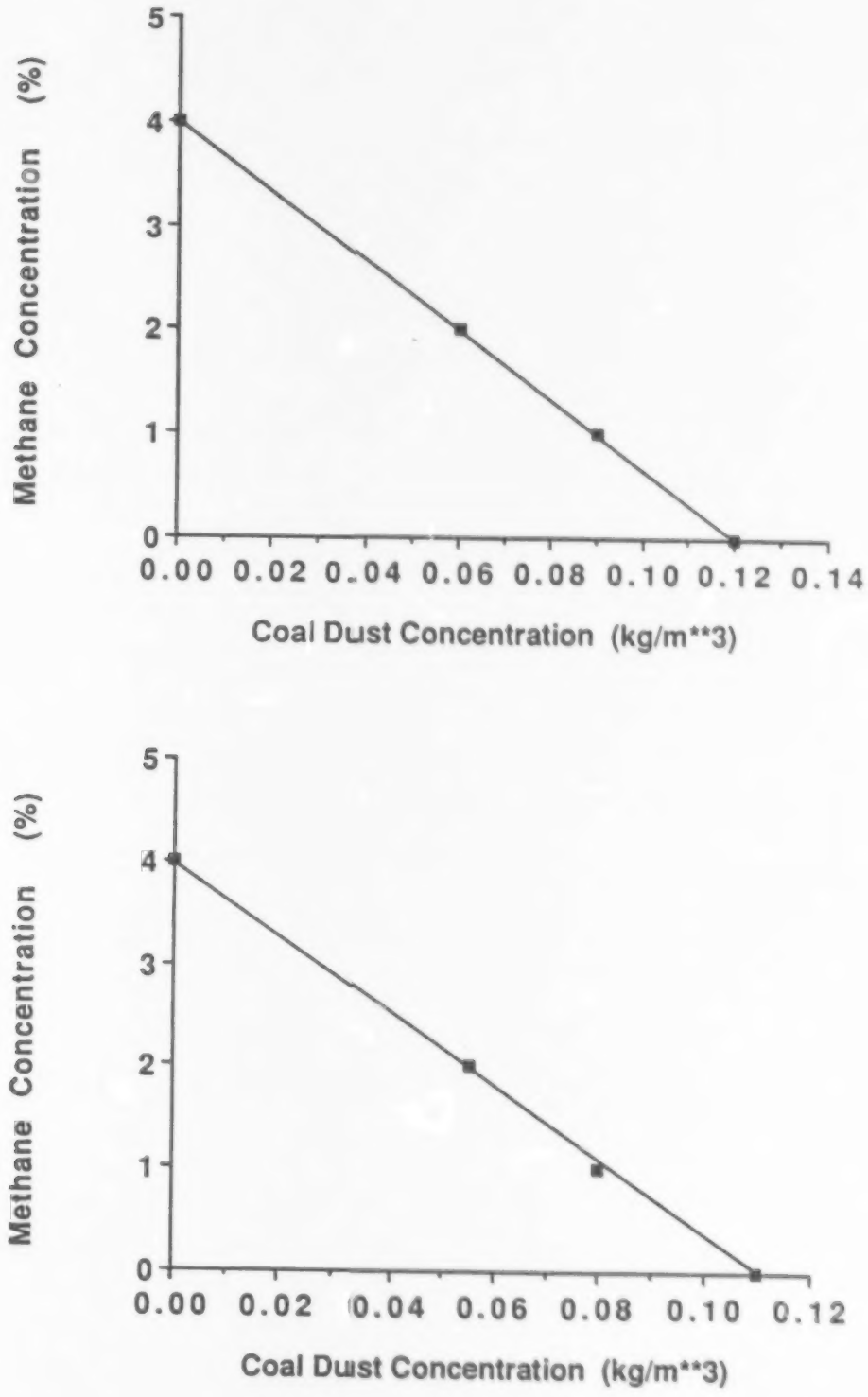

Fig. 4.13 Lean flammability limits of Phalen 1 coal (upper plot) and Phalen 2 coal (lower plot).

and a nonflammable zone to the left. These observations agree with similar work conducted at the U.S. Bureau of Mines and reported by Cashdollar et al. (1987). It is interesting to note that in the present study, the experimentally determined (i.e. apparent) lean limit for methane was approximately 4% by volume. This indicates that the 5 kJ chemical ignitors used here may have been somewhat excessive in terms of ignition energy and were therefore overdriving the system.

4.2 Phase II Results

Phase II of the experimental program involved coal dust/dolomite/air and methane/coal dust/dolomite/air mixtures. The results given in Figs. 3.19 to 3.36 display the same trend with respect to repeatability as did the phase I tests. A point worth repeating here is the fact that a single dust concentration, 0.5 kg/m^3, was used in all the inerting tests. This particular concentration was chosen because for all conditions of coal type, particle size and methane concentration, the maximum explosion pressure had peaked and the maximum rate of pressure rise was at or very near to its peak value.

Typical results from the inerting work are given in Figs. 4.14 and 4.15, showing only mean values of P_{max} and $(dP/dt)_{max}$ with smooth curves drawn through the data. The results shown are for the Lingan 1 (Fig. 4.14) and Phalen 2 (Fig. 4.15) coals, both with no methane present. The maximum explosion pressure undergoes only a slight decrease with an increase in dolomite percentage, up to near the inerting level. At this point, there is a sudden and rapid drop in P_{max}. The maximum rate of pressure rise, on the other hand, exhibits a fairly smooth and continuous decrease from the onset of dolomite addition. The general trends shown in Figs. 4.14 and 4.15 are consistent with those observed by Cashdollar and Hertzberg (1989) in a recent laboratory study of limestone inerting requirements.

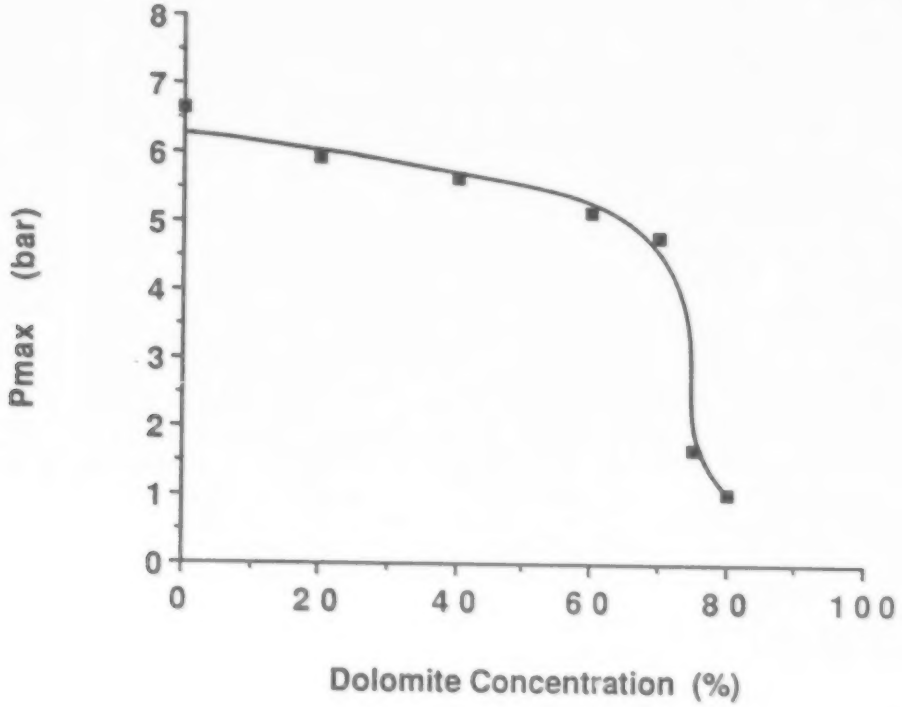

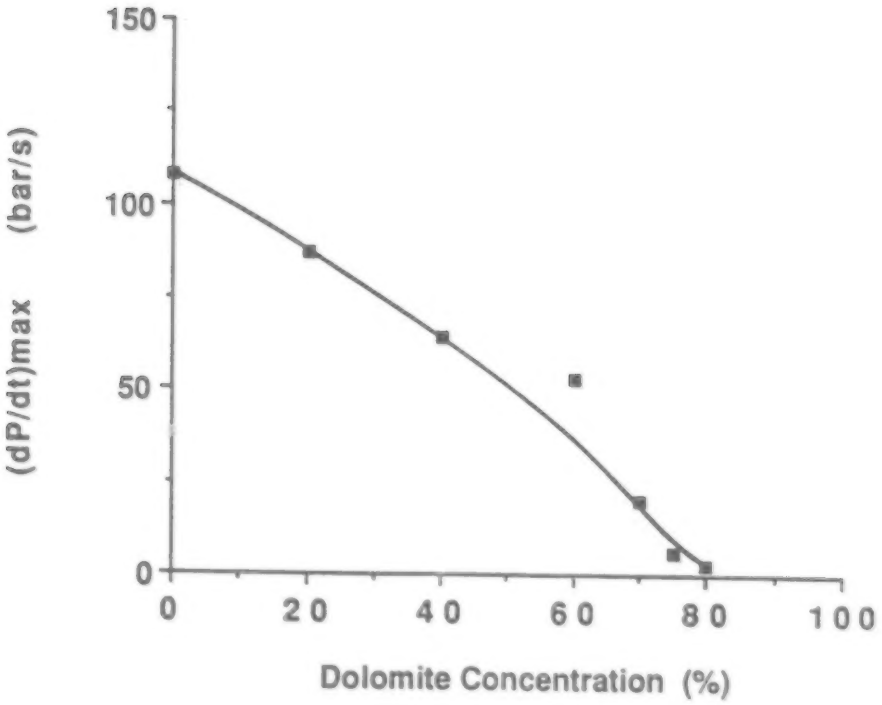

Fig. 4.14 P_{max} and $(dP/dt)_{max}$ at various dolomite concentrations (Lingan 1, 0.5 kg/m^3 coal dust, 0% methane).

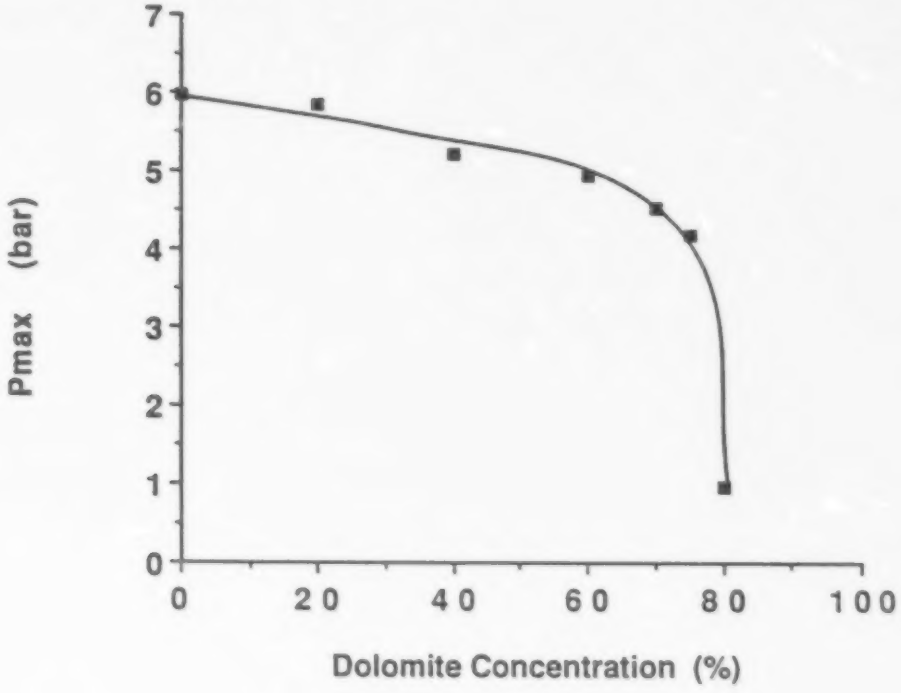

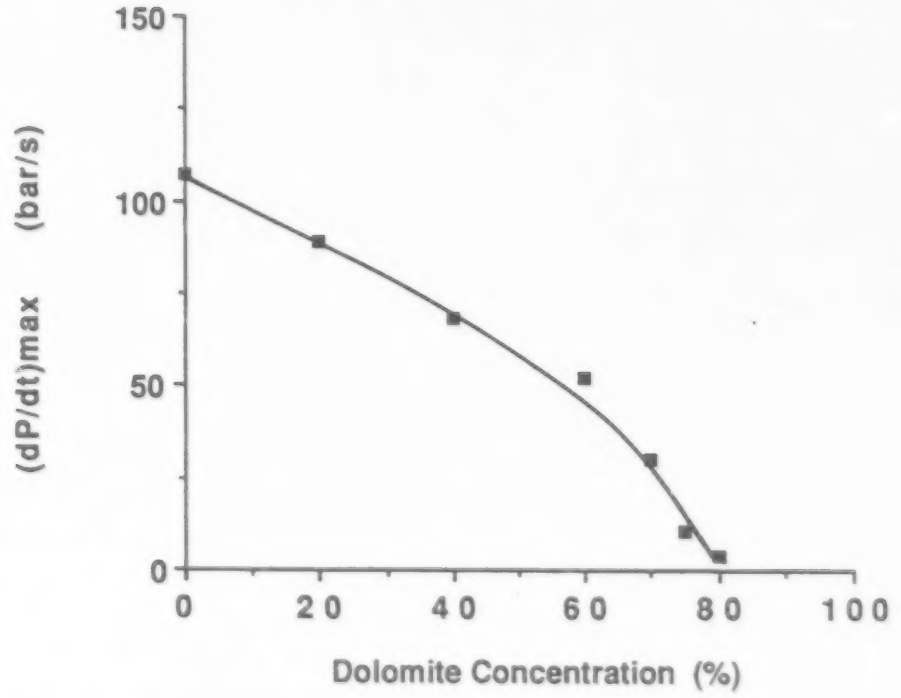

Fig. 4.15 P_{max} and $(dP/dt)_{max}$ at various dolomite concentrations (Phalen 2, 0.5 kg/m^3 coal dust, 0% methane).

The phase II data were checked for trends with respect to methane admixture, coal particle size and coal volatile content, and were found to be consistent with the results from phase I. For example, Fig. 4.16 shows the effect of methane admixture on P_{max} and $(dP/dt)_{max}$ for the Prince 2 coal. Adding methane to the oxidizing atmosphere has the expected effect of increasing $(dP/dt)_{max}$ at all dolomite percentages. The increase in P_{max} with methane addition is more pronounced near the inerting level; this agrees with the behaviour of P_{max} from the phase I work (Fig. 4.3).

Of primary interest in the dolomite inerting studies was the percentage of dolomite required to inert each explosive mixture. The inerting level was determined using the same P_{max} and $(dP/dt)_{max}$ criteria as in the lean limit work, i.e. $P_{max} \geq 2$ bar and $(dP/dt)_{max} \geq 5$ bar/s (or $K_{St} \geq 1.5$ bar • m/s). The inerting range was first narrowed down to within 5%. For example, the Prince 2 coal shown in Fig. 4.16 (no methane) satisfied the P_{max} criterion at the 80% dolomite level, but not at 85% dolomite. A similar situation existed for the $(dP/dt)_{max}$ criterion, thus indicating that the inerting requirement was between 80% and 85% dolomite. The data were then interpolated between the "go" and "no go" dolomite percentages to give a value for the inerting level.

The inerting requirements thus obtained are shown in Table 4.2. The results are presented in two ways: as the percentage of dolomite in the total solids mixture (dolomite plus coal dust), and as the percentage of incombustibles in the total solids mixture. This last parameter, the total incombustible content or TIC, is composed of the dolomite and the ash and moisture in the coal.

4.2.1 Methane admixture

The effect of methane addition is to increase the amount of dolomite required for inerting (TIC is always affected in the same way as dolomite percentage). This is analogous to the extension of the lean flammability limit which is brought about by

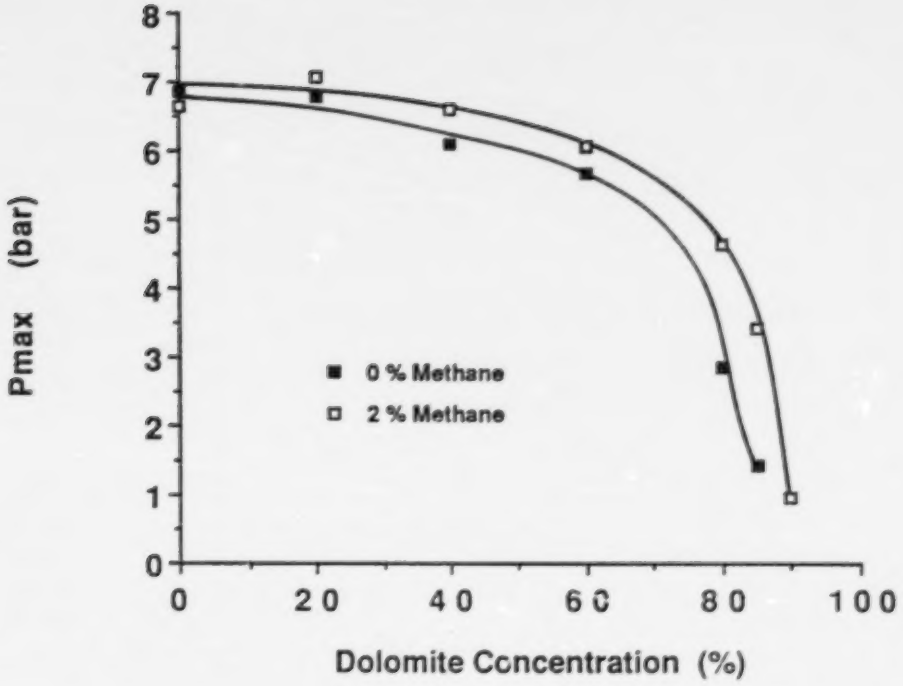

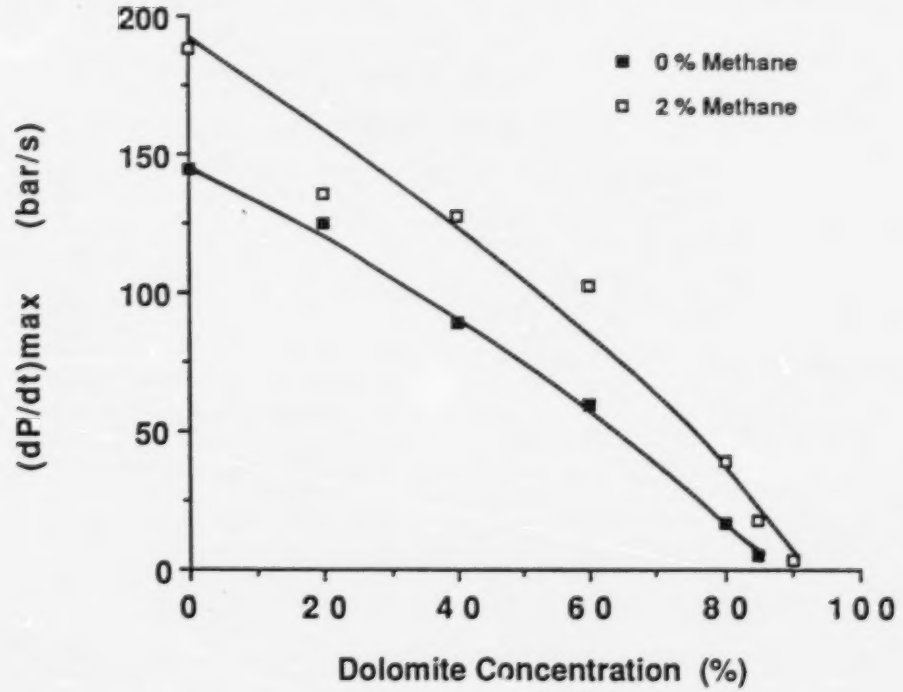

Fig. 4.16 Effect of methane admixture on dolomite inerting requirements of Prince 2 coal.

Table 4.2 Dolomite inerting requirements for coal dust/air and methane/coal dust/air mixtures.

Coal Type and Size	Methane Concentration [%]	Dolomite Concentration [%]	Total Incombustible Content [%]
Prince 1	0	80	83
Prince 1	1	84	87
Prince 1	2	88	90
Prince 2	0	84	87
Prince 2	1	86	88
Prince 2	2	89	91
Lingan 1	0	74	79
Lingan 1	1	79	83
Lingan 1	2	84	87
Lingan 2	0	84	86
Lingan 2	1	87	89
Lingan 2	2	89	91
Phalen 1	0	64	77
Phalen 1	1	69	80
Phalen 1	2	74	83
Phalen 2	0	78	85
Phalen 2	1	84	89
Phalen 2	2	86	91

methane admixture, and is illustrated by Table 4.2. Alternatively, this effect is shown graphically by Figs. 4.17 to 4.19. The inerting ratio, which is the ratio of dolomite to coal dust, is seen to substantially increase for each percentage of methane added.

As a result of full-scale mine tests, the U.S. Bureau of Mines has developed an empirical formula to predict the additional rock dust (limestone) required for each percent of methane: A = (100 - I)/5, where A is the additional limestone (in percent) and I is the total incombustible content (in percent) needed with no methane present. Table 4.3 gives the experimental values and predicted values (from the Bureau of Mines formula) of the additional dolomite required to inert for each extra percent of methane. The relationship is shown graphically in Fig. 4.20, with the straight line at 45 degrees representing the ideal case of perfect agreement between experimental and predicted values.

The actual agreement between the two sets of data is reasonably good, particularly when the following points are considered. First, the Bureau of Mines formula was developed from large-scale tests using limestone as the inerting material, whereas the present study was carried out in a small-scale vessel with dolomite as the rock dust. Second, the experimental program followed in the current work was extensive and did not deal with only one type and size of coal. Rather, the coal dusts used were of various particle sizes, volatile contents and ash contents.

4.2.2 Coal particle size

The influence of coal particle size on the dolomite inerting requirements can be seen from Table 4.2 and also Figs. 4.17 to 4.19. Decreasing the mass mean diameter by reducing particle size throughout the entire size distribution substantially increases the inerting level for both the Lingan and the Phalen coals. This is especially apparent for the required dolomite percentage, and, to a lesser degree, for the total incombustible content.

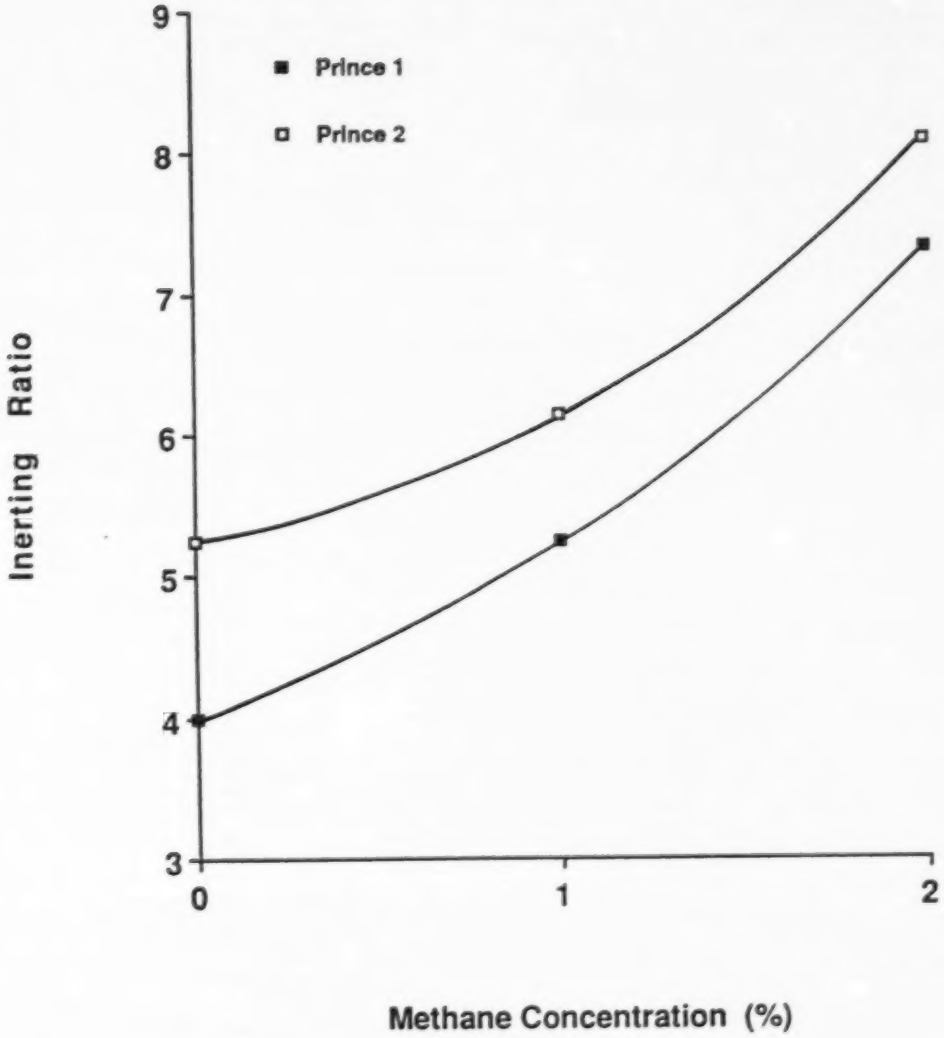

Fig. 4.17 Effect of methane addition on inerting ratio for Prince coals.

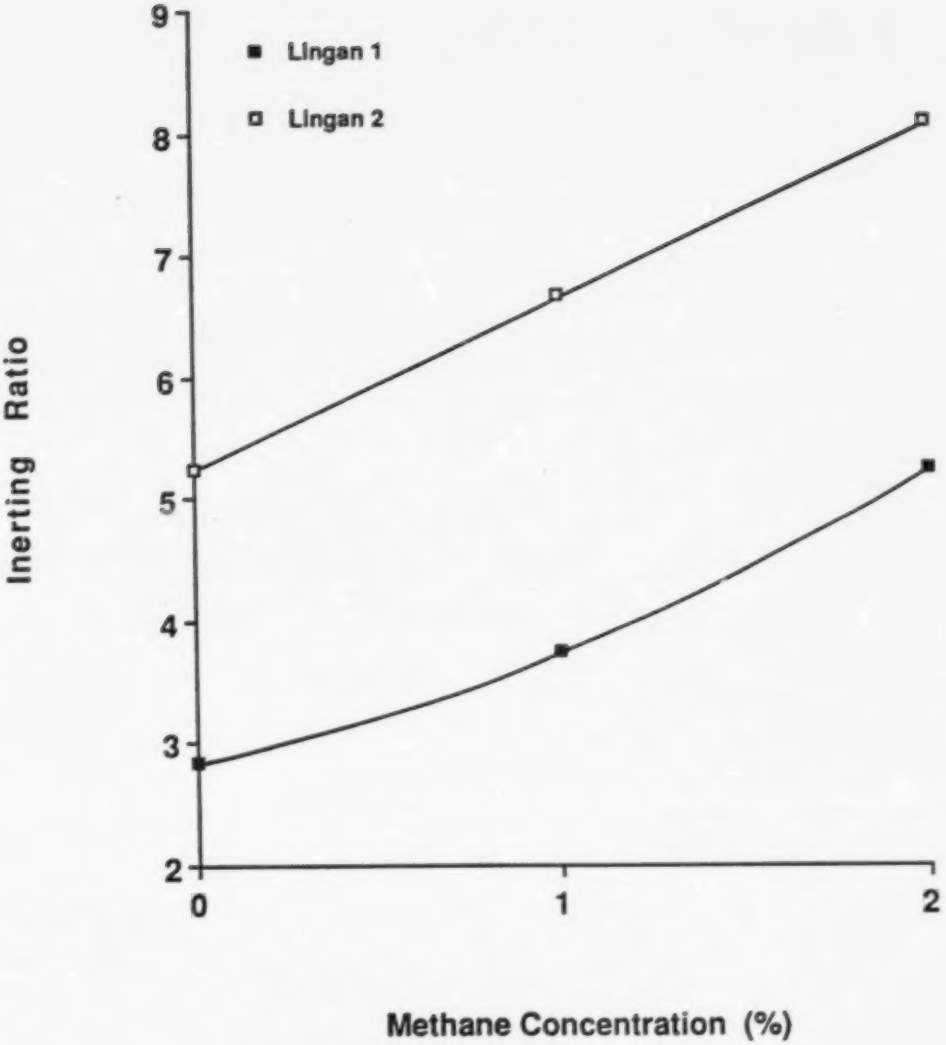

Fig. 4.18 Effect of methane addition on inerting ratio for Lingan coals.

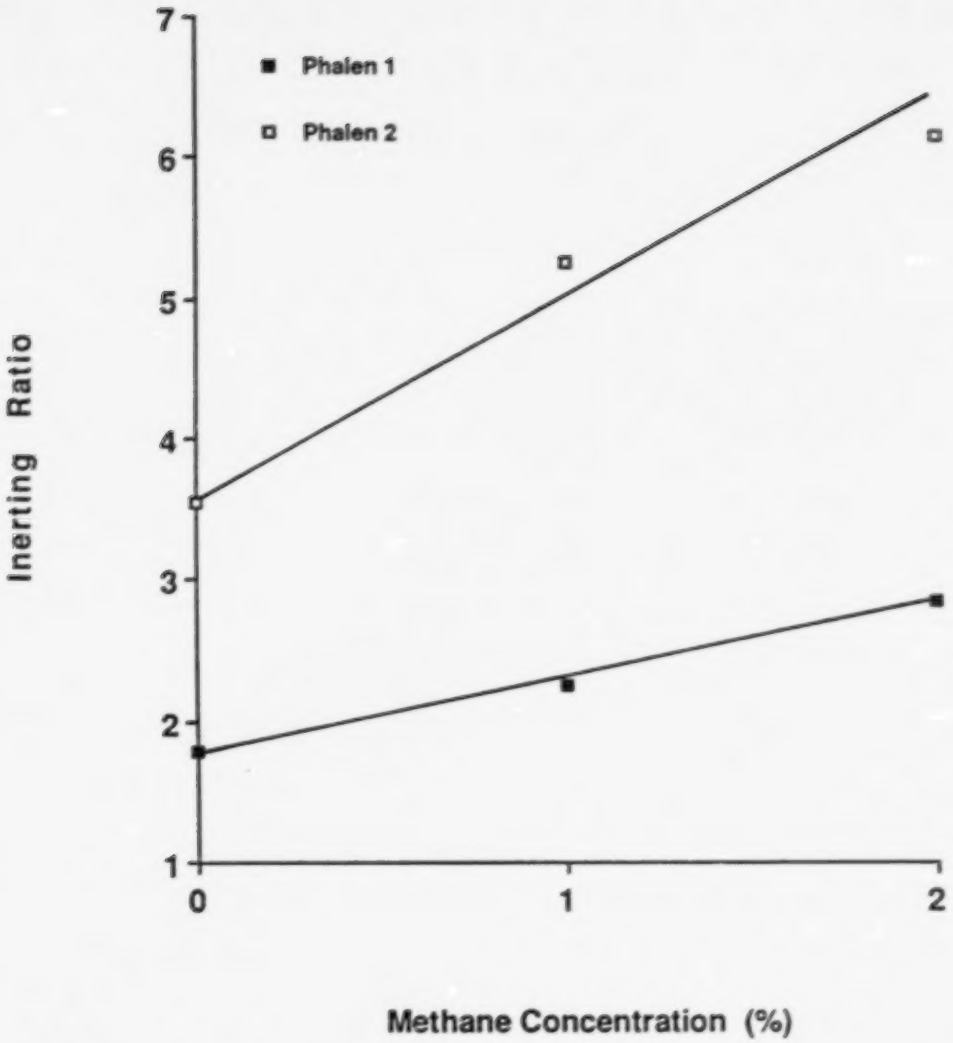

Fig. 4.19 Effect of methane addition on inerting ratio for Phalen coals.

Table 4.3 Experimental and predicted values of additional dolomite due to methane addition.

Coal Type and Size	Methane Concentration [%]	Experimental Value of Additional Dolomite [%]	Predicted Value of Additional Dolomite [%]
Prince 1	1	3	3
Prince 1	2	8	7
Prince 2	1	2	3
Prince 2	2	5	5
Lingan 1	1	5	4
Lingan 1	2	10	8
Lingan 2	1	3	3
Lingan 2	2	5	6
Phalen 1	1	5	5
Phalen 1	2	10	9
Phalen 2	1	6	3
Phalen 2	2	8	6

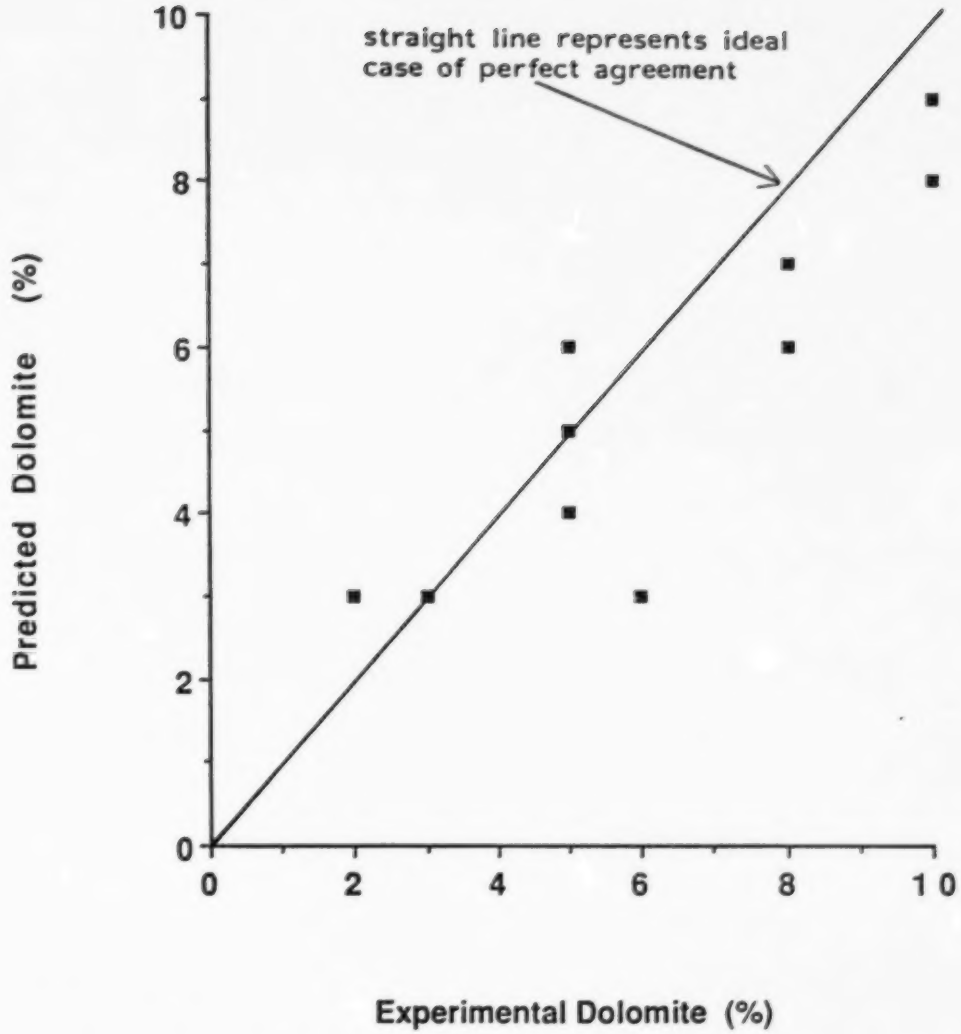

Fig. 4.20 Relationship between experimental and predicted values of additional dolomite due to methane addition.

For the Prince coals, even with the slight decrease in volatile content from Prince 1 to Prince 2, there is still an increase in inerting requirements when the mass mean diameter is decreased from 23 μm to 19 μm. This implies that the particle size distribution of the coal can play a dominant role in establishing the level of dolomite concentration needed to suppress an explosion.

4.2.3 Coal volatile content

The effect of coal volatile content on the inerting level can be seen from the results for the Prince 1 (36% volatiles), Lingan 1 (32% volatiles) and Phalen 1 (26% volatiles) coals. Again, the particle size distributions are not identical, but are approximately the same. In the absence of methane the percentage dolomite required to inert decreases in direct proportion to decreasing volatile content, from 80% for Prince 1 to 74% for Lingan 1 to 64% for Phalen 1. It must be remembered, however, that the Phalen coals had ash contents which were about double those for the Prince and Lingan coals. It is not surprising, therefore, that when the inerting requirements are expressed on a total incombustible content basis, the difference between the Lingan 1 and Phalen 1 coals is greatly reduced.

Some measure of the effect of volatile content for smaller coals can be gained by examining the Prince 2 and Phalen 2 results. There are slightly more fines (< 20 μm) in the Phalen 2 coal than in Prince 2, but the remainder of the size distributions are similar. Here, there is still a requirement for a greater dolomite percentage at the 34% volatile level than at the 26% level. The values are 84% dolomite for Prince 2 with no methane and 78% dolomite for Phalen 2 with no methane. Clearly though, the difference in inerting requirements for the two coals is now much less than for the larger sizes of the same two coals. This observation is consistent with the work of Cashdollar and Hertzberg (1989) and was explained by them in terms of an increased rate of devolatilization from the smaller dusts, particularly for the lower volatility coal.

4.3 Applicability to Coal Mining Industry

In the final section of this chapter the applicability of the current results to the coal mining industry is discussed. This is done by first considering the key test parameters of turbulence level and ignition source. The discussion then shifts to an examination of two properties of the test material – coal particle size and coal ash content.

4.3.1 Turbulence level

Turbulence plays a large role in determining the explosion characteristics of a dust (particularly $(dP/dt)_{max}$) and is, therefore, a dominant concern in dust explosion research (Amyotte et al., 1988). In closed-vessel testing, with an air blast used to disperse the dust throughout the vessel, some degree of turbulence will always be present in the test apparatus before ignition. Factors which strongly influence the turbulence level in dust explosion testing include the dispersion reservoir volume, the dispersing air pressure, the ignition delay time and the dispersion nozzle itself. In the current work, these parameters were 1 L, 13.8 bar (g), 410 ms and the U.S. Bureau of Mines perforated design, respectively.

The choice of these values, particularly the dispersing air pressure and ignition delay time, was governed by the desire to obtain measurements of maximum explosion pressure and size-normalized maximum rate of pressure rise (K_{St}) which were comparable to those determined at the U.S. Bureau of Mines in a 20-L test vessel for Pittsburgh seam bituminous coal dust. The U.S. Bureau of Mines small-scale results have been consistently shown to compare favourably with the data from large-scale testing at the Bureau's Bruceton and Lake Lynn Experimental Mines (Cashdollar et al., 1987). Thus, the rationale for setting the turbulence level in the present work was to give the test results some relevance to what would be expected in an actual mine setting. It must be remembered, however, that this turbulence level is

moderate and that a higher dispersing air pressure and shorter ignition delay time would yield higher values of the K_{St} parameter.

4.3.2 Ignition source

Recognition of the importance of ignition source strength is essential in applying explosibility data for dusts to a practical system. It is well-established that energetic ignition sources are required for determination of lean flammability limits and rock dust inerting requirements. While electrical sparks are important as low-energy industrial ignition sources, many ignition sources found in industry are quite massive, often extending into the kJ range. This is of particular concern in the coal mining industry where primary explosions of methane have been responsible for initiation of a coal dust explosion (as described in the first chapter of this report). Use of the 5 kJ chemical ignitors was therefore justified on the basis of being relevant to the actual industrial setting of the coal dust used as test material.

4.3.3 Coal particle size

The current study has shown that coal particle size has a significant effect on several dust explosibility parameters, perhaps most notably the dolomite inerting level. A key question which must be addressed, therefore, is whether or not the particle sizes used in this work are representative of those for actual mine dust. Table 4.4. gives the particle size analyses for several dust samples collected from various locations in the Prince, Lingan and Phalen mines. The samples were collected and analyzed by CBDC.

Comparison of Tables 2.1 and 4.4 shows that the coals having comparable, although not identical, size distributions are Prince 1 and Prince C, Lingan 1 and Lingan B, and Phalen 1, Phalen B and Phalen C. It is interesting to note that half of the coal dusts shown in Table 4.4 are coarser than the test samples in Table 2.1. The

Table 4.4 Particle size analyses of CBDC colliery dust samples.

Colliery	Location	<125 μm [weight %]	<75 μm [weight %]	<45 μm [weight%]	<20 μm [weight%]
Prince (Prince A)	No. 7 W Bottom Level, Stage Loader	67	57	43	23
Prince (Prince B)	No. 7 W Bottom Level, At Spillpoint No. 2 Drive	94	81	55	28
Prince (Prince C)	No. 7 W Wall, Jack Control Blocks	97	91	72	36
Lingan (Lingan A)	No. 11 E Top of Wall, Top Corner	64	48	31	16
Lingan (Lingan B)	No. 10 E Bottom Level, No. 1 Drive Spillpoint	92	80	62	41
Phalen (Phalen A)	No. 1 W Bottom Level, Outside Spillpoint	53	32	18	11
Phalen (Phalen B)	No. 1 W Bottom Level, Stage Loader	95	88	71	43
Phalen (Phalen C)	No. 1 W Wall, No. 30, No. 40 Roof Supports	95	86	70	48

larger size fractions in the current work (Prince 1, Lingan 1 and Phalen 1) thus appear to be representative of the finer mine sizes. The smaller size fractions used in this study (Prince 2, Lingan 2 and Phalen 2) are useful in showing some of the effects of generating even finer coal dusts. Further support for the use of fine size fractions in laboratory testing is given by Sapko et al. (1989). Their review paper on prevention and suppression of coal mine explosions indicates that the coal dust being generated at present is finer than in earlier years, and that this float coal dust is the most dangerous in terms of explosibility.

The final point to be discussed here is how the experimentally determined inerting levels compare with those required by government regulation. Canada is among the strictest countries in the world in this respect; the inerting requirements listed for Canada by Sapko et al. (1989) are 75% total incombustible content for methane concentrations less than 1% and 80% total incombustible content for methane concentrations greater that 1%. The inerting requirements for coal dust/air mixtures shown in Table 4.2 are in all cases greater than 75% TIC, and the 75% level is therefore inadequate for explosion suppression of these dusts. It must be remembered, however, that these requirements are for fine size fractions and that inerting levels are strongly dependent on coal particle size. There is also the consideration that the inerting levels given in Table 4.2 are the result of tests conducted in a 26-L chamber with 5 kJ chemical ignitors. As noted by Cashdollar and Hertzberg (1989), the possible apparatus dependence of inerting level and the known variation of the level with ignition energy mean that laboratory-scale inerting requirements should perhaps be considered as relative rather than absolute values.

Whether there is a need for a differentiated approach to rock dusting, as in the United States, is a question which could best be answered by further testing on coarse samples. Inerting regulations for coal dust in the United States currently call for a general level of 65% TIC, but also stipulate 80% TIC in returns where coal dust is finer.

What is clear from the present work, though, is that there is no apparent rationale for relaxing the current Canadian rock dusting regulations.

4.3.4 Coal ash content

The present work was conducted using run-of-mine coal. As previously mentioned, the Phalen coals had a particularly high ash content when compared to the Prince and Lingan coals. This is part of the reason for reporting the inerting requirements on a basis of total incombustible content as well as dolomite percentage. It was considered prudent, however, to briefly examine the explosion behaviour of one of the coals after it had been cleaned.

A small sample of "pure" Phalen coal was obtained from CBDC and was ground and sieved into the following size fractions, by weight: 100% < 125 μm, 83% < 75 μm, 58% < 45 μm, 35% < 20 μm; D_w = 34 μm. Figure 4.21 shows that although the sample was somewhat larger than the Phalen 1 coal, P_{max} was slightly increased and $(dP/dt)_{max}$ was significantly increased over the corresponding Phalen 1 values. The lean flammability limit determined from the data in Fig. 4.21 is approximately 0.1 kg/m^3; this is lower than the previously reported Phalen 1 lean limit of 0.12 kg/m^3. These observations are consistent with a lower ash content and higher volatile content in the "pure" Phalen coal than in the Phalen 1 coal.

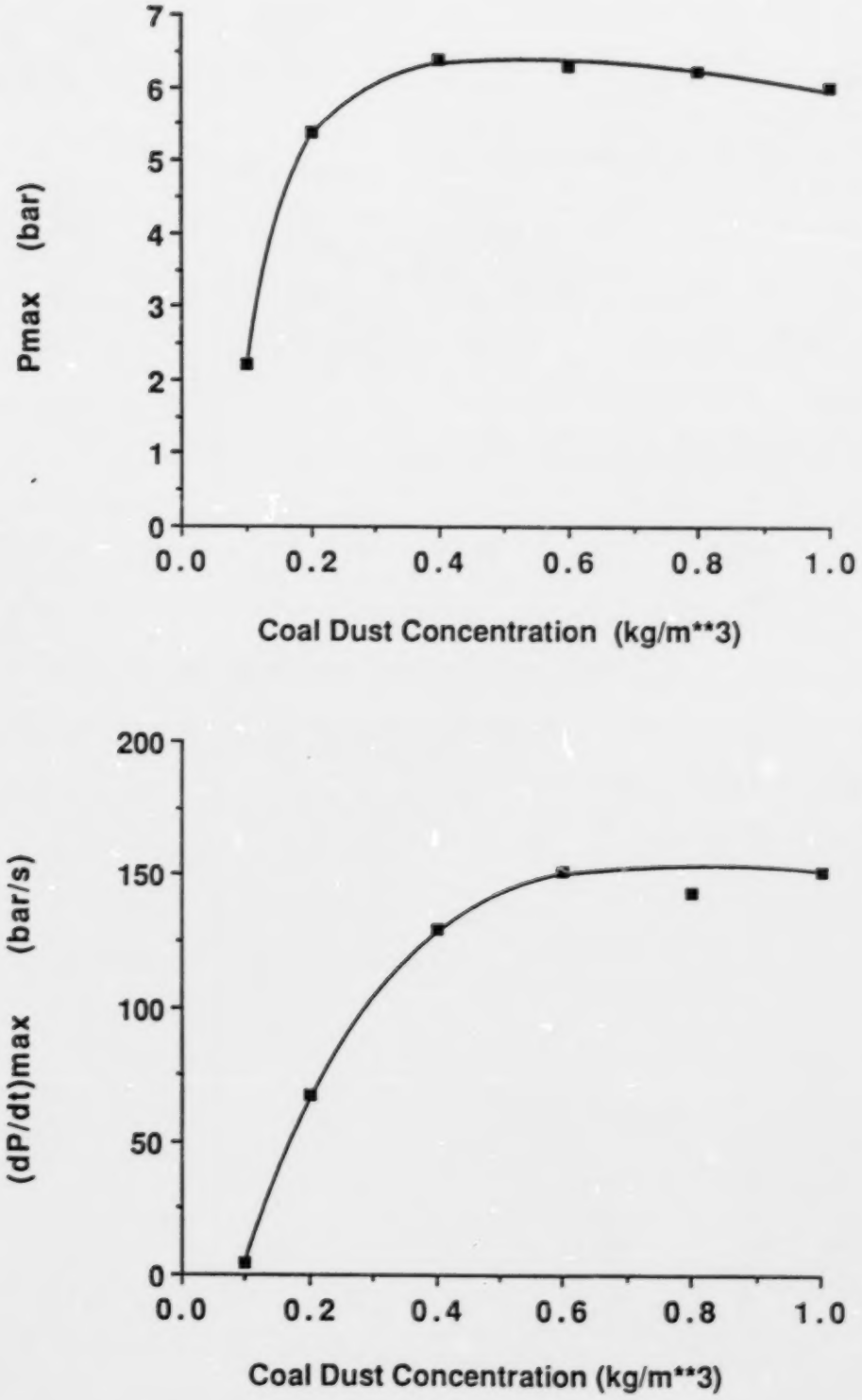

Fig. 4.21 P_{max} and $(dP/dt)_{max}$ at various coal dust concentrations (Phalen "pure", 0% methane).

CHAPTER 5

CONCLUSIONS AND RECOMMENDATIONS

In this chapter, the main findings of this work are summarized and recommendations arising from the work are given.

5.1 Summary of Conclusions

The principal conclusions which have been drawn from this study are as follows:

1. Methane addition to the oxidizing atmosphere of a coal dust/air mixture results in an increase in P_{max} and $(dP/dt)_{max}$ at a given dust concentration when such a mixture is ignited. The effect is greatest at low dust concentrations and becomes small at high dust concentrations, particularly for P_{max}.
2. Methane admixture also causes the peak values of P_{max} and $(dP/dt)_{max}$ to occur at dust concentrations which are less than for coal dust alone.
3. The effect on P_{max} and $(dP/dt)_{max}$ of reducing the coal particle size is similar to that of methane admixture. This observation is consistent with the phenomenological model of dust flame propagation by devolatilization and subsequent volatiles combustion.
4. Coal volatile content has a significant effect on P_{max} and $(dP/dt)_{max}$; these parameters are higher the greater the volatile content of the coal.
5. The lean flammability limit of coal dust/air mixtures displays a marked dependence on coal volatile content, with lower lean limits being obtained for higher volatility coals. There is also evidence of a particle size dependence of the lean limit for coals having broad particle size distributions.

6. The lean flammability limit of hybrid mixtures of methane/coal dust/air varies linearly with the percent methane in the oxidizing atmosphere and as such is predicted by Le Chatelier's law.
7. With respect to explosion inerting levels, the effect of methane admixture is to increase the amount of dolomite required (in other words, the total incombustible content needed). The additional amount of dolomite needed in the presence of methane can be predicted with reasonable accuracy by the empirical formula developed by the U.S. Bureau of Mines.
8. The particle size distribution of a coal plays a significant role in establishing the level of dolomite concentration needed to suppress an explosion, with finer size coals requiring more inert material.
9. Coal volatile content also has a substantial effect on inerting levels, in a manner similar to that for particle size.
10. Our results have demonstrated that there is no rationale for relaxing the current requirements for rock dusting operations in Canada.

5.2 Recommendations for Further Work

Based on the experience gained and conclusions drawn from this study, we recommend that the following work would be of value in better understanding the coal dust explosion hazard:

1. Inerting tests at coal dust concentrations other than 0.5 kg/m^3, to examine inerting requirements over a range of hazardous concentrations.
2. Inerting tests with limestone, to compare with the effectiveness of dolomite in suppressing coal dust explosions.
3. Inerting tests with coarse particles, to investigate the particle size dependence of inerting level for dust particles larger than those used in this study.

4. Experiments using various ignition energies and geometries, to simulate potential ignition sources in a coal mine.
5. Further sampling of mine dust, to identify representative particle size distributions for laboratory testing.

REFERENCES

Abrahamsen, A.R. (1987), "The U.K. Approach to Dust Explosibility Assessment and Its Relevance to Explosion Prevention and Protection", *Industrial Dust Explosions, ASTM STP 958*, K.L. Cashdollar and M. Hertzberg (Eds), pp. 60-73, American Society for Testing and Materials, Philadelphia.

Alameddin, A.N. and Luzik, S.T. (1987), "Coal Dust Explosions in the Cement Industry", *Industrial Dust Explosions, ASTM STP 958*, K.L. Cashdollar and M. Hertzberg (Eds), pp. 217-233, American Society for Testing and Materials, Philadelphia.

Amyotte, P.R., Chippett, S. and Pegg, M.J. (1988), "Effects of Turbulence on Dust Explosions", *Prog. Energy Combust. Sci.* **14**, 293-310.

Amyotte, P.R. and Pegg, M.J. (1989), "Lycopodium Dust Explosions in a Hartmann Bomb: Effects of Turbulence", *J. Loss Prev. Process Ind.* **2**, 87-94.

Cashdollar, K.L. and Hertzberg, M. (1985), "20-L Explosibility Test Chamber for Dusts and Gases", *Rev. Sci. Instrum.* **56**, 596-602.

Cashdollar, K.L., Sapko, M.J., Weiss, E.S. and Hertzberg, M. (1987), "Laboratory and Mine Dust Explosion Research at the Bureau of Mines", *Industrial Dust Explosions, ASTM STP 958*, K.L. Cashdollar and M. Hertzberg (Eds), pp. 107-123, American Society for Testing and Materials, Philadelphia.

Cashdollar, K.L. and Hertzberg, M. (1989), "Laboratory Study of Rock Dust Intering Requirements: Effects of Coal Volatility, Particle Size, and Methane Addition", *Proc. 23rd Int. Conf. SMRI*, pp. 965-975, Washington, D.C.

Dixon-Lewis, G., Bradley, D. and El-Din Habik, S. (1987), "Burning of Coal and Organic Dusts in Air", *Archivum Combustionis* **7**, 85-98.

Geysen, W.J., Belmans, R. and Scheys, L. (1987), "A Sugar Dust Explosion and Some Measures to Limit Its Consequences", *Industrial Dust Explosions, ASTM STP 958*, K.L. Cashdollar and M. Hertzberg (Eds), pp. 234-242, American Society for Testing and Materials, Philadelphia.

Hertzberg, M., Cashdollar, K.L., Lazzara, C.P. and Smith, A.C. (1982a), "Inhibition and Extinction of Coal Dust and Methane Explosions", *RI 8708*, U.S. Bureau of Mines, Pittsburgh.

Hertzberg, M., Cashdollar, K.L., Ng, D.L. and Conti, R.S. (1982b), "Domains of Flammability and Thermal Ignitability for Pulverized Coals and Other Dusts: Particle Size Dependences and Microscopic Residue Analyses", *19th Symp. (Int.) Combust.*, pp. 1169-1180, The Combustion Institute, Pittsburgh.

Hertzberg, M., Cashdollar, K.L. and Zlochower, I.A. (1986a), "Flammability Limit Measurements for Dusts and Gases: Ignition Energy Requirements and Pressure Dependences", *21st Symp. (Int.) Combust.*, pp. 303-313, The Combustion Institue, Pittsburgh.

Hertzberg, M., Zlochower, I.A. and Cashdollar, K.L. (1986b), "Volatility Model for Coal Dust Flame Propagation and Extinguishment", *21st Symp. (Int.) Combust.*, pp. 325-333, The Combustion Institute, Pittsburgh.

Hertzberg, M. and Cashdollar, K.L. (1987), "Introduction to Dust Explosions", *Industrial Dust Explosions, ASTM STP 958*, K.L. Cashdollar and M. Hertzberg (Eds), pp. 5-32, American Society for Testing and Materials, Philadelphia.

Kauffman, C.W. (1987), "Recent Dust Explosion Experiences in the U.S. Grain Industry", *Industrial Dust Explosions, ASTM STP 958*, K.L. Cashdollar and M. Hertzberg (Eds), pp. 243-264, American Society for Testing and Materials, Philadelphia.

Lee, J.H.S., Knystautas, R., Bond, F., Craft, N. and Kang, P.Y. (1984), "The Influence of Turbulence on Dust Explosion and the Effect of Methane on Coal Dust Explosion", *Contract Report No. 0ST 84-00016*, CANMET, EMR, Canada.

Mintz, K.J. (1989), "The Explosibility of Three Canadian Coals", *MRL 89-50 (TR)*, CANMET, EMR, Canada.

Nagy, J., (1981), "The Explosion Hazard in Mining", *RI 1119*, U.S. Bureau of Mines, Pittsburgh.

Sapko, M.J., Greninerg, N.B. and Watson, R.W. (1989), "Review Paper: Prevention and Suppression of Coal Mine Explosions", *Proc. 23rd Int. Conf. SMRI*, pp. 791-806, Washington, D.C.

Swift, I. (1982), "Developments in Dust Explosibility Testing: The Effect of Test Variables", *Fuel-Air Explosions*, J.H.S. Lee and C.M. Guirao (Eds), pp. 375-403, University of Waterloo Press, Ontario.

Watson, R.W.(1981), "Prevention and Suppression of Gas Explosions in Mines", *Proc. Aus. I.M.M. Illawarra Branch Ignitions, Explosions and Fires in Coal Mines Symp.*, 6.1-6.13.